[redacted]

MARTIN MARIETTA ENERGY SYSTEMS LIBRARIES
3 4456 0360779 1

ORNL 1128
Progress
9a

AEC RESEARCH AND DEVELOPMENT REPORT

PHYSICS OF SOLIDS INSTITUTE

QUARTERLY PROGRESS REPORT

FOR PERIOD ENDING JULY 31, 1951

LABORATORY RECORDS

OAK RIDGE NATIONAL LABORATORY
CENTRAL RESEARCH LIBRARY
CIRCULATION SECTION
4500N ROOM 175
LIBRARY LOAN COPY
DO NOT TRANSFER TO ANOTHER PERSON
If you wish someone else to see this report, send in name with report and the library will arrange a loan.
UCN-7969 (3 9-77)

CLASSIFICATION CHANGED TO: DECLASSIFIED
BY AUTHORITY OF: AEC-7-12-60
BY: M. Bowman 8/26/60

OAK RIDGE NATIONAL LABORATORY
OPERATED BY
CARBIDE AND CARBON CHEMICALS COMPANY
A DIVISION OF UNION CARBIDE AND CARBON CORPORATION
UCC
POST OFFICE BOX P
OAK RIDGE, TENNESSEE

[redacted]

SECRET

SECURITY INFORMATION

ORNL 1128

This document consists of 77 pages.

Copy 9 of 136 . Series A.

Contract No. W-7405, eng. 26

METALLURGY DIVISION

J. H. Frye, Jr. Director

PHYSICS OF SOLIDS INSTITUTE

D. S. Billington, Acting Director

QUARTERLY PROGRESS REPORT

for Period Ending July 31, 1951

EDITED BY

D. S. Billington and J. T. Howe

DATE ISSUED

FEB 26 1952

OAK RIDGE NATIONAL LABORATORY
operated by
CARBIDE AND CARBON CHEMICALS COMPANY
A Division of Union Carbide and Carbon Corporation
Post Office Box P
Oak Ridge, Tennessee

RESTRICTED DATA

This document contains Restricted Data as defined in the Atomic Energy Act of 1946. Its transmittal or the disclosure of its contents in any manner to any unauthorized person is prohibited.

SECRET

SECURITY INFORMATION

MARTIN MARIETTA ENERGY SYSTEMS LIBRARIES
3 4456 0360779 1

ORNL 1128
Progress

INTERNAL DISTRIBUTION

1. G. T. Felbeck (C&CCC)
2-3. Chemistry Library
4. Physics Library
5. Biology Library
6. Health Physics Library
7. Metallurgy Library
8-9. Training School Library
10-13. Central Files
14. C. E. Center
15. C. E. Larson
16. W. B. Humes (K-25)
17. W. D. Lavers (Y-12)
18. A. M. Weinberg
19. E. H. Taylor
20. E. J. Murphy
21. E. D. Shipley
22. D. S. Billington
23. F. C. VonderLage
24. R. C. Briant
25. J. A. Swartout
26. S. C. Lind
27. F. L. Steahly
28. A. H. Snell
29. A. Hollaender
30. M. T. Kelley
31. G. H. Clewett
32. K. Z. Morgan
33. J. S. Felton
34. A. S. Householder
35. C. S. Harrill
36. C. E. Winters
37. D. W. Cardwell
38. E. M. King
39. C. B. Ellis
40. J. T. Howe
41. C. P. Keim
42. L. K. Jetter
43. E. J. Boyle
44. W. D. Manly
45. C. D. Susano
46. W. W. Parkinson
47. R. J. Gray
48. B. S. Borie
49. D. E. Hamby
50. E. E. Stansbury
51. G. P. Smith
52. J. E. Cunningham
53. E. C. Miller
54. A. Brasunas
55. A. G. H. Andersen
56. J. O. Betterton, Jr.
57. R. B. Oliver
58. P. Patriarca
59. T. H. Blewitt
60. W. E. Taylor
61. J. H. Crawford, Jr.
62. A. F. Cohen
63. J. C. Wilson
64. O. Sisman
65. W. J. Sturn
66. M. T. Robinson
67. R. H. Kernohan
68. M. T. Metcalf
69. G. W. Keilhotz
70. R. S. Livingston (Y-12)
71. R. J. Jones (Y-12)
72. D. D. Cowen
73. P. M. Reyling
74-78. Central Files (O.P.)

RESTRICTED DATA

This document contains Restricted Data as defined in the Atomic Energy Act of 1946. Its transmittal or the disclosure of its contents in any manner to any unauthorized person is prohibited.

EXTERNAL DISTRIBUTION

79-86.	Argonne National Laboratory
87-89.	Atomic Energy Commission, Washington
90-93.	Brookhaven National Laboratory
94-97.	Carbide and Carbon Chemicals Company (Y-12)
98-100.	Knolls Atomic Power Laboratory
101-102.	General Electric Company, Richland
103.	Hanford Operations Office
104-107.	Los Alamos
108-109.	New York Operations Office
110.	Patent Branch, Washington
111-125.	Technical Information Service, Oak Ridge
126-129.	University of California Radiation Laboratory
130.	Massachusetts Institute of Technology (Kaufmann)
131.	Battelle Memorial Institute
132-134.	North American Aviation
135.	Westinghouse Electric Corporation
136.	Savannah River Operations Office, Wilmington

RESTRICTED DATA

This document contains Restricted Data as defined in the Atomic Energy Act of 1946. Its transmittal or the disclosure of its contents in any manner to any unauthorized person is prohibited.

SECRET

SECURITY INFORMATION

Physics of Solids Institute quarterly progress reports previously issued in this series are as follows:

ORNL-1025	Period Ending January 31, 1951
ORNL-1095	Period Ending April 30, 1951

RESTRICTED DATA

This document contains Restricted Data as defined in the Atomic Energy Act of 1946. Its transmittal or the disclosure of its contents in any manner to any unauthorized person is prohibited.

SECRET

SECURITY INFORMATION

TABLE OF CONTENTS

	PAGE NO.
INTRODUCTION AND SUMMARY	1
1. BUILDING STATUS	6
Hot Cells	6
2. SOLID STATE REACTIONS	11
Bombardment of P-Type Germanium	11
Silicon Bombardment Experiments	12
An Automatic Multirange Recording Device for Measuring Varying Potentials	13
Cryostat for Pile Irradiation	14
Lithium-Iron Cyclotron Bombardment	14
3. RADIATION METALLURGY	20
Neutron Irradiation of Age Hardening Alloys	20
Effect of Precipitate Particles on Resistivity of Cu-Be Alloys	24
Recovery of Radiation Hardening in Copper-Base Solid-Solution Alloys	28
Creep Under Irradiation	29
Cantilever creep	29
4. ENGINEERING PROPERTIES	35
Liquid-Metals Loop	35
Liquid-Metals In-Pile Stress-Corrosion Loop	37
Nuclear Heating	37
Pile-Induced Radiation	40
Physical Properties of Irradiated Elastomers	41
Irradiation of Graphite-Uranium Rods	47
5. LIQUID FUELS	50
Radiation Damage to Liquid Fuels	50

RESTRICTED DATA

This document contains Restricted Data as defined in the Atomic Energy Act of 1946. Its transmittal or the disclosure of its contents in any manner to any unauthorized person is prohibited.

PAGE NO.

6. CRYSTAL PHYSICS 51

Y-12 Cyclotron Studies 51
Radiation-cooled targets 51
Water-cooled targets 53
X-Ray Work 54
In-Pile Thermal Conductivity of Structural Materials at High Temperatures 55
Electrical and Thermal Conductivity of Metals 55
Metal Crystals 55
Change in resistivity of copper crystals from pile irradiation 57
Effect of radiation on the X-ray reflection coefficients 62
Effect of radiation on the stress-strain curves of polycrystalline copper 63
Study of the radiation effects on disordered Cu_3Au 63
LITR facility 66

RESTRICTED DATA
This document contains Restricted Data as defined in the Atomic Energy Act of 1946. Its transmittal or the disclosure of its contents in any manner to any unauthorized person is prohibited.

LIST OF TABLES

TABLE NO.	TITLE	PAGE NO.
2.1	Initial Values of N-Type Silicon Samples	13
2.2	Capsule Irradiation Conditions	17
2.3	Results of Capsule Irradiations	17
4.1	Nuclear Heating Rate for Several Materials	39
4.2	Graphite Bars Fabricated by BMI	48
4.3	Radiation Induced Changes in Graphite Bars	48
6.1	Electrical Resistivity of Copper Crystals	56
6.1	Summary	56
6.2	Measurements of the Electrical Resistance of Copper Single Crystals by Comparison with the Resistance of a Standard Control Specimen	58
6.3	Effect of Interstitials on the Elastic Coefficients of Copper	60

RESTRICTED DATA

This document contains Restricted Data as defined in the Atomic Energy Act of 1946. Its transmittal or the disclosure of its contents in any manner to any unauthorized person is prohibited.

LIST OF FIGURES

FIGURE NO.	TITLE	PAGE NO.
1.1	Master Slave and Tell Manipulators	6
1.2	Front Face of Hot Cells 4, 5a, 5b, and 6	7
1.3	Entrances to Hot Cells 4, 5a, 5b, and 6	8
1.4	Front Face of Cells 1, 2, and 3	9
1.5	Entrances to Cells 1, 2, and 3	10
2.1	Conductivity vs. Integrated Fast-Neutron Flux for N-Type Silicon at ~48°C	13
2.2	New Iron Specimen Capsule and Target Box	15
2.3	New Iron Specimen Capsule and Target Box	16
2.4	Cross-Section of Iron Specimen from Irradiation No. 1	18
2.5	Cross-Section of Iron Specimen from Irradiation No. 1	18
2.6	Cross-Section of Iron Specimen from Irradiation No. 1	19
3.1	Comparison of Resistance Changes of Solution-Quenched Cu-Be During Thermal Aging and During Neutron Exposure	21
3.2	Comparison of Aging of Single Crystal and Polycrystalline Cu-Be Specimens	21
3.3	Effect of Neutron Irradiation on Subsequent Aging of Cu-Be Specimens at 325°C.	22
3.4	Effect of Low-Temperature Aging on Subsequent Aging of Cu-Be Specimens at a Higher Temperature	23
3.5	Effect of Radiation on Rate of Precipitation in Cu-Be Specimens as Measured by Changes in Resistance	23
3.6	Effect of Neutron Irradiation on Subsequent Aging of Cu-Ti Specimens at 300°C	24

RESTRICTED DATA

This document contains Restricted Data as defined in the Atomic Energy Act of 1946. Its transmittal or the disclosure of its contents in any manner to any unauthorized person is prohibited.

FIGURE NO.	TITLE	PAGE NO.
3.7	Effect of Neutron Irradiation on Subsequent Aging of Cu-Ti Specimens at 350°C	24
3.8	Schematic Illustration of Potential and Charge Distribution in the Vicinity of a Platelet Having the Composition Cu-Be in a Matrix of Cu_9Be_1	
	a. Potential Due to Ionic Charge	25
	b. Charge Density Due to Trapped Electrons	25
	c. Resultant Charge Distribution	26
3.9	Approximation of Platelet Shape and Potential Well Used to Calculate the Ionic Potential Perturbation	
	a. Shape Assumed for Platelet	26
	b. Potential Well Assumed for Ionic Perturbation	26
3.10	Geometrical Representation of the Energy Levels in a Potential Well	28
3.11	Composite Plot of Three Bench and Three In-Pile Cantilever Creep Curves of Type 347 Stainless Steel Specimens at 1500°F	30
3.12	In-Pile Cantilever Creep Test of Type 347 Stainless Steel at 1500°F; Maximum Stress, 1700 psi	31
3.13	In-Pile Cantilever Creep Test of Type 347 Stainless Steel at 1500°F; Maximum Stress, 1700 psi	31
4.1	Absorption of Bremsstrahlung Activity from Li^8 Beta	35
4.2	Bremsstrahlung Activity from In-Pile Lithium Loop	36
4.3	Run No. 1, Rate of Heat Loss as a Function of Temperature for a Copper Specimen in a Large Calorimeter	40
4.4	Short Time Gamma Decay of Hastelloy	40
4.5	Long Time Gamma Decay of Hastelloy	40
4.6	Absorption of Gamma Radiation from Hastelloy	41

RESTRICTED DATA

This document contains Restricted Data as defined in the Atomic Energy Act of 1946. Its transmittal or the disclosure of its contents in any manner to any unauthorized person is prohibited.

FIGURE NO.	TITLE	PAGE NO.
4.7	Gamma Decay of Thorium	41
4.8	Physical Properties of Irradiated Natural Rubber	42
4.9	Physical Properties of Irradiated Thiokol ST	42
4.10	Physical Properties of Irradiated Hycar PA-21	43
4.11	Physical Properties of Irradiated GR-150	43
4.12	Physical Properties of Irradiated Silastic 7-170	44
4.13	Physical Properties of Irradiated Neoprene W	44
4.14	Physical Properties of Irradiated Hycar OR-15	45
4.15	Physical Properties of Irradiated GR-S50	45
5.1	Liquid-Fuel Sample Container with Thermocouple Well and Pressure Fittings	50
5.2	Capsule and Pressure Measuring Device	50
6.1	Eutectic-Containing Fuel Pin	51
6.2	Equilibrium Temperature of Eutectic-Containing Fuel Pin as a Function of Proton Beam Power	52
6.3	The 220 Reflection from an Unirradiated and an Irradiated Copper Crystal	62
6.4	Effect of Radiation on the Stress-Strain Curves of Polycrystalline Copper	63

RESTRICTED DATA

This document contains Restricted Data as defined in the Atomic Energy Act of 1946. Its transmittal or the disclosure of its contents in any manner to an unauthorized person is prohibited.

INTRODUCTION AND SUMMARY

This report covers work performed in the Physics of Solids Institute of the Metallurgy Division for the period May 1 to July 31, 1951.

BUILDING STATUS

Hot Cells. Handling of active materials was begun in the hot cells during the quarter, although all details and equipment conversion and installation are not yet complete.

SOLID-STATE REACTIONS

Bombardment of P-Type Germanium. P-type germanium has been bombarded and measurements have been made showing agreement with the Lehman-James model which predicts that bombardment will cause the Fermi level ζ to approach a limiting or saturation value. For materials in which the original value of ζ was above ζ_{limit}, bombardment caused a depression toward ζ_{limit}, and for materials in which ζ was originally below ζ_{limit} bombardment produced a rise of ζ toward ζ_{limit}. The saturation value for the Fermi level has been determined to be between 0.168 and 0.105 ev with work continuing toward a more accurate value.

Silicon Bombardment Experiments. Methods were worked out for attaching test leads to silicon samples to permit taking Hall effect and resistivity measurements. Two N-type samples were bombarded with fast neutrons and values were determined at 53 and 42°C respectively for electron concentration and initial rate of carrier removal per incident neutron. Conductivity decreased under bombardment to approximately the calculated conductivity of intrinsic silicon at the temperature of exposure.

Conductivity data taken as the samples changed temperature during pile shutdowns and startups is in agreement with the fact that the saturation conductivity occurs at approximately the intrinsic conductivity.

An Automatic Multirange Recording Device for Measuring Varying Potentials. An automatic recording device has been designed and built for measuring the changing electrical properties of semiconductors during bombardment. Some of the construction details and capabilities of the device are discussed.

Cryostat for Pile Irradiations. The cooling jacket has been installed in hole 52 and all auxiliary equipment is in the shops. Slight modification of the cryostat is expected to be completed shortly so that operation should begin within a few months.

Lithium-Iron Cyclotron Bombardment. Three iron capsules containing lithium were irradiated in the Berkeley 60-in. cyclotron using a 36-Mev alpha-particle beam. Two control samples experienced similar temperature treatments without radiation exposure. None of the five capsules have been opened for post-run examination.

A complete analysis of the first three capsules irradiated during the quarter ending April 31 is given.

RADIATION METALLURGY

Neutron Irradiation of Age Hardening Alloys. Hardness, resistance, and X-ray-diffraction studies were made of both single crystal and polycrystalline Cu-Be specimens and comparisons were made between "irradiation aging" and normal thermal aging.

Evidence is presented which lends support to the hypothesis that irradiation aging is a pre-precipitation process similar to the early stages of low-temperature thermal aging.

Irradiation of Cu-Ti alloys cause a decrease in the speed of aging at 300 and 350°C as compared to non-irradiated specimens. Further investigations will be conducted.

Ag-Cu specimens were irradiated and then aged at 75°C. No resistance changes were noted in either the exposed or control samples.

It was found that Ni-Be does not irradiation age, therefore the effect of irradiation in Cu-Be is not characteristic of the beryllium atom.

Effect of Precipitate Particles on Resistivity of Cu-Be Alloys. A theoretical and mathematical investigation is given in an attempt to explain the resistance effects observed in both radiation aging and low-temperature thermal aging solution-quenched Cu-Be age-hardening alloys as compared to changes observed in the copper alloys.

Dimensions of spherical precipitate nuclei are considered too large to interfere with the electron wave. Precipitate nuclei in the form of platelets might possibly cause some interference in their small dimension.

Recovery of Radiation Hardening in Copper-Base Solid-Solution Alloys. A repetition of former annealing experiments on radiation-hardened copper alloys produced recovery of the alloys in the same order as previously noted. None of the samples used thus far were annealed before irradiation sufficiently to completely remove work hardening. New samples have been fully annealed and are being exposed in the reactor.

Creep Under Irradiation. Three cantilever creep tests of type 347 stainless steel were run in the X reactor and a comparison was made with three bench tests run under the same conditions without radiation. Up to about 100 hr the creep rates are about the same. Thereafter the irradiated specimens begin to creep faster showing about 10% greater creep strain after 200 hr and about 20% more after 250 hr. Creep rates of the irradiated specimens showed definite decreases during pile shutdowns, as opposed to slight increases in one previous experiment.

Decreases in creep strain under irradiation as reported by other workers are thought to be due to the fact that their tests were run at much higher creep rates than the cantilever tests. The high rates of strain and the bombardment-hardening of annealed materials could reasonably produce the changes reported.

Hollow liquid-coolant filled tensile specimens and the related controllers, support frames, and furnace forms have been received, and extensive bench tests will be run before any attempts are made to run them in the Low Intensity Training Reactor (LITR). Use of a measuring device other than the microformer is expected; several methods will be tested for adaptability and accuracy.

ENGINEERING PROPERTIES

Liquid-Metals Loop. Lithium was circulated through hole 58 of the X reactor for a period of one week in order to study the Bremsstrahlung activity from the decay of Li^8. The average energy of the Bremsstrahlung arising from circulation of the lithium in type 316 stainless steel tubes was determined to be of the order of 0.06 Mev.

The measured activity of the lithium and cursory visual examination indicated no appreciable corrosion at an in-pile temperature of about 1000°F. Further investigation will be made when the tubes become less radioactive.

The next loop will be run using sodium at 1500°F in inconel tubes.

Liquid-Metals In-Pile Stress-Corrosion Loop. Design has been begun on a circulating-liquid-sodium loop to be run in the LITR at 1500°F. Creep measurements will be made on a 5-in. test section under 1500 psi stress.

Nuclear Heating. An investigation was started to determine the rates of heat production in various materials by nuclear bombardment in order to provide a basis for predicting the cooling requirements for the experimental apparatus. Two similar calorimeters were constructed, one of 5-in. diameter and 5-in. length for LITR use, the other of a long 3/4-in. diameter tube for use in the X reactor. The use of the calorimeters is discussed.

Pile-Induced Radiation. Decay curves are given for four Hastelloy alloys after they had been irradiated for six months in the X reactor.

Decay curves were also taken for several thorium samples, some containing small amounts of beryllium, columbium, zirconium, and titanium. The curves and energy of radiation indicate the predominant activity to be Pa^{233}.

Physical Properties of Irradiated Elastomers. Tensile strength, elongation, set at break, compression set, strain at 400 psi compression, change in weight, specific gravity, Shore durometer hardness, and Shore elasticity were measured for eight commercial plastics before and after irradiation in hole 19 of the X reactor.

Silastic, Neoprene, GR-S, Hycar OR, natural rubber, and Hycar PA are hardened by irradiation, but butyl (GR-1) and Thiokol became sticky and tarry.

Description of the test procedures and results of the tests to all the elastomers are given.

Irradiation of Graphite-Carbon Rods. Twelve uranium-free graphite rods were irradiated in the X pile as a preliminary step in the study of radiation damage to uranium-graphite materials. The rods exposed represented 12 different types of graphite. The samples were irradiated in the center of hole 1768 for two weeks corresponding to an integrated flux of $1 \times 10^{18}/cm^2$. Dimensions, weight, and natural vibration frequency were measured to determine the elastic modulus, electrical resistivity, and relative thermal conductivity. Some changes in future techniques will be made to increase the accuracy of the results for future measurements on the graphite-containing enriched uranium.

LIQUID FUELS

Radiation Damage to Liquid Fuels. Liquid fuels have been canned and heated to 1500°F both in the presence of radiation and without radiation. The 58-psi starting pressure of helium did not vary appreciably during the period. The samples are now being chemically analyzed as well as being examined for metallurgical changes.

CRYSTAL PHYSICS

Y-12 Cyclotron Studies. A study of radiation damage to the Aircraft Reactor Experiment (ARE) materials is

being made using the Y-12 86-in. cyclotron for proton bombardment.

Fuel pin targets (Fig. 6.1) are made of a 6 in. length of 1/4-in.-o.d. inconel tubing having a .010-in. wall thickness. A 4-in. length at one end is flattened to present a flat surface to the beam; the remaining cylindrical portion serves as an expansion chamber.

An estimate of the heat to be dissipated in the cyclotron is made by use of a calutron for preliminary bombardment with a high flux of low-energy protons.

Four fuel pins thus far studied were held at 700 to 725°C at the front face by means of beam heating. Beam currents were 2 to 3 μa of 20-Mev protons. Heat was dissipated from the target by radiation cooling. Two of the pins were exposed for 1 hr and two for 4 hr at approximately the same beam currents and temperatures. Only preliminary analytical results have been obtained thus far.

Spectroscopic analyses will be made of the eutectic for traces of inconel elements; the fuel will be assayed to determine if any changes have occurred in the ratios of uranium and fluorine; mass spectrographic analyses will detect changes in quantities of the fluorides of uranium.

The container tube will be metallurgically examined for corrosion, intergranular penetration, and grain alteration.

To permit an increase in the beam current a water-cooled block has been designed for mounting the fuel pins. One block-mounted pin has been bombarded. A beam current of 20 amp was required to maintain the face at approximately 1500°F. Radioactivity of the specimen has thus far prevented analysis. Two further types of water-cooled target mounts have been built and will be run in the near future.

X-Ray Work. A Hilger X-ray-diffraction unit was placed in operation during the quarter. The Hilger tube in continuously evacuated and has an anode made up of copper, cobalt, chromium, and silver targets, allowing quick selection of four distinct X-ray wave lengths. X-ray radiation from the Hilger tube is being used temporarily to operate a North American Philips Geiger-counter spectrometer.

Work done during this quarter consisted of zinc and copper crystal orientation and identification and comparison of various materials.

In-Pile Thermal Conductivity of Structural Materials at High Temperatures. The thermal conductivity of inconel at 820°C was found to decrease by a factor of two after less than one week of exposure in the X pile; after the initial decrease the value remains approximately constant. An in-pile temperature anneal removed approximately 20% of the damage; further exposure, however, caused the conductivity to return to its original equilibrium value. Confirmatory experiments will be run on inconel, and the work will be expanded to include types 310 and 316 stainless steels.

Electrical and Thermal Conductivity of Metals. Work began this quarter on an apparatus for making in-pile measurements of electrical conductivity and changes in thermal conductivity of metals at below 400°C. Magnetoresistance will be measured

before and after irradiation at temperatures up to 800°C.

Metal Crystals. The change in electrical resistivity of copper crystals resulting from a bombardment is reported. It is observed that the induced change of resistivity has a temperature dependence. This temperature dependence cannot be explained by changes in the Debye characteristic temperature. The effect of neutron irradiation on the X-ray reflection coefficients of copper crystals and the stress-strain curves of neutron-irradiated polycrystalline copper are also reported. A proposed experiment on the effect of irradiation on disordered Cu_3Au is also discussed in some detail.

OPEN PUBLICATION

J. W. Cleland, J. H. Crawford, Jr., K. Lark-Horovitz,* J. C. Pigg, "The Effect of Fast Neutron Bombardment on the Electrical Properties of Germanium," *Phys. Rev.* **83**, 312 (1951).

*Consultant from Purdue University.

1. BUILDING STATUS

HOT CELLS

S. E. Dismuke

Cells 3, 4, 5a, and 6 were placed in operation during the quarter and have proved quite satisfactory. Both the Master Slave and Tell manipulators shown in Fig. 1.1 have been used with encouraging success.

Cells 1 and 2 are complete, but in order to avoid contamination, they will not be used until after the semi-permanent apparatus is installed.

The chip collection system in cell 1 has been rebuilt, and tests have shown that the redesigned unit is satisfactory. It consists of a cyclone separator, an Aerotech dust collector, and a Fiberglas filter in series with a fan.

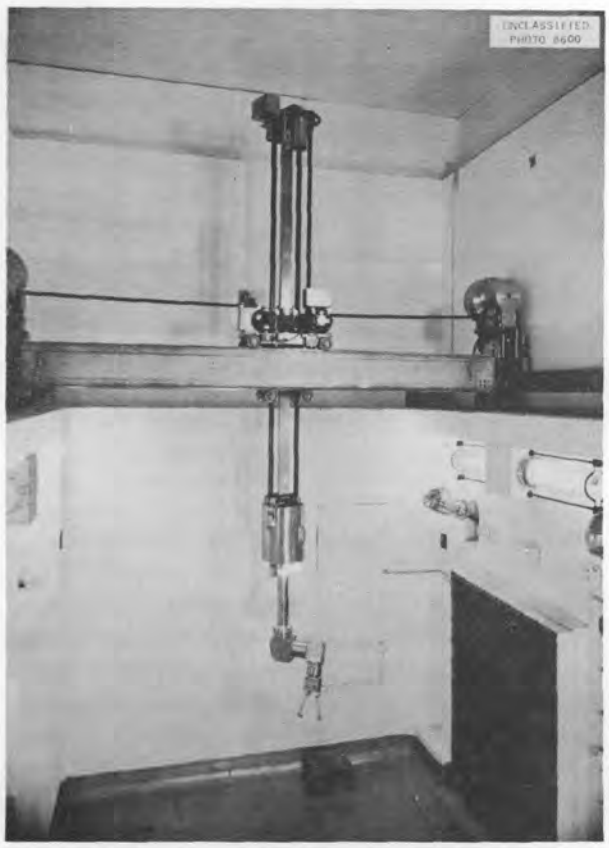

Fig. 1.1. Master Slave and Tell Manipulators.

The hydraulic system for operation of the intercell barrier doors has been tested, and installation will be completed some time in September.

Windows in several of the cells have given some trouble due to blistering and holes in the Amercote lining. Most of the hot work to date has been such that the water-filled windows have given adequate protection. As a result there has been some delay in fixing the trouble.

The remote controlled lathe is complete, but difficulties in making a few of the parts operate properly are holding up installation.

The Special Design Section of the Engineering Department has designed a remote polishing device that is near completion; it will be tested by R. J. Gray of the Metallurgy Division before it is used for work with contaminated materials. The remote polisher consists of a standard polishing unit with a special housing so arranged that the specimen holder rotates about an axis offset several inches from the axis of the polishing wheel. The same motor drives both the polishing wheel and the specimen holder. Design of a remote specimen mounting press for auxiliary use with the polisher is near completion.

Work is beginning on the installation of a metallograph in cell 2. It will be mounted through a recess on the north (entrance) side of the cell.

Pictures of the completed cells and some of their related equipment are shown in Figs. 1.2-1.5. Figure 1.2 shows the front face of cells 4, 5a, 5b, and 6; the Master Slave manipulators can be seen in operating position. Cell walls are constructed of concrete block and painted with strippable cocoon paint. Steel plates 4 in. in thickness form the cell roofs.

Figure 1.3 pictures the entrances to cells 4, 5a, 5b, and 6. The movable walls and the cell exhaust ducts may be observed in this view. In the lower right-hand corner an edge of the storage tank can be seen. This tank is approximately 6 ft wide by 23 ft long by 13 ft deep and may be filled with water for storage of hot specimens.

Figure 1.4 shows the front face of cells 1, 2, and 3. The Tell manipulator may be seen through the nearest window; its control box hangs on the outside face to the left of the window. Control equipment for a resistivity measuring unit is shown on casters in front of the cells.

In Fig. 1.5 the entrances to cells 1, 2, and 3 are shown. To the right of the picture and just to the left of cell 1 may be seen the loading chamber for charging the cells, and just below the loading chamber is the hydraulic power unit for operating the intercell barrier doors.

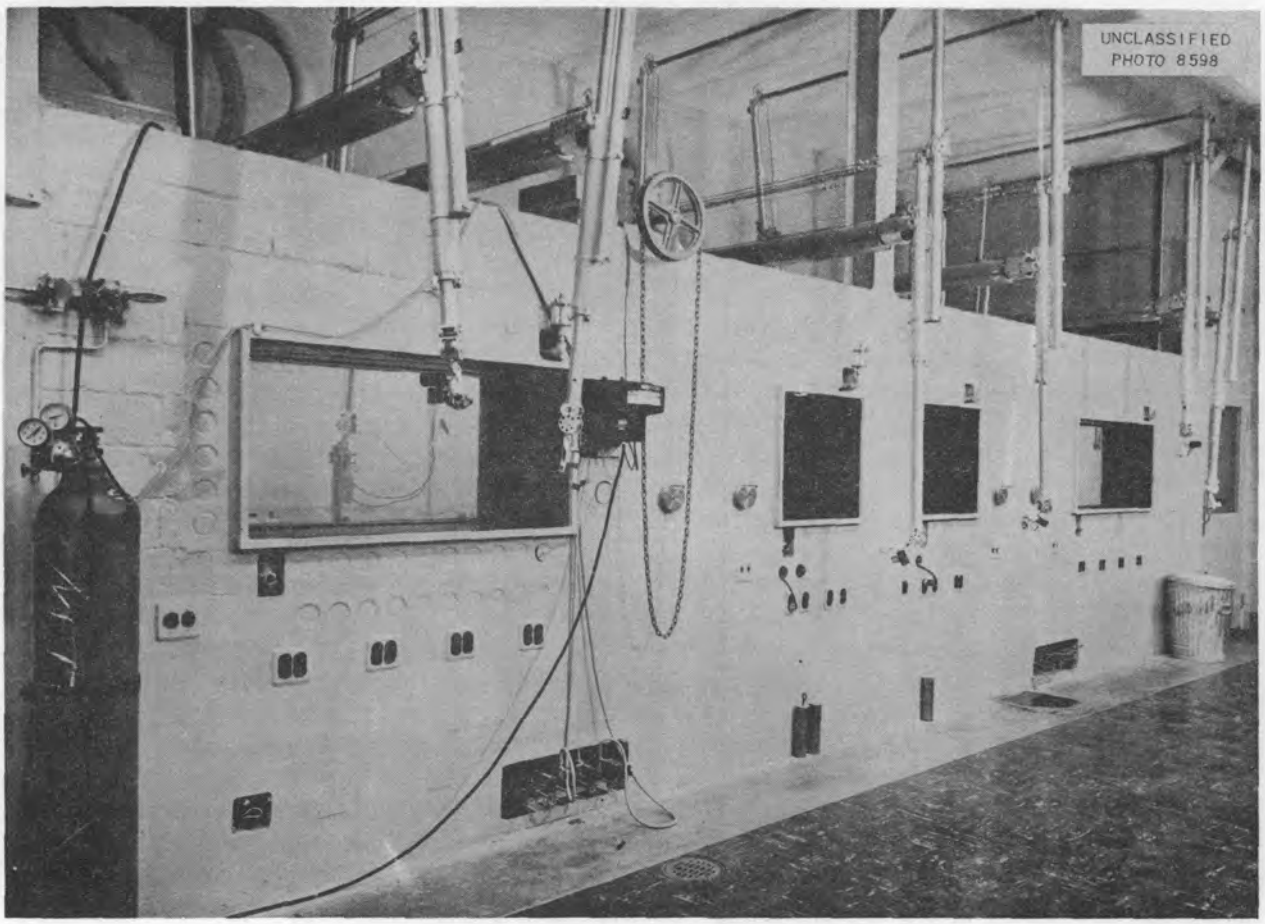

Fig. 1.2. Front Face of Hot Cells 4, 5a, 5b, and 6.

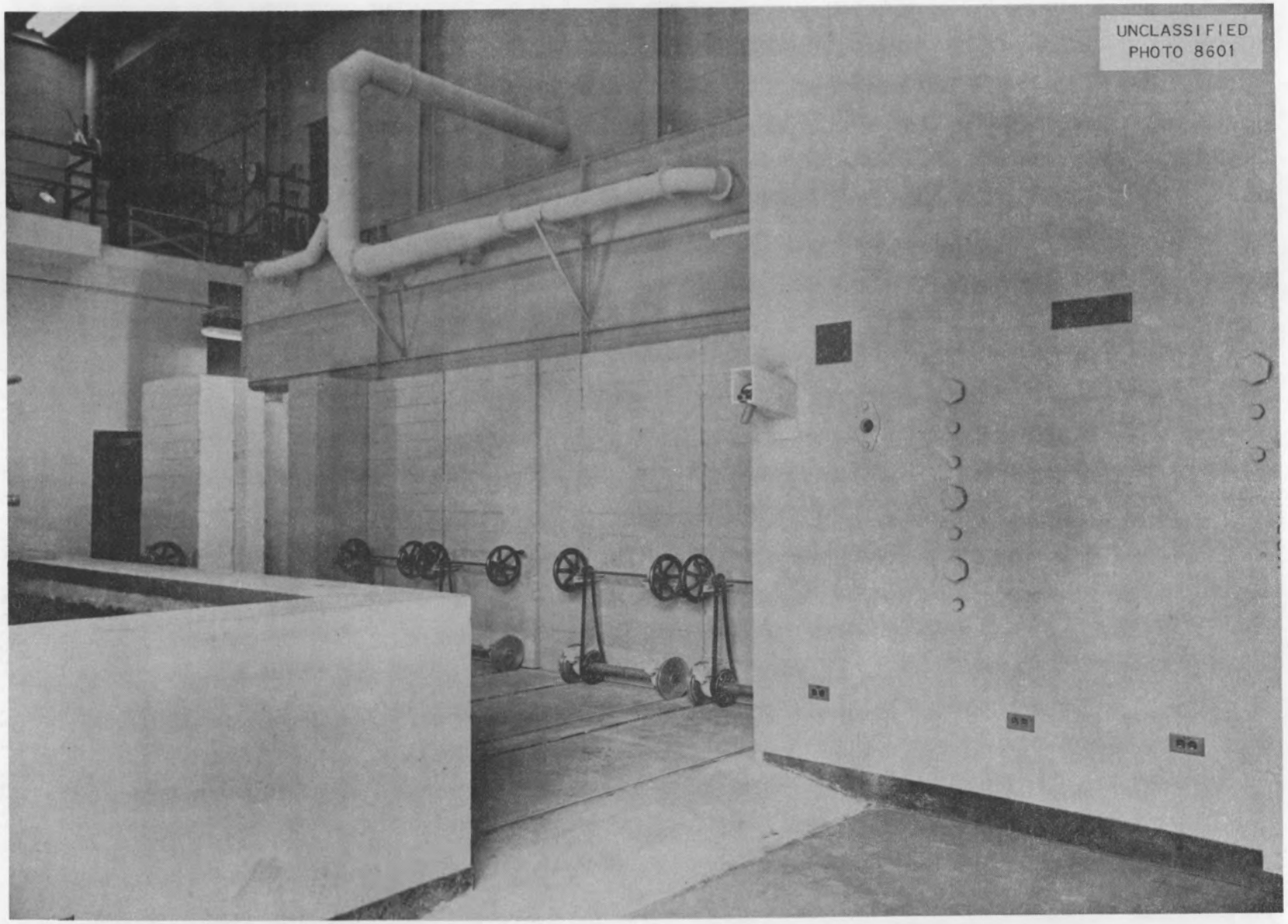

Fig. 1.3. Entrances to Hot Cells 4, 5a, 5b, and 6.

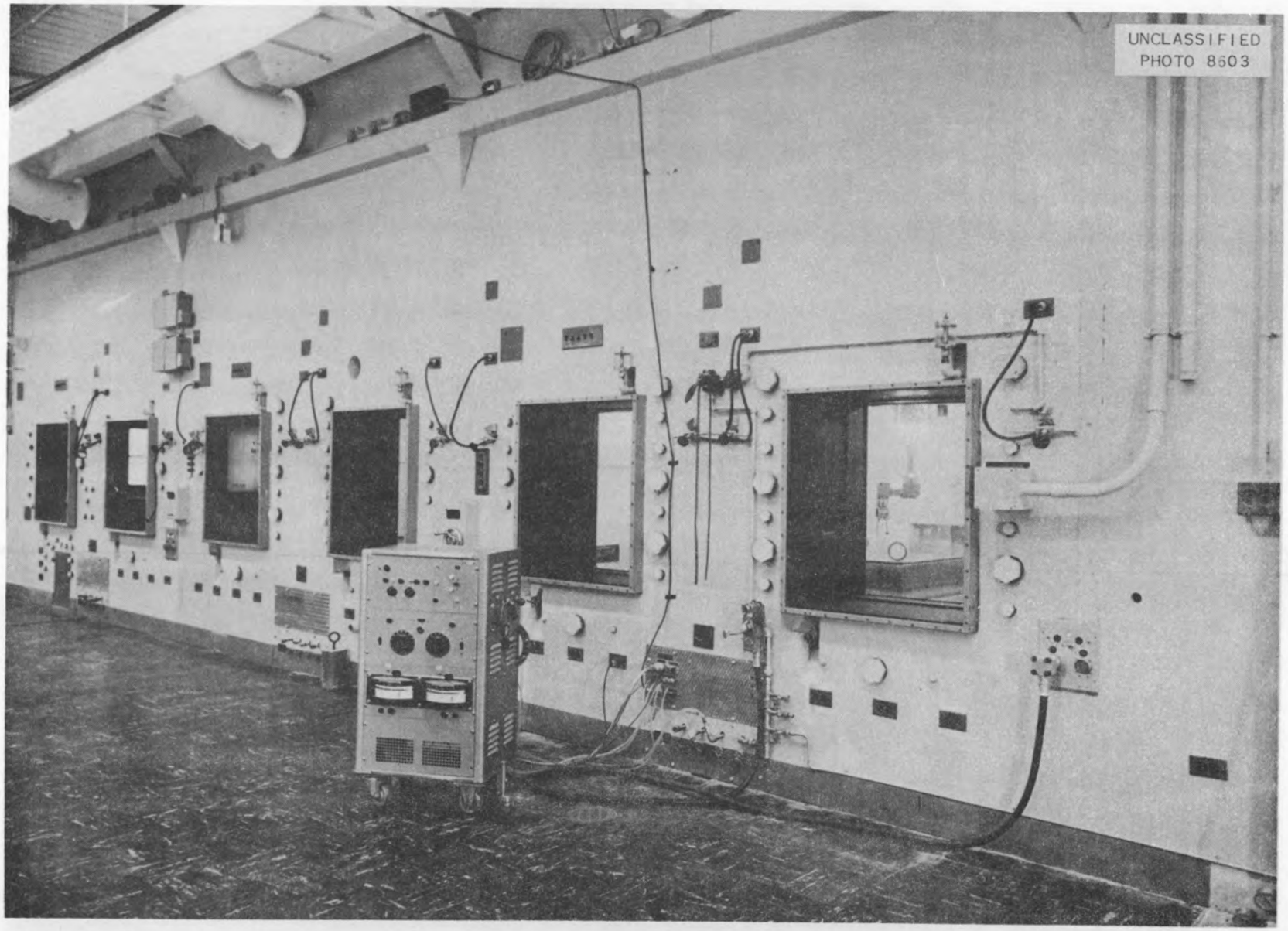

Fig. 1.4. Front Face of Cells 1, 2, and 3.

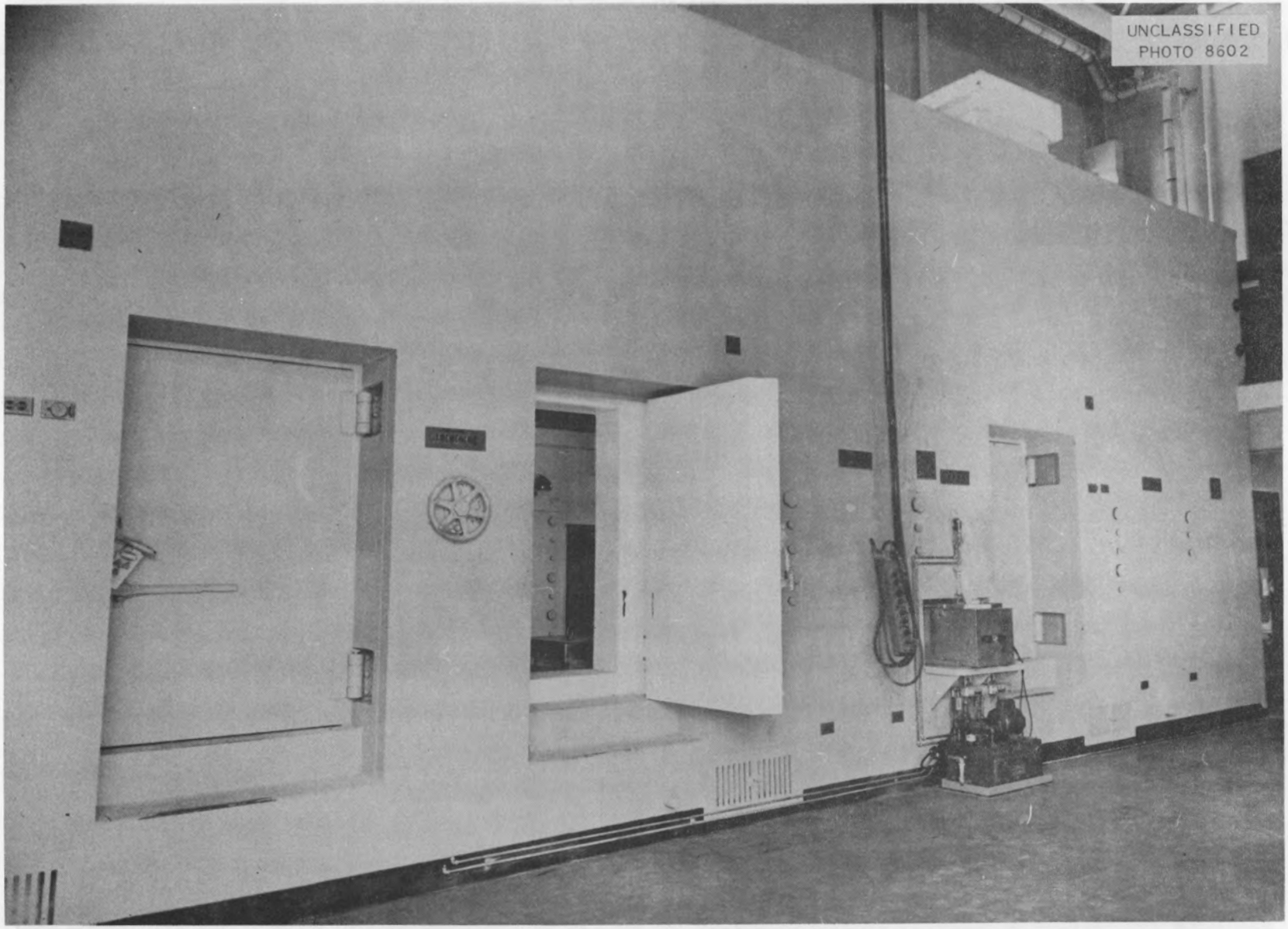

Fig. 1.5. Entrances to Cells 1, 2, and 3.

2. SOLID STATE REACTIONS

BOMBARDMENT OF P-TYPE GERMANIUM

J. W. Cleland K. Lark-Horovitz*
J. H. Crawford, Jr. J. C. Pigg
F. W. Young, Jr.

In a previous report[1] it was shown that low-resistivity P-type Germanium (approximately 0.005 ohm-cm) decreased in conductivity on fast-neutron bombardment at approximately 50°C and that somewhat high-resistivity P-type material (approximately .1 ohm-cm) showed a decrease in conductivity at -78°C, even though this material increased in conductivity at about 50°C. This behavior was shown to be in agreement with a model proposed by Lehman and James[2] in which both hole traps (donors) and electron traps (acceptors) are introduced below the middle of the forbidden energy band in equal concentrations. Because of the importance of these results it is desirable to discuss agreement between them and the model in greater detail.

According to the Lehman-James model, bombardment causes introduction of an electron trap or acceptor and a hole trap or donor for each displaced atom (vacancy-interstitial pair). These traps are presumably associated with the vacancy and interstitial atom, respectively. The introduction of these levels causes the Fermi level ζ to approach a limiting or saturation value ζ_{limit}. Thus, if the original value of ζ lies above ζ_{limit}, as is the case for N-type and high-to-moderate-resistivity P-type material, bombardment will cause a depression of ζ toward ζ_{limit}. Conversely, if ζ originally lies below ζ_{limit}, as in the case of low-resistivity P-type material, bombardment causes a raising of ζ toward ζ_{limit}. The dependence of electron and hole concentrations on ζ are

$$n_e = \frac{2(2\pi m_e^* kT)^{3/2}}{h^3} \cdot e^{(\Delta\epsilon_g - \zeta)/kT} \quad (1)$$

and

$$n_h = \frac{2(2\pi m_h^* kT)^{3/2}}{h^3} \cdot e^{-\zeta/kT}, \quad (2)$$

where the subscripts e and h refer to electrons and holes, respectively, $\Delta\epsilon_g$ is the forbidden energy band width, and ζ is measured from the top of the filled band. From these equations it is evident that a depression of ζ will cause a decrease in n_e in N-type germanium. Depression of ζ across the middle of the forbidden energy band will cause conversion to P-type and further depression of ζ will cause an increase in the hole concentration. On the other hand, elevation of ζ in P-type material will cause a decrease in hole concentration with a corresponding decrease in conductivity.

Corresponding to ζ_{limit}, there will be a limiting value of the hole concentration $(n_h)_{limit}$ above which one would expect a decrease in conductivity with bombardment. This value

*Consultant from Purdue University.

[1] J. W. Cleland, J. H. Crawford, Jr., J. C. Pigg, and F. W. Young, Jr., "Evidence for Hole Traps in Germanium Resulting from Fast-Neutron Bombardment," *Physics of Solids Institute Quarterly Progress Report for Period Ending April 30, 1951*, ORNL-1095, p. 36 (Nov. 12, 1951).

[2] K. Lark-Horovitz, *Reading Conference on Properties of Semiconducting Materials*, Appendix II, by G. W. Lehman and H. M. James (to be published); G. W. Lehman, "Fermi Levels in Semiconductors," *Phys. Rev.* 81, 321 (1950).

can be obtained directly from Eq. (2). Thus

$$(n_h)_{limit} = \frac{2(2\pi m_h^* kT)^{3/2}}{h^3} \cdot e^{-\zeta_{limit}/kT} . (3)$$

It can be shown that to the approximation used in the model, ζ_{limit} is temperature independent. Thus $(n_h)_{limit}$ is seen to have an exponential dependence on the reciprocal of the absolute temperature. These features of the model are qualitatively verified by experimental results.

More extensive bombardment experiments have been carried out on P-type germanium with carrier concentrations extending over a larger range in order to "bracket" more closely the value of ζ_{limit}. At 55°C a sample whose hole concentration was 7.23×10^{16} cm^{-3} showed an increase in conductivity, while a sample with $n_h = 7.02 \times 10^{17}$ cm^{-3} showed a decrease in conductivity on bombardment. From Eq. (3), using the electronic rest mass for m_h^*, it can be shown that 0.168 ev > ζ_{limit} > 0.105 ev. Further experiments are under way which are designed to determine ζ_{limit} more exactly.

SILICON BOMBARDMENT EXPERIMENTS

J. W. Cleland K. Lark-Horovitz*
J. H. Crawford, Jr. J. C. Pigg
F. W. Young, Jr.

The study of the effect of fast-neutron bombardment on the properties of silicon have been continued. Considerable difficulty has been encountered in attaching test leads to the samples, but a method has been worked out which has been found to be suitable. Gold spots are fused on to the sample in the appropriate positions for Hall effect and resistivity measurements by means of a compressed air-gas torch and either borax or commercial aluminum solder flux. After this drastic heat treatment is given to the sample it is necessary to vacuum anneal it at approximately 500°C for periods up to 60 hr to remove the lattice defects frozen in by quenching. After the anneal the test leads can be soldered directly to the gold spots with soft solder.

Two N-type samples furnished us by Bell Laboratories have been bombarded. The initial values of electron concentration n_e, the exposure temperature T_e, and the initial rate of carrier removal per incident neutron

$$\left[\frac{dn_e}{d(nvt)_{fast}} \right]_I$$

are listed in Table 2.1. The conductivity vs. bombardment curve for one of these samples is shown in Fig. 2.1. It is interesting to note that the conductivity decreased five orders of magnitude during the bombardment to a value of 10^{-5} ohm^{-1}-cm^{-1}, which corresponds approximately to the calculated conductivity of intrinsic silicon at the temperature of exposure (approximately 50°C). The curve appears to saturate after about 7×10^{18} nvt. There is also definite evidence of small increases in conductivity at constant temperature during pile shutdown, which indicates annealing of the radiation damage.

Although the initial electron concentrations of the two samples are almost identical, the slope of the sample exposed at the lower temperature is somewhat higher than that of the sample with the higher temperature of exposure. However, the relative trapping efficiency of the bombardment-introduced traps is expected

*Consultant from Purdue University.

TABLE 2.1

Initial Values of N-Type Silicon Samples

(Furnished by Bell Laboratories)

SAMPLE	n_e^0 (cm^{-3})	T_e (°C)	$\left[\frac{dn_e}{d(nvt)_{fast}}\right]_I$
1	1.21×10^{16}	53	-1.52
2	1.24×10^{16}	42	-1.82

to be greater the lower the temperature, and the initial slope should be proportional to the relative trapping efficiency. Therefore, the observed difference in slope is in the proper direction. These slopes are smaller

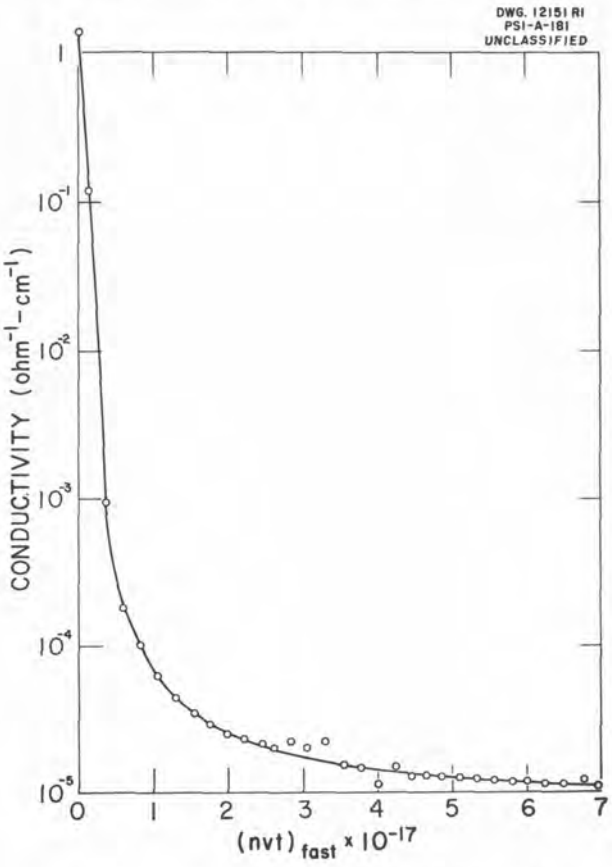

Fig. 2.1. Conductivity vs. Integrated Fast-Neutron Flux for N-Type Silicon at ~ 48°C.

by a factor of three than that reported previously for N-type silicon[3]. The earlier result was obtained on a low-resistivity N-type sample (ρ = .0037 ohm^{-1}-cm^{-1}) which was bombarded in a different position in the pile at 47°C. The large difference in initial slope may be due to one or a combination of the following factors: (1) The slope may be dependent on the carrier concentration which is quite different for the two cases, and (2) the relative values of the fast flux in the two positions are not known more accurately than 50%.

A large number of log conductivity vs. $1/T$ curves were obtained as the samples cooled and heated during pile shutdowns and startups. These curves gave good straight lines and the slopes corresponded to a trap depth of .5 ± .1 ev. Although too much emphasis should not be placed on the slope of these curves over such a short temperature range (in this case about 20°C), it is interesting that the energy value so obtained is about one-half the forbidden gap width of silicon and is thus in agreement with the fact that the saturation conductivity occurs at approximately the intrinsic conductivity. More extensive measurements of this nature are being planned in order to obtain a better idea of the depth of traps as well as their energy distribution introduced by bombardment into both P-type and N-type silicon.

AN AUTOMATIC MULTIRANGE RECORDING DEVICE FOR MEASURING VARYING POTENTIALS

J. C. Pigg

In measurements of the changing electrical properties of semiconductors during neutron bombardment

[3] J. W. Cleland, J. H. Crawford, Jr., K. Lark-Horovitz, and J. C. Pigg, "Silicon Bombardment Experiments," ORNL-1095, *op. cit.*, p. 35.

in the nuclear reactor, it is desirable to use automatic recording methods whenever possible. A device has been constructed and is currently being used which fulfills the requirements of the semiconductors under consideration. The components are (1) a 0 to 3 mv, 12-point Brown Electronik Recorder with a four-pole 12-position selector switch ganged to the Brown input selector switch; (2) a system of limit switches which activate appropriate stepping relays for automatic circuit changed; (3) a system of scale indication; (4) a Vibrating Reed Electrometer for high-resistance measurements, and (5) constant current, constant voltage, and variable power supplies.

By means of the limit switches and relays, proper scale and circuit changes can be made to keep the data within the range of the recorder and provide a linear plot for changes up to 12 orders of magnitude.

Each major component is connected to a needle plug terminal board so that any circuit within the range of the available components can be readily employed.

By means of the selector switch ganged with the recorder input switch the external circuit can be changed for each point.

Standard modifications and components are used throughout. A complete report in the form of an instruction manual for the instrument will be published in the near future.

CRYOSTAT FOR PILE IRRADIATION

R. P. Metcalf and J. T. Howe

The cooling jacket and shielding have been installed in hole 52 of the X reactor and the cold case assembly of the helium refrigeration system was relocated for use with the cryostat while in the pile. A panel board for permanent location of controls and instruments was drawn up and installation was requested.

Detection of corrosion in the silver-to-aluminum joint of a helium line to the cryostat required redesign of the joint. Drawings are in the shop, and it is hoped that all work will be completed in time for in-pile operation of the cryostat during the latter part of the next quarter.

LITHIUM-IRON CYCLOTRON BOMBARDMENT

North American Aviation, Inc.
W. W. Parkinson

To provide information about the behavior of structural materials under irradiation while in contact with liquid metals, bombardments of iron in contact with molten lithium are being carried out in the Berkeley 60-in. cyclotron. Since the original equipment could not be made to operate satisfactorily about 900°C (1652°F), it was necessary to develop a new iron specimen capsule to be bombarded in a different type of high-temperature target box. Photographs of this capsule were presented in the previous quarterly progress report,[4] and the arrangement of the capsule, with its heater, in the target box is shown in Figs. 2.2 and 2.3. With this apparatus, three capsules, in addition to the three reported earlier, have been irradiated with the direct 36-Mev alpha-particle beam.

Before assembly of the capsules for irradiation the specimen plate which made up the face of one end of

[4] North American Aviation, Inc. and W. W. Parkinson, "Lithium-Iron Cyclotron Bombardment," ORNL-1095, p. 61 ff.

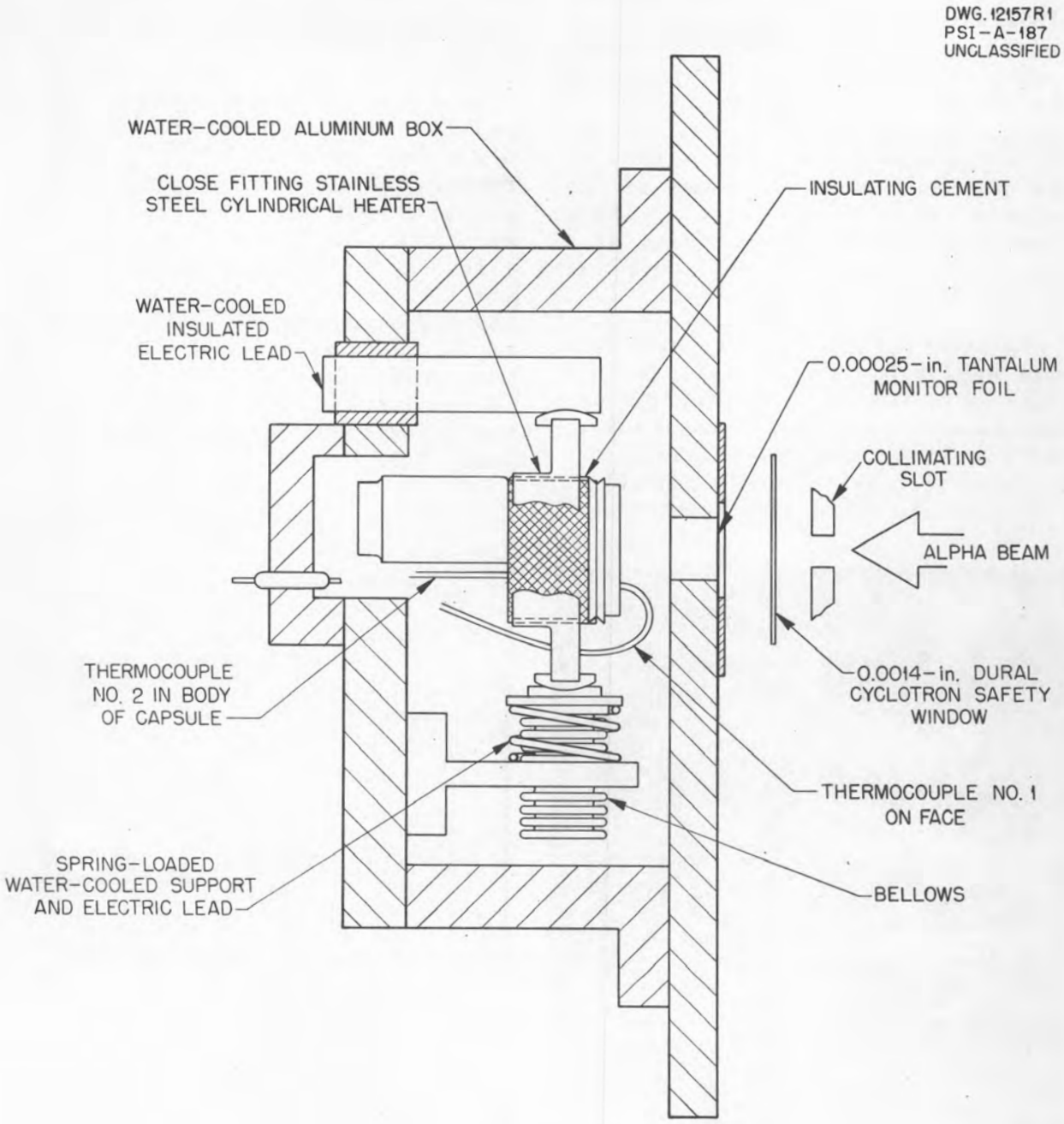

Fig. 2.2. New Iron Specimen Capsule and Target Box.

the capsule was tested as follows: (1) The plate was annealed, then polished and etched for a few seconds in "nital" solution; (2) the hardness was measured both inside and outside the area to be bombarded; and (3) these zones were photomicrographed. The capsules were assembled and filled with lithium as described in the earlier report. An area 0.608 x 0.250 in. on the face of each capsule was bombarded under conditions listed in

Table 2.2. The mean energy of the alpha particles incident on the capsules was 36.6 Mev with an uncertainty of about 1 Mev, depending on the tuning and other conditions of the cyclotron. The temperature tabulated is that of the thin face at the bombarded area; the body of the capsule ran 5 to 15° higher. There were occasional fluctuations of a few seconds duration 10° above and 20° below these temperatures.

In order to provide corrosion data more applicable to our samples than those obtained at other sites where temperature gradients, exposure times, and container shapes differed, two capsules were heated under conditions comparable to those of a bombardment.

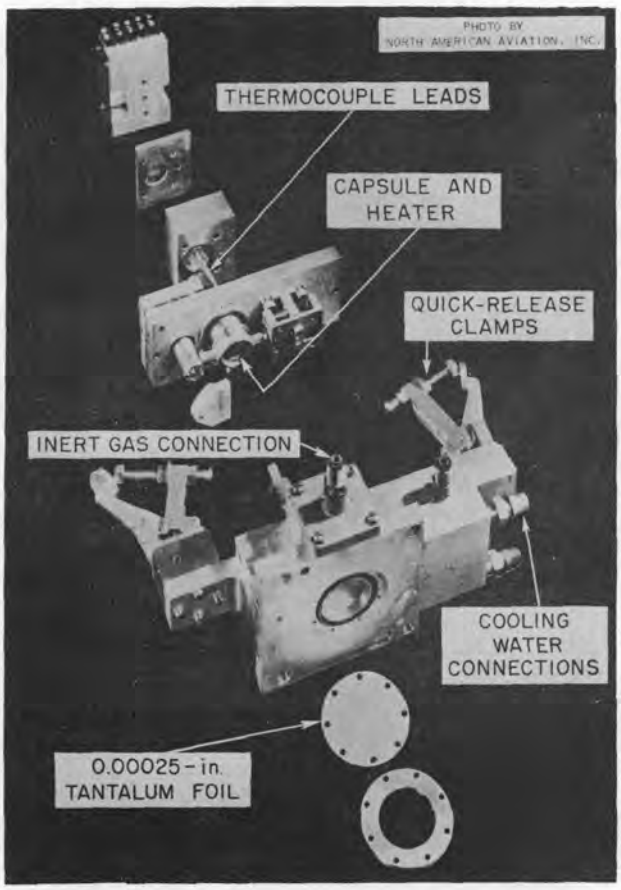

Fig. 2.3. New Iron Specimen Capsule and Target Box.

The treatment of these capsules is also recorded in Table 2.2.

None of the capsules have been opened for examination after irradiation. The capsules irradiated as described previously[4] have been opened; the lithium charges have been analyzed and their activities have been measured. This work for the first capsule irradiated, along with the X-ray-diffraction measurements, the photomicrographs, and the analysis of the iron, was reported in the last quarterly report.[4] The results for the later capsules, together with those for the first, are recorded in Table 2.3.

To continue the examination of the first capsule, the microhardness was measured to have an average value of 89.5 Knoop hardness numbers in the irradiated zone and 89.3 in the unirradiated zone, compared with an average of 106.5 over the whole surface before bombardment. A survey of grain size was made at 39 points over the surface of this specimen to ascertain the limits of the region in which grain growth had occurred. This region was found to be roughly confined to the irradiated area. Measurements on the photomicrographs of the unirradiated area of the specimen show that the grain size of this area changed very little during irradiation.

Photomicrographs of the cross-section of this specimen (between backing strips of other metal) were made of the irradiated and unirradiated zones. These photomicrographs (Figs. 2.4 - 2.6) show that in some of the grains, apparently distributed at random through the irradiated zone, a change in the internal structure has taken place. No conclusions have been drawn yet as to the nature or cause of this change.

TABLE 2.2

Capsule Irradiation Conditions

RUN NO.	TEMPERATURE (°C)	TIME AT TEMPERATURE (hr)	EXPOSURE (μa-hr)	REMARKS
4	625	18.0	35.0	
5	625	48.0	20.0	Control bombardment without lithium in capsule; long period required to obtain exposure.
6	915	4.7	10.3	Heater circuit opened; capsule developed leak and lithium ignited when heater was inspected.
Control	906	5.7	None	Check on corrosion without irradiation.
Control	625	17.2	None	Check on corrosion without irradiation.

TABLE 2.3

Results of Capsule Irradiations

RUN NO.	TEMPERATURE (°C)	TIME AT TEMPERATURE (hr)	EXPOSURE (μa-hr)	IRON IN Li CHARGE[a] (%)	RADIOACTIVITY OF CHARGE[b] (counts/min)
1	625	9.0	25.1	0.008	2
2	910	6.2	13.6	0.23[c]	2700[c]
3	675	17.3	3.8	0.004 to 0.006	2
Control	906	5.7	None	0.004 to 0.006	None

[a] Surface-to-volume ratio for all except run 2 was 5.1 cm^2/cm^3 and 1.24 g of lithium in each capsule.

[b] Activity was measured on step 1 of a Berkely Scaler, Model Decimal 2000.

[c] During run 2 a leak developed in the capsule, allowing the lithium charge and the interior of the capsule to be exposed to the helium atmosphere of the target box. Lithium escaped to reduce the charge to 0.87 g, making the surface-to-volume ratio 5.5 cm^2/cm^3. The run was terminated when the tantalum window closing the target box ruptured and exposed the hot capsule to air. The oxidized condition of the exterior of the capsule may have allowed iron oxide to flake off into the charge during its removal for analysis.

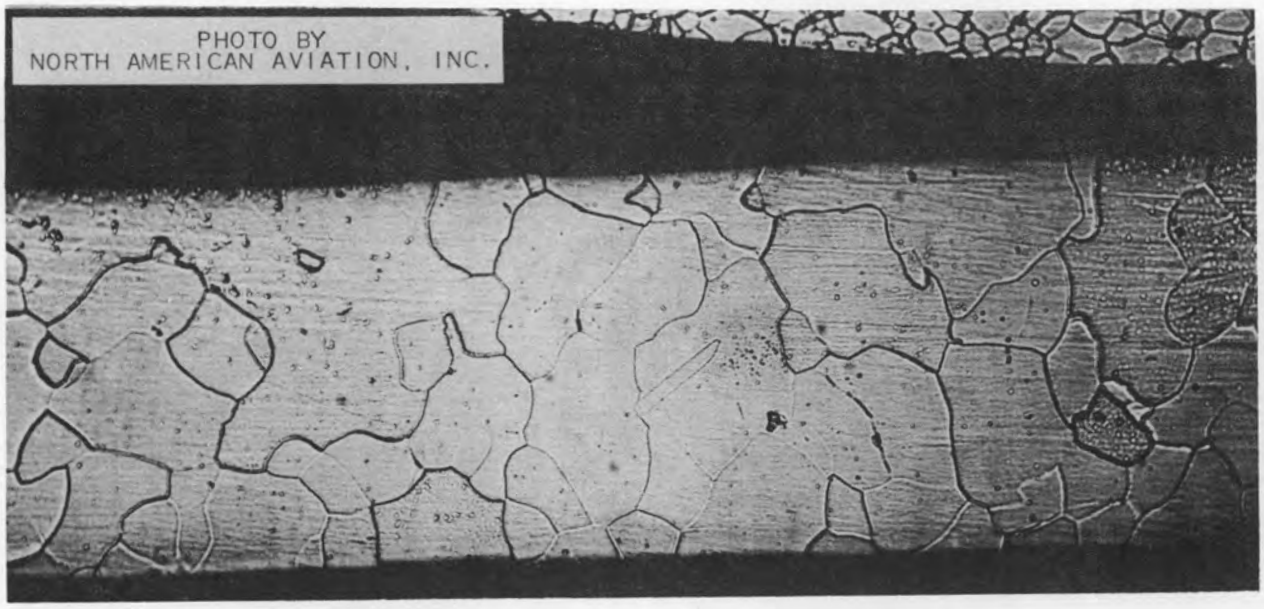

Fig. 2.4. Cross-Section of Iron Specimen from Irradiation No. 1. 3% Nital etch; 250X.

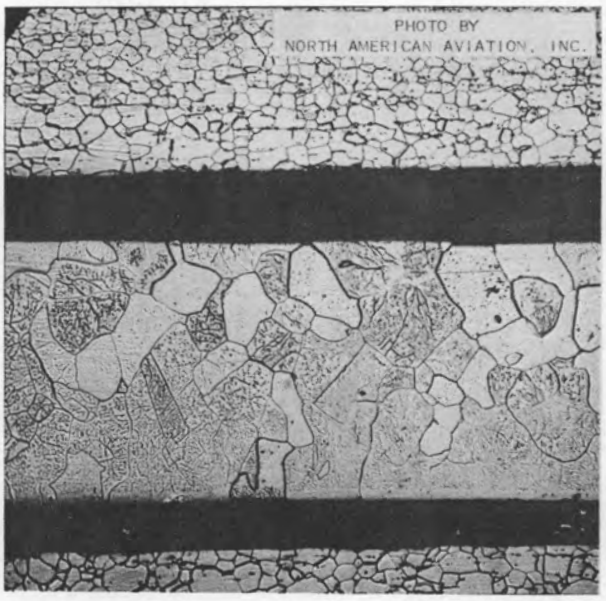

Fig. 2.5. Cross-Section of Iron Specimen from Irradiation No. 1. 3% Nital etch. Original photograph taken at 250X; reduced approximately 35% in reproduction.

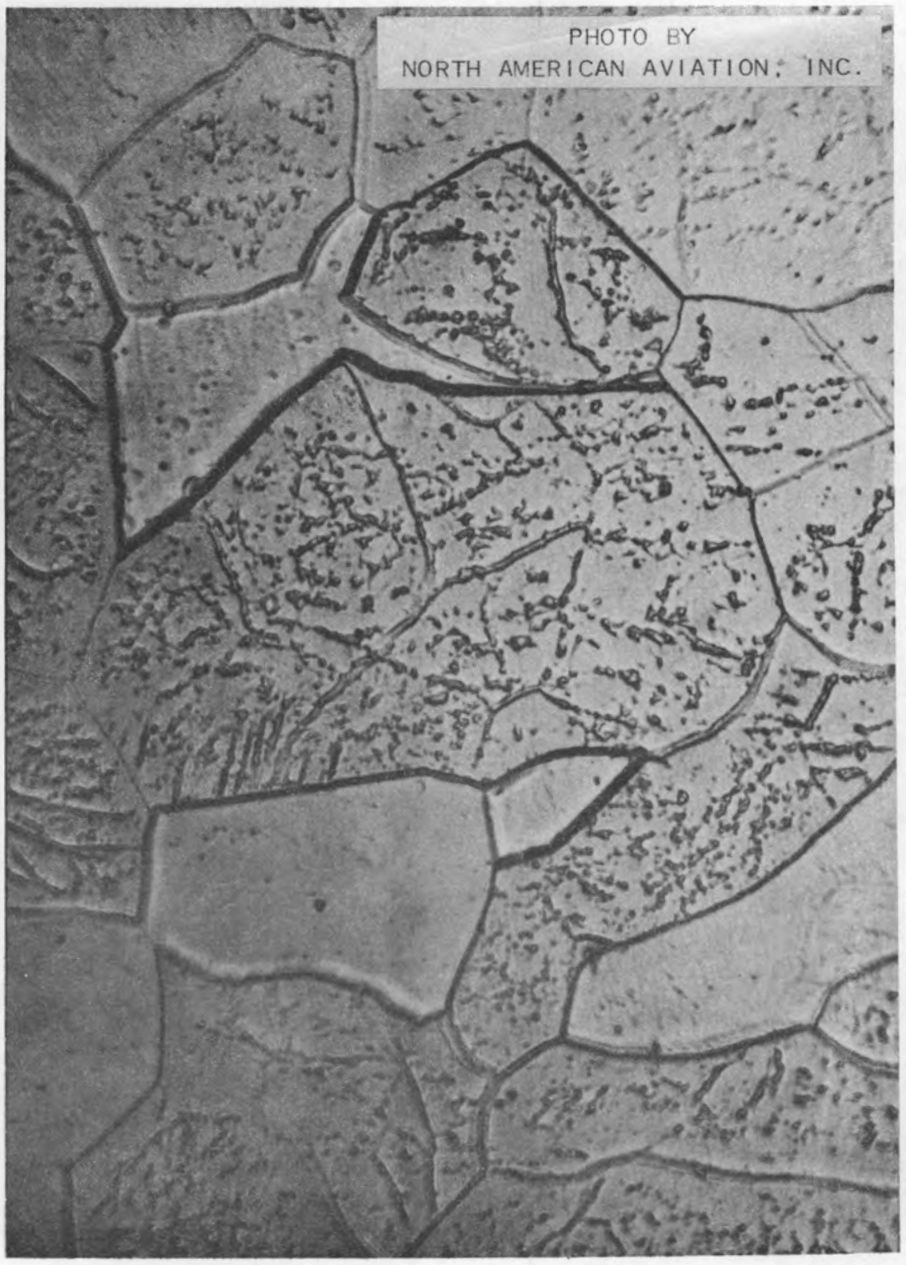

Fig. 2.6. Cross-Section of Iron Specimen from Irradiation No. 1. 3% Nital etch; 1000X.

3. RADIATION METALLURGY

NEUTRON IRRADIATION OF AGE HARDENING ALLOYS

W. E. Taylor G. T. Murray
F. M. Blacksher

Evidence of pre-precipitation or precipitation in a solution-annealed Cu-Be alloy due to neutron bombardment was presented in the last progress report.[1] The term "irradiation aging" was introduced to describe this phenomenon. The basis for the precipitation or pre-precipitation hypothesis was the similarity between irradiation aging and low-temperature thermal aging. During the past quarter data have been obtained which lend additional support to a pre-precipitation hypothesis.

Previously reported data[1] on the comparison of low-temperature thermal aging to irradiation aging suggested the possibility that the effect of irradiation was similar to thermal aging at 75°C. Consequently, a solution-annealed Cu-Be electrical resistance specimen was thermally aged at 75°C, and the change in resistance was compared (Fig. 3.1) with the change obtained from the in-pile experiment previously reported. The 75°C thermally aged curve does bear a striking resemblance to the irradiation-aged curve.

If the irradiation effect is a nucleation or precipitation process the question arises as to what condition the material will attain if it is irradiated until no appreciable rate of change is observed. If the rate of growth is not affected much the material should reach a pseudo-equilibrium when the supersaturated solid solution becomes so depleted in beryllium that nuclei cannot form, or when some type of equilibrium is created between the formation and disruption of nuclei by irradiation.

Such a condition would be evidenced by a saturation value of the resistance. The irradiation curves are being extended in an effort to determine if saturation occurs. It appears as though an extremely long time of exposure will be required for the irradiation aging to attain such an equilibrium at the flux rates now available.

Precipitation in Cu-Be alloys occurs predominantly at the grain boundaries during the early stages of thermal aging, so a grain boundary effect might occur during irradiation-aging specimens. Single crystal solution-annealed electrical resistance specimens were irradiation aged and thermally aged. The comparison of the single crystal and polycrystalline crystal aging curves is shown in Fig. 3.2. The single crystal specimen appears to age thermally at a much slower rate than the polycrystalline specimen. This slower rate is to be expected due to the absence of grain boundary precipitation and somewhat less to the lower beryllium content (1.8% Be by weight) of the single crystal specimen compared to the polycrystalline specimen (2.2% Be by weight). However, the change in resistance during irradiation of the solution-annealed single crystal specimen was of the same order of magnitude as that obtained during irradiation of a solution-annealed polycrystalline specimen for comparable exposures. This is indicated

[1] W. E. Taylor, G. T. Murray, and F. M. Blacksher, "Radiation Effects in Supersaturated Solid Solutions," *Physics of Solids Institute Quarterly Progress Report for Period Ending April 30, 1951*, ORNL-1095, p. 51 (to be issued).

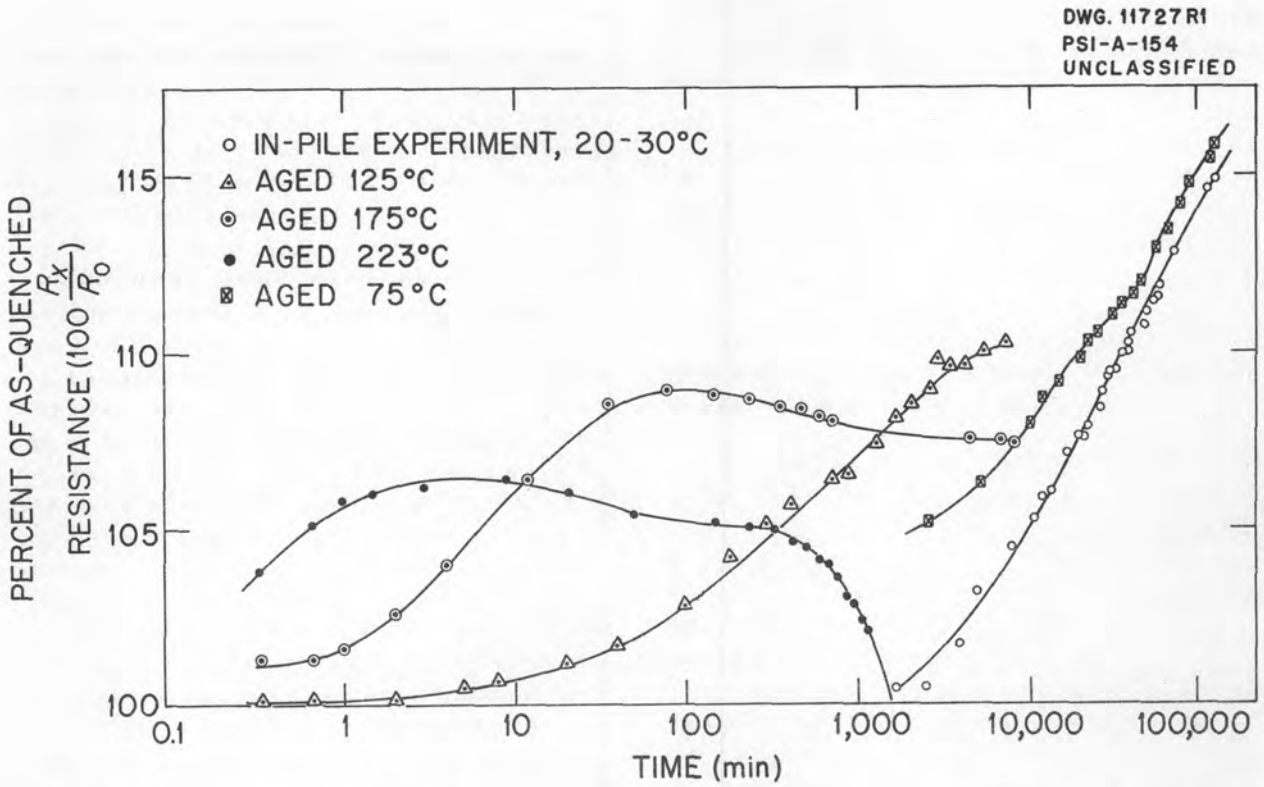

Fig. 3.1. Comparison of Resistance Changes of Solution-Quenched Cu-Be During Thermal Aging and During Neutron Exposure.

in Fig. 3.2. Thus irradiation aging does not involve any grain boundary effect. Also the comparison of irradiation aging and low-temperature thermal aging now will show a similarity at a much higher thermal-aging temperature (in the neighborhood of 125 to 175°C) if single crystals are used in both instances. An attempt will be made to determine this temperature.

It was found that irradiation of a solution-annealed polycrystalline specimen considerably altered the subsequent rate of precipitation. The aging behavior at 325°C of an irradiated and a nonirradiated specimen is compared in Fig. 3.3. The increase in electrical resistance due to irradiation recovers almost completely

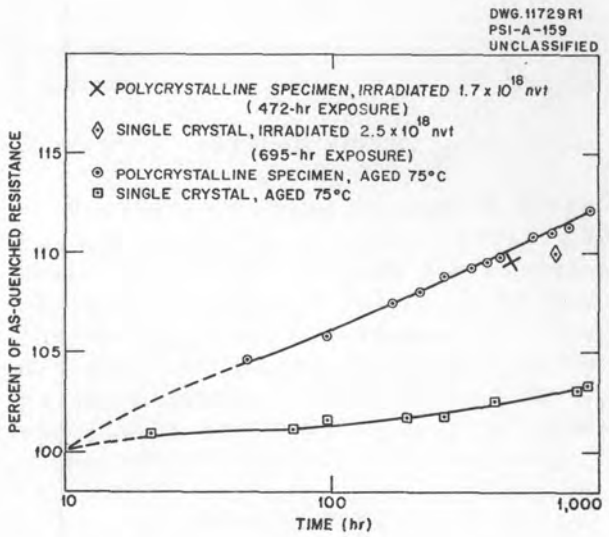

Fig. 3.2. Comparison of Aging of Single Crystal and Polycrystalline Cu-Be Specimens.

after 20 sec at this temperature. On further aging the precipitation process in the irradiated specimen appears to be advanced compared to the standard. This can be explained on the basis of the formation of nuclei during irradiation. The rapid recovery will occur if some of these nuclei are redissolved while the advanced aging can be attributed to the growth of the nuclei which are not redissolved. Similar retrogression phenomena would be expected to occur if nuclei formed at low temperatures were subjected to higher temperatures. The results of such an experiment are shown in Fig. 3.4. The specimen which was pre-aged at 125°C exhibits a resolution of nuclei and an advanced aging process at 325°C compared to the standard. This behavior is similar to that exhibited by the irradiated specimen. This correspondence again suggests a similarity between irradiation aging and low-temperature thermal aging.

Although in most respects the radiation effects in Cu-Be are analogous to nucleation, the shift

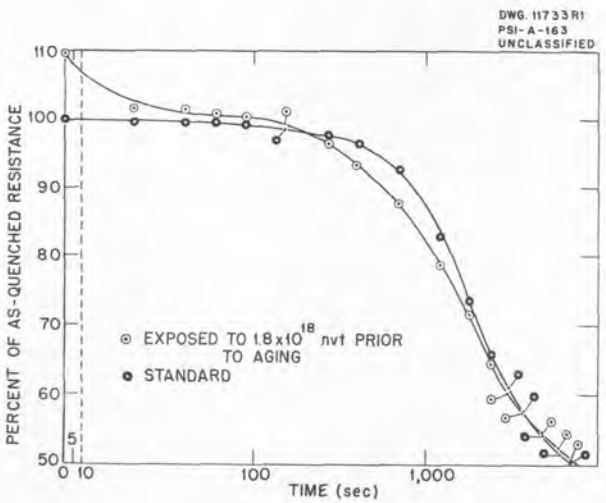

Fig. 3.3. Effect of Neutron Irradiation on Subsequent Aging of Cu-Be Specimens at 325°C.

of the X-ray line suggests that perhaps clusters rich in beryllium are being broken up by the irradiation. There are thus two possible mechanisms:

1. Disruption of clusters rich in beryllium which would lead to greater dispersion of beryllium atoms with a consequent reduction in lattice parameter, increase in resistance and hardness, etc. The effect on subsequent aging could be explained by increased rates of diffusion due to the presence of interstitials and vacancies in the lattice.

2. Formation of clusters rich in beryllium which would act as nuclei. By comparison with the effects of nucleation during thermal aging the radiation effects can be explained. This mechanism apparently gives no explanation for the radiation-induced line shift.

Thermal aging of samples during irradiation offers a possible means of distinguishing between those effects. If mechanism (1) occurs, the early stages of aging should be retarded. If mechanism (2) occurs, the early stages of aging should be accelerated.

In the preliminary test the effect of radiation on the rate of precipitation, as measured by changes in resistance, was determined by aging two specimens at 250°C; one was aged in the presence of radiation (fast-neutron flux = 10^{10} nvt), the other without radiation. Resistance was measured at the aging temperature for both specimens. The curves obtained are shown in Fig. 3.5. The specimen which was aged in the presence of radiation aged much faster during the early stages and

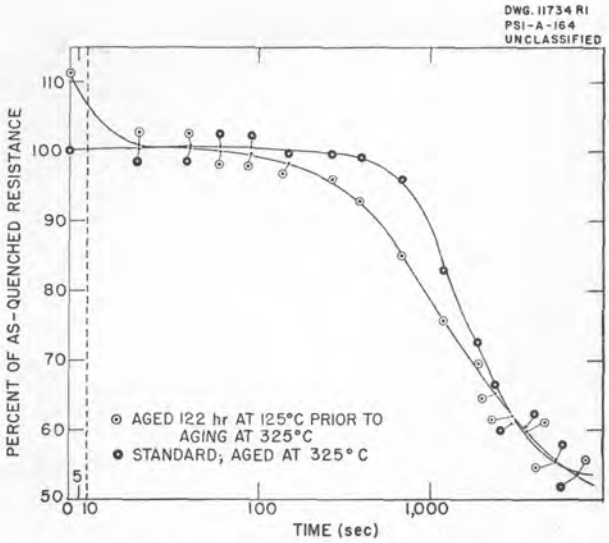

Fig. 3.4. Effect of Low-Temperature Aging on Subsequent Aging of Cu-Be Specimens at a Higher Temperature.

slower during the later stages than the unirradiated specimen. This effect can be explained on the basis that radiation primarily affects the rate of nucleation and has little if any effect on the rate of growth. An increase in the nucleation rate will speed up the early stage of aging and therefore the later stage must be slowed somewhat in comparison to the nonirradiated specimen as a result of the decrease in the beryllium concentration of the matrix. Additional experiments at different temperatures and fluxes are required to confirm this explanation.

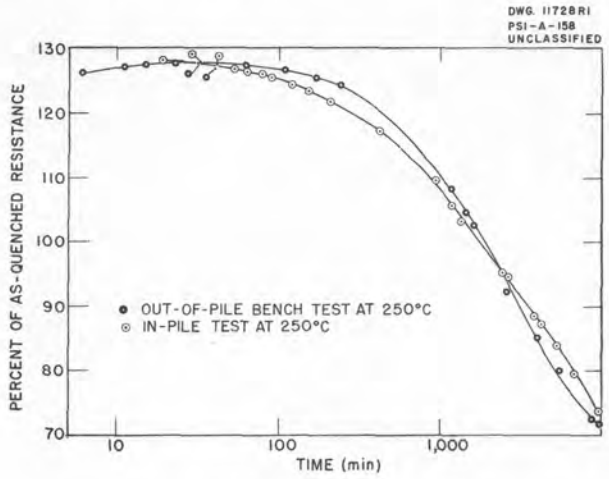

Fig. 3.5. Effect of Radiation on Rate of Precipitation in Cu-Be Specimens as Measured by Changes in Resistance.

The anomalous line shift of the Cu-Be (331) line due to irradiation[1] was investigated further. A single phase alloy (1.8% Be) was made and specimens were irradiated in an effort to exclude the excess beryllium as a variable. The line shift of such specimens due to irradiation was of the same order of magnitude as that obtained from irradiated specimens containing beryllium in excess of that for complete solid solubility.

The possibility was considered of relating the line shift to a contraction of the lattice caused by the strains created around the nuclei. However, no such shift has been detected in specimens aged thermally for 120 hr at 125°C.

The changes due to irradiation of solution-annealed Cu-Ti alloys previously reported[1] indicated that the behavior of Cu-Ti during irradiation was similar to the behavior of copper-base simple solid-solution alloys. It may therefore be concluded that Cu-Ti does not irradiation age. The effect of radiation on subsequent aging has been investigated and has been found to be very different from that of Cu-Be specimens. Aging curves determined by electrical resistance measurements for aging at 300 and 350°C are shown in Figs. 3.6 and 3.7. The standard specimen appears to age much faster than the irradiated specimen. This phenomenon is being investigated further.

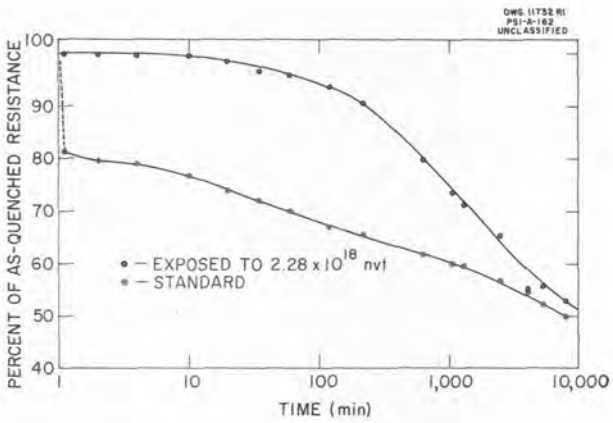

Fig. 3.6. Effect of Neutron Irradiation on Subsequent Aging of Cu-Ti Specimens at 300°C.

Electrical resistance specimens of a Ag-Cu alloy were exposed in the solution-annealed condition to a flux of 2.2×10^{18} nvt. No change in the electrical resistance could be measured. A Ag-Cu specimen was aged thermally at 75°C for the same period of time that the others were irradiated. No change in resistance could be detected. Thus, it appears that Ag-Cu will not irradiation age.

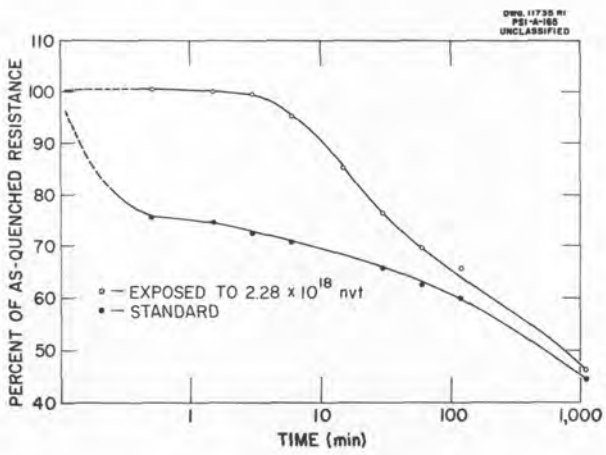

Fig. 3.7. Effect of Neutron Irradiation on Subsequent Aging of Cu-Ti Specimens at 350°C.

The effect of irradiation in Cu-Be alloy may be characteristic of the beryllium atom. To investigate this possibility, specimens of a solution-quenched Ni-Be alloy (approximately 2% Be by weight) were exposed to a flux of 8.0×10^{17} nvt. No change in resistance could be measured. The hardness increased 13 DPH numbers. The increase in hardness is of the same order of magnitude as that measured for copper-base simple solid-solution alloys. The effect of irradiation on nickel-base simple solid-solutions is not known. A Ni-Be electrical resistance specimen was aged thermally at 75°C for the same length of time that the others were exposed to radiation. No change in resistance could be measured. This result indicates that in contrast to the behavior of Cu-Be specimens, Ni-Be does not age at low temperatures.

From the results for the Ni-Be alloy it may be concluded that (1) Ni-Be does not irradiation age, and (2) the effect of irradiation in Cu-Be is not characteristic of the beryllium atom.

EFFECT OF PRECIPITATE PARTICLES ON RESISTIVITY OF Cu-Be ALLOYS

W. E. Taylor and J. S. Koehler*

Investigation of the effect of radiation on solution-quenched Cu-Be age-hardening alloys indicates a characteristic increase in resistance which is much greater than radiation-induced changes in other copper alloys.[2] A similar large resistance increase is observed when this alloy is aged at low temperatures. Other

*Consultant from University of Illinois.

[2] W. E. Taylor, G. T. Murray, and F. M. Blacksher, "Annealing of Radiation Hardening of Copper and Copper Alloys," ORNL-1095, *op. cit.*, p. 45.

radiation effects in this alloy are also similar to those brought about by aging. It is therefore of interest to investigate the nature of such resistance increases in order to understand radiation effects in this material and possibly others of a similar nature, i.e., supersaturated solid solutions.

As an explanation of the resistance changes observed during aging, Mott[3] has suggested that interference of scattered electron waves can occur when the precipitate particles are nearly the dimensions of the electron wave. The electron wave length is given by

$$\lambda = \frac{h}{\sqrt{2mE_0}} , \qquad (1)$$

where

h = Planck's constant,

m = mass of the electron,

E_0 = height of the Fermi level above the bottom of the conduction band.

Using the value of E_0 = 7.04 ev,[4] we obtain for the wave length of the conduction electrons in copper, $\lambda = 4.6 \times 10^{-8}$ cm. This value, or even two or three multiples, is much too small to consider as the dimension of a spherically shaped precipitate nucleus. Precipitate nuclei in the form of platelets might conceivably be a few multiples of this value in their small dimension.

An attempt is being made to estimate theoretically the effect of such nuclei based on the model shown in Fig. 3.8*a*. Assuming that the valence electrons are loosely bound, the excess positive charge on the beryllium ion would lead to a depression of the potential in any region containing a high concentration of beryllium. As a first approximation a square potential well is assumed which is just deep enough to trap the extra valence electrons associated with the beryllium ions. These trapped electrons will penetrate a small distance into the region outside of the well as a result of the tunnel effect (Fig. 3.8*b*). The positive and negative charges will therefore not be exactly balanced at any given point, and a double-charged layer at each edge of the potential well will result (Fig. 3.8*c*). This charge distribution will be calculated, and the resulting scattering potential will be determined.

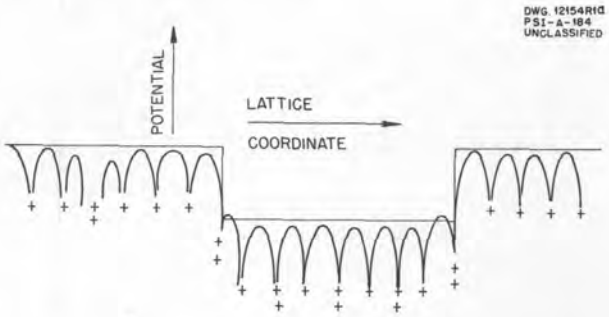

Fig. 3.8*a*. Potential Due to Ionic Charge.

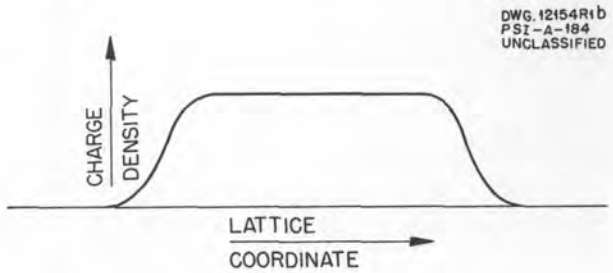

Fig. 3.8*b*. Charge Density Due to Trapped Electrons.

[3] N. F. Mott, "Discussion of a Paper by Gaylor," *J. Inst. Metals* 60, 267 (1937).

[4] F. Seitz, *Modern Theory of Solids*, McGraw-Hill, New York, p. 146, 1940.

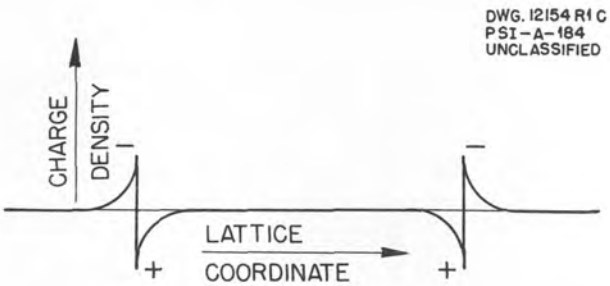

Fig. 3.8*c*. Resultant Charge Distribution.

To calculate the potential in and around the precipitate nucleus we will assume the formation of a square platelet (Fig. 3.9*a*) which is coherent with the surrounding matrix lattice. We will further assume:

1. The platelet is of the Cu-Be composition which is also its composition when it becomes a macroscopic size.

2. The electron density within the platelet is 1.5 per atom, corresponding to a valence of +1 for copper and +2 for beryllium.

3. The electron density in the surrounding matrix is 1.1 per atom.

4. The perturbed potential due to the ionic charge is a square potential well (Fig. 3.9*b*) having the dimensions

$$V_p = -D$$

$$\left\{ -\frac{t}{2} < Z < \frac{t}{2} \right.$$

$$\left. \text{and } -\frac{d}{2} < x,\ y < \frac{d}{2} \right\}. \quad (2)$$

5. The excess electrons are trapped in discrete energy levels in the potential well to a height D, i.e., the potential well is completely filled. The problem then is to calculate D of a correct value to just trap the excess 0.4 electrons per atom for any given size of platelet.

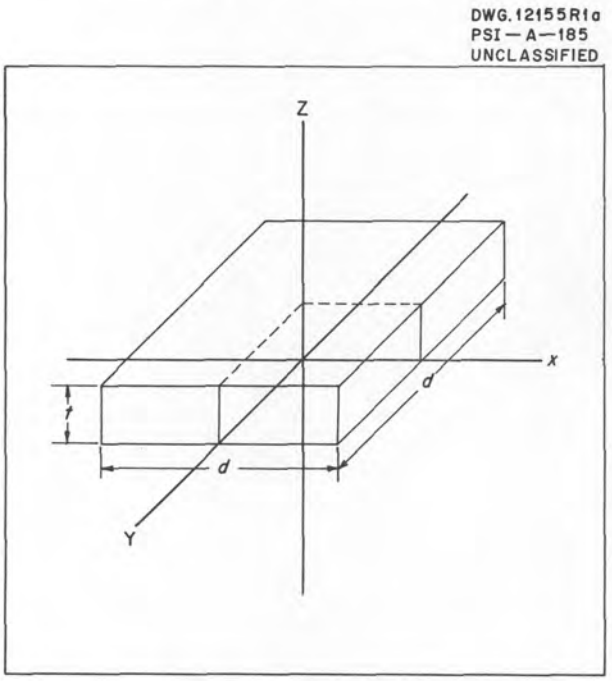

Fig. 3.9*a*. Shape Assumed for Platelet.

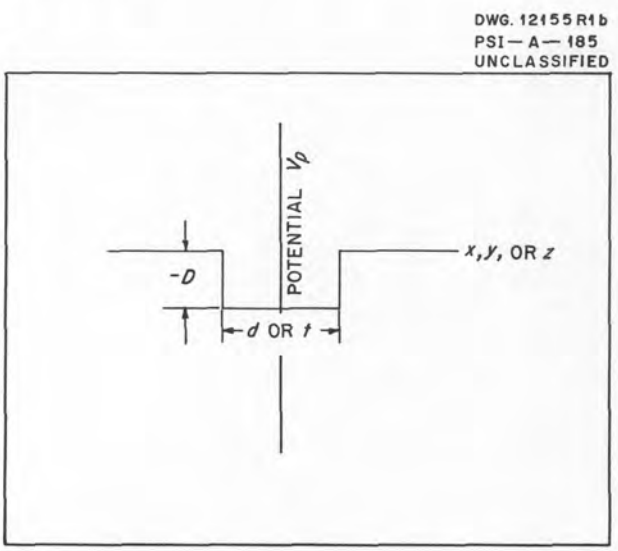

Fig. 3.9*b*. Potential Well Assumed for Ionic Perturbation.

The number of atoms in the platelet is given by

$$N_a = \frac{d^2 t}{\frac{4}{3}\pi r_0^{\,3}} , \qquad (3)$$

where r_0 is the distance between atoms. The excess of electrons in the platelet is given by

$$N_e = (1.5 - 1.1)N_a$$

or

$$N_e = \frac{2.4 d^2 t}{8\pi r_0^{\,3}} . \qquad (4)$$

Equation (4) may be rewritten as

$$N_e = \frac{2.4 R^2 P^3}{8\pi} , \qquad (4a)$$

where $R = d/t$ and $P = t/r_0$, the thickness expressed in atomic distances.

The energy difference between any trapped electron and the bottom of the potential well is

$$E = \frac{h^2 k^2}{2m} = \frac{h^2}{8m}\left(\frac{n_x^{\,2} + n_y^{\,2}}{d^2} + \frac{n_z^{\,2}}{t^2}\right), \qquad (5)$$

where k is the wave vector, and the n's are the number of nodes in the standing waves and, being of the nature of quantum numbers, are necessarily restricted to positive integers (1, 2, 3, ... N_i).

We must not determine $E = D$ such that there are $N_e/2$ levels with lower energy. We are primarily interested in the factor

$$\left[\frac{n_x^{\,2} + n_y^{\,2}}{d^2} + \frac{n_z^{\,2}}{t^2}\right] ,$$

so that Eq. (5) is better written in the form

$$\left[\frac{n_x^{\,2}}{R^2} + \frac{n_y^{\,2}}{R^2} + n_z^{\,2}\right] = \frac{8 m r_0^{\,2} E P^2}{h^2} . \qquad (5a)$$

The integers n may be considered to occupy a sphere in a space defined by n_x/R, n_y/R, and n_z (Fig. 3.10). Consider those points whose coordinants are $n_x = n_y/R$ and n_z with $n_i = 1, 2, \ldots$. This is a lattice defined in one octant by the translation $1/R$, $1/R$, and 1, each point corresponding to an energy level and dividing the lattice into unit cells of volume $1/R^2$. Now 1/8 of each point may be considered as belonging to the unit cell, and since there are eight corners in the cell, there will be one cell for each energy level. Thus R^2 times the volume of the octant will give the number of energy levels. The volume of this octant is

$$V = 1/8 \cdot \frac{4\pi}{3} \cdot \frac{a^2 b}{R^2} , \qquad (6)$$

where a is the largest value taken by n_x or n_y, and b is the largest value taken by n_z, so that the number of levels is

$$N_L = R^2 V = \frac{\pi a^2 b}{6} . \qquad (7)$$

Moreover we see from Fig. 3.10 that by virtue of our definition of coordinates

$$a = Rb , \qquad (8)$$

so that

$$N_L = \frac{\pi R^2 b^3}{6} . \qquad (9)$$

Since each level may be occupied by two electrons we have

$$N_L = \frac{N_e}{2} = \frac{R^2 b^3}{6} . \qquad (9a)$$

DWG.12153R1
PSI-A-183
UNCLASSIFIED

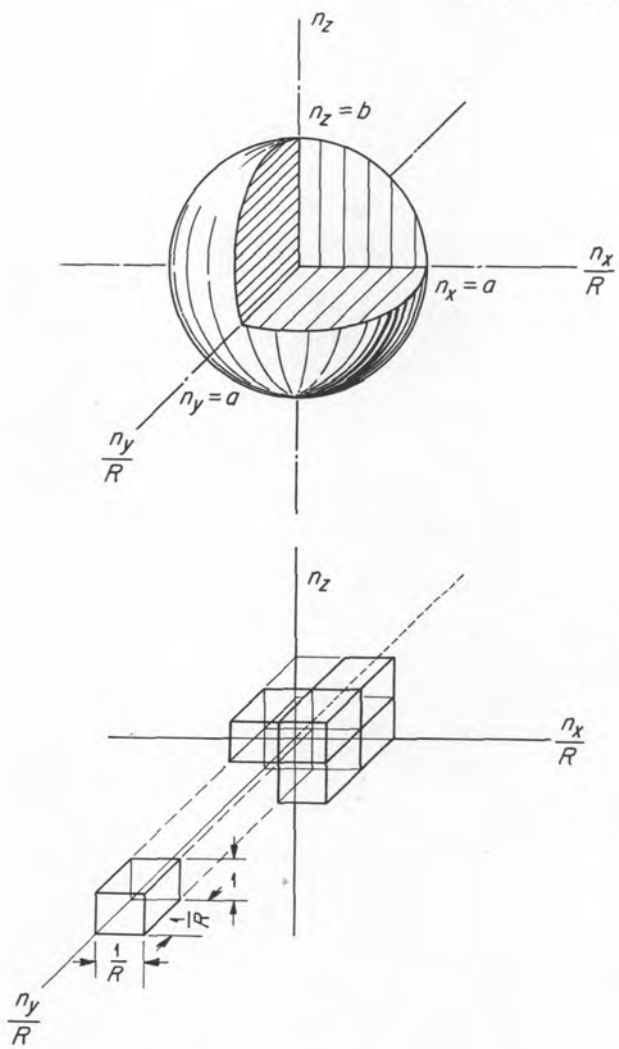

Fig. 3.10. Sphere and Cells Formed by $\frac{n_x}{R}$, $\frac{n_y}{R}$, and n_z.

Substituting from Eq. (4a), we have

$$\frac{2.4R^2P^3}{16} = \frac{R^2 b^3}{6} ; \qquad (10)$$

simplifying and solving for b, we have

$$b = \frac{P}{2}\left[\frac{7.2}{\pi^2}\right]^{1/3} . \qquad (11)$$

Now b is the value which n_z would have if n_x/R and n_y/R were zero (Fig. 3.10), so that Eq. (5a) for the highest energy levels becomes

$$\frac{P^2}{4}\left[\frac{7.2}{\pi^2}\right]^{2/3} = \frac{8mr_0{}^2EP^2}{h^2} . \qquad (12)$$

Solving for E, we have

$$E = \left[\frac{7.2}{\pi^2}\right]^{2/3} \cdot \frac{h^2}{32mr_0{}^2} , \qquad (13)$$

and substituting values, we have

$$D = E = 3.82 \times 10^{-12} \text{ ergs} = 2.39 \text{ ev.}$$

This potential will now be used to calculate the electronic charge around the platelet. Further results will be given in later reports.

RECOVERY OF RADIATION HARDENING IN COPPER-BASE SOLID-SOLUTION ALLOYS

W. E. Taylor G. T. Murray
F. M. Blacksher

Additional experiments have been made to investigate the recovery of

radiation hardening in copper alloys. Samples of Cu-Zn, Cu-Ge, Cu-Ga, and Cu-As containing 2 and 4 atom % alloy constituent were annealed 15 min at successively higher temperatures. The temperature intervals were 50°C starting at 200°C. More rapid recovery was again noted in the order zinc, gallium, germanium, and arsenic alloys. It was noted that considerable recovery of the arsenic alloys had occurred after 6 months at room temperature.

During the preparation of additional samples of these materials for radiation exposure it was found that of the above samples those previously used had not been sufficiently annealed to completely eliminate work hardening. New samples have been completely annealed and are being exposed in the reactor.

CREEP UNDER IRRADIATION

J. C. Wilson J. C. Zukas
R. A. Weeks W. W. Davis

Cantilever Creep. A set of three fairly reproducible cantilever creep tests of type 347 stainless steel has been completed in the X reactor at a fast flux of $\approx 4 \times 10^{10}$ n/cm^2-sec. Two of the three accompanying bench tests show good agreement with one another, but the third test differs markedly from the other two. Discounting the latter, it appears that bench and in-pile tests are virtually indistinguishable up to about 100 hr. Thereafter the specimens under bombardment creep faster so that they show approximately 10% greater total creep strain after 200 hr of operation and almost 20% more after 250 hr. Observations of creep rate immediately prior to, during, and subsequent to pile shutdowns after approximately 160 hr of bombardment show that there is a marked decrease in creep rate during this temporary absence of neutron flux. This substantiates the conclusions regarding total creep strain above.

The apparatus was a slightly modified version of one previously described;[5] all tests were run at 1500°F, and the maximum fiber stress was 1500 psi. A composite plot of the above tests appear in Fig. 3.11. The tests whose results appear as curves *A* and *B* were both charged during weekly 12-hr shutdowns and were creeping before the pile was started; test *C* was charged during a very short shutdown and was under bombardment before loading. It is suspected that a faulty strain gage (used to equalize the strain in all specimens, see below) may have permitted an excessive load to have been applied to the third bench test (curve *O*). In the lower right-hand corner of Fig. 3.11 the portions of curves *A* and *B* adjacent to the 160-hr shutdowns are reproduced in greater detail. Along each curve is the creep rate, relative to curve *A*, just preceding the shutdown. The rate values for curve *B* were determined from a manual plot of the data whereas those for curve *A* were determined directly from the chart record of microformer output voltage vs. time. The data during a 9-hr shutdown on curve *C* indicated a reduced rate, but insufficient points were obtained for a detailed plot. From the graphs it is patent that the creep rate decreased during pile shutdowns which occurred at the indicated points in the strain-time history of the specimen. Possibly the rate change can be associated with the influence of radiation on

[5] "In-Pile Creep," *Aircraft Nuclear Propulsion Project Quarterly Progress Report for Period Ending December 10, 1950*, ORNL-919, p. 225, esp. p. 227 (Feb. 26, 1951).

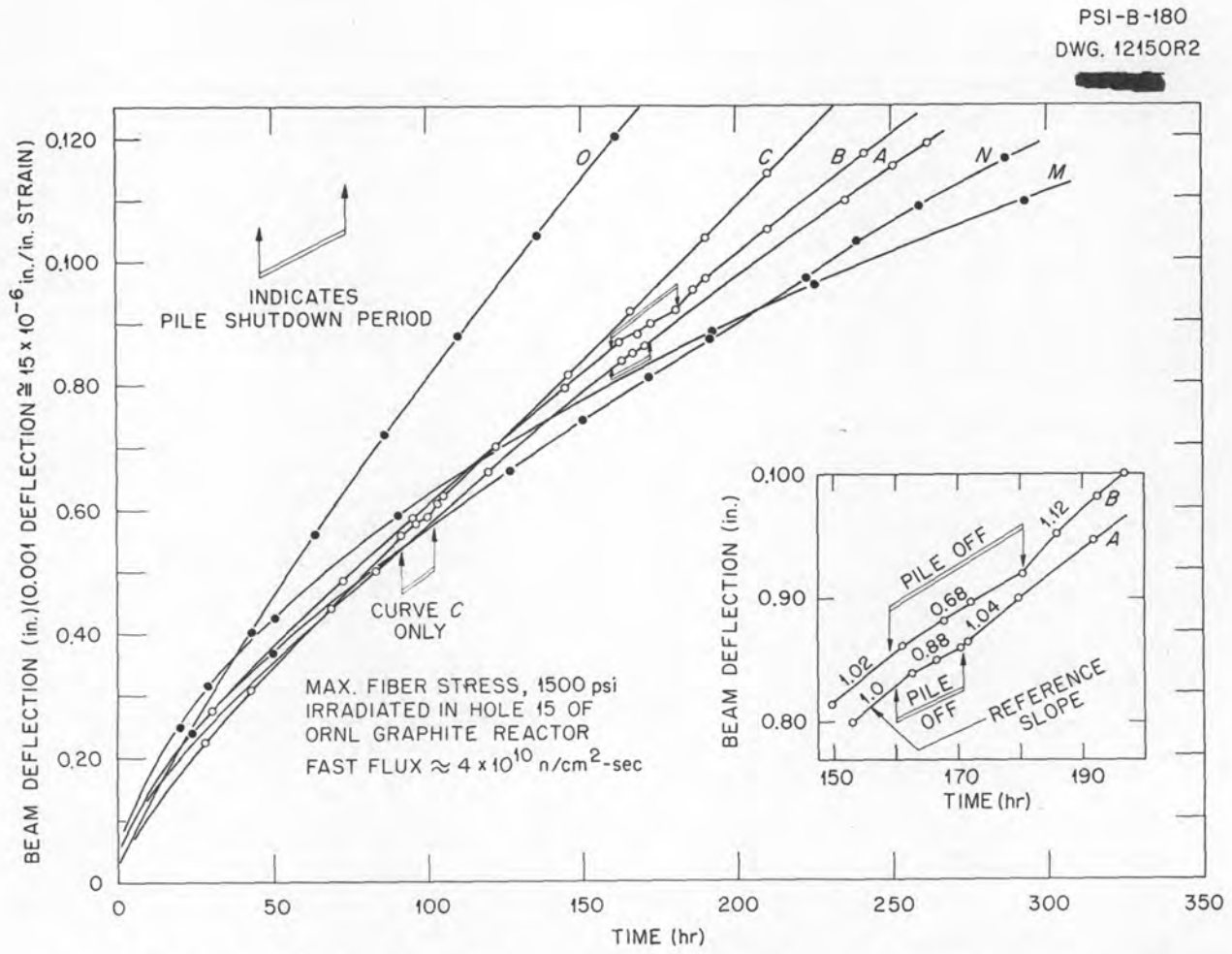

Fig. 3.11. Composite Plot of Three Bench and Three In-Pile Cantilever Creep Curves of Type 347 Stainless Steel Specimens at 1500°F.

the microformer, but the work of Cook and Johnson[6] indicates that there are no effects of sufficient magnitude to account for the differences noted here. The flux-dependent change in microformer output voltage reported earlier[7] is likewise too small to affect greatly the rate changes discussed above.

The earlier tests[7] differed from those reported here in that the stress was applied during heating to the operating temperature whereas the apparatus now used is loaded at will after the operating temperature has been reached. Also, some modifications, noted below, have improved the reliability of the data. The first test (Fig. 3.12) was run during irradiation on a specimen with no previous creep history; the second test (Fig. 3.13) had a creep history on the bench before irradiation in the pile. The first showed a linear strain-time relationship from about

[6] L. A. Cook and W. E. Johnson, "In-Pile Test of Microformer," *Proceedings of the Irradiation Damage Conference at Westinghouse Atomic Power Division, March 6-7, 1951*, TID-5021, p. 50.

[7] J. C. Wilson, J. C. Zukas, and W. W. Davis, "Creep Under Irradiation," ORNL-1095, *op. cit.*, p. 46.

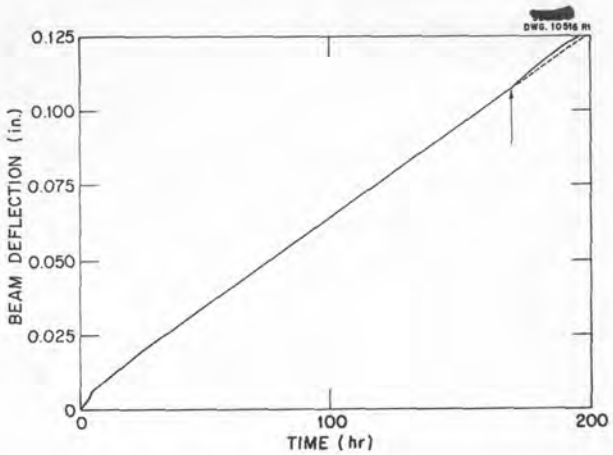

Fig. 3.12. In-Pile Cantilever Creep Test of Type 347 Stainless Steel at 1500°F; Maximum Stress, 1700 psi.

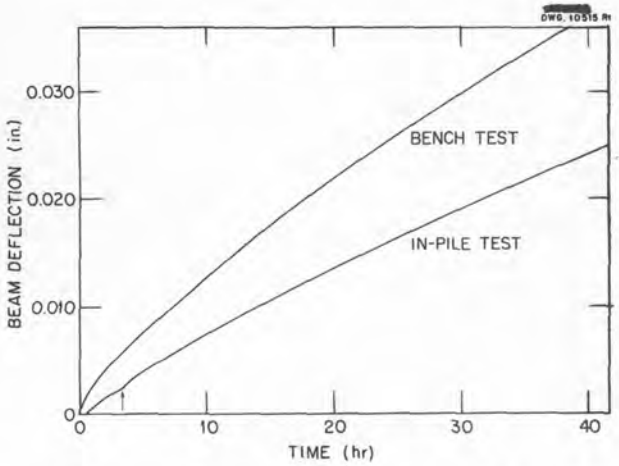

Fig. 3.13. In-Pile Cantilever Creep Test of Type 347 Stainless Steel at 1500°F; Maximum Stress, 1700 psi.

40 hr of operation until an extended shutdown at about 160 hr. In the same test a possible 3% rate increase was reported during the shutdown, and a transient increase in rate immediately after resumption of bombardment was observed. The present data indicate that the curves are not linear during the period from 40 to 160 hr, but the curvature is somewhat less than in the absence of radiation. Also the work during this quarter shows a marked decrease in rate during reactor shutdowns as opposed to slight increase for the earlier experiments. The increase in rate upon resumption of bombardment appears in both instances. The second of the earlier curves shows reduced creep following resumption of the creep test in the pile after 40 hr of bench testing. This result is not necessarily contrary to the present findings since the reduction in creep reported was early in the creep history during which period no conclusions are drawn in the present instance.

In summary, under the present test conditions good evidence is found of an increase in creep strain after about 100 or more hours under neutron bombardment, and there are indications of no effect or diminished creep for shorter exposure times. In contrast to the above view, other workers in the field have reported apparently different results. Yockey *et al.*[8] have found only diminished creep of aluminum under cyclotron bombardment with 38-Mev alpha particles. It should be noted, however, that the creep rate during these tests was several thousand times greater than in the work reported here. In view of the well-known hardening of annealed materials under bombardment and the high rate of strain (several percent per hour) employed in the cyclotron, deformation could reasonably be expected to occur mainly by slip processes and a discrepancy between the results reported is not unreasonable. At the strain rates of the cantilever test (about 0.001%/hr) the present knowledge of the mode of deformation is insufficient to support conjectures on the effects of

[8] H. P. Yockey *et al.*, *Effect of Cyclotron Irradiation on Creep of Aluminum*, NAA-SR-121 (June 8, 1951).

bombardment. The single NEPA creep test at Hanford[9] showed a decrease in all stages; it was operated at a strain rate some 30 times greater than that of the cantilever tests.

Several modifications of the original apparatus have improved the reproducibility of the data. The aluminum-base plate supporting the specimen and the microformer has been replaced with one made of fired lavite because of suspected deformation in the aluminum member whose temperature may have been as high as 800°F during operation. It is believed that this substitution has been responsible for the generally lower creep deformation observed in the latest tests.

Specimen geometry, particularly in the region of the fillet at the supported end, should be the same in all specimens to obtain reproducible results. Since some variation existed in specimens received from the shop, an attempt was made to assure the same stress in all specimens by loading them all to the same elastic strain (cold). This was done by cementing 1/8 in. long SR-4 strain gages to each specimen on the gage length near the support end fillet.[10] To compensate for the weight of the loading beam, which contributes a sizeable fraction of the stress, a value of zero strain was found by taking the average of the strain gage readings with the specimen inverted and then righted. The loading weights on each beam were then adjusted to read the same strain (corresponding to 1500 psi) from zero on each individual specimen.

Temperature control of the apparatus exterior of the specimen (required because of variations of pile and cooling air temperatures and flow rate of the latter) has been improved by controlling separately the ambient of the high-temperature furnace and the temperature of the microformer itself.

In the revised form of the apparatus the loading beam and the stress-applying weight are restrained by a thin nichrome wire which may be fused at will to load the specimen at any desired time. This determines the origin of the strain-time curve accurately, whereas before, the origin was arbitrarily selected as the strain when the operating temperature had been reached. The output voltage of the microformer now actuates a suppressed zero pen recorder which is sufficiently sensitive to permit accurate strain rate measurements over a period of but a few hours.

Following several more confirmatory bench tests to check the above results, a series of irradiations in the LITR will be made. The apparatus will be further modified by reducing the weight of the unit as much as possible to minimize gamma heating. It is hoped that the microformer can be used, although gamma heating makes this questionable. The sliding wire type extensometer described in an earlier report[11] is sufficiently well developed to be substituted for the microformer without any great sacrifice in accuracy of measurement of total strain.

The ANP program requires information on creep and/or stress corrosion of possible constructional materials

---

(9) "Radiation Damage to Nonmetallic Reactor Materials," *NEPA Project Quarterly Progress Report for Period January 1 - March 31, 1951*, NEPA-1792, p. 91, esp. p. 93.

(10) Figure 9.3, ORNL-919, *op. cit.*, p. 228.

(11) J. C. Wilson, M. J. Feldman, J. C. Zukas, and W. W. Davis, "Creep Under Irradiation," *Physics of Solids Institute Quarterly Progress Report for Period Ending January 31, 1951*, ORNL-1025, p. 44, esp. p. 45 (July 17, 1951).

in contact with static or flowing liquid metals or compounds. To this end a tensile apparatus using a hollow tubular specimen with reduced section in the gage length has been designed to be loaded by direct stressing applied by a member extending outside the LITR. The interior of the specimen may be filled with any desired fluid. The first tests are planned for inconel specimens containing static liquid sodium at 1500°F. In view of the danger to the reactor should such an apparatus fail, extensive bench tests will be made under the same test conditions in the absence of radiation. All controllers, supporting frames, furnace forms, and specimen materials have been received. The specimens have been machined, and the hood in which the tests are to be carried out is being installed. The apparatus will test tubular specimens 0.100 in. i.d. with 0.040-in. walls reduced to 0.020 in. over a 1-in. gage length. In the bench rigs the loading weight will be hung on the bottom of the specimen, and the extension will be measured by a cathetometer or trial models of the extensometers of the projected in-pile rigs.

If the test is to be run with small total extensions (such as 0.2% maximum) the extensometer must be able to measure a range of about 0.002 in. to within 1%. The possibility of using microformers in the LITR is doubtful because of the gamma heating, and in the MTR it will be impossible to use them. A consideration of the problems involved in measuring such small displacement shows that high precision depends not only on the measuring device but also on the manner in which the strain indications are transmitted to it. It should be possible to take readings both during pile operations and shutdowns, and this, because of gamma heating, demands remarkable temperature control (better than about 1°C) of all metallic elements of the system whose length change would affect the results. Ideally, the extensometer should be in a temperature-controlled zone as near the specimen as possible. The possibilities of an air micrometer are being investigated for use in this application. Using a device such as described by Ribaud,[12] a reasonably linear range of measurement over about 0.003 in. with a sensitivity of about 1/4% has been obtained. The same apparatus is now being operated at higher temperatures to see if it can be used at the test temperature. In this case it will be possible to incorporate it in the apparatus adjacent to the specimen where temperature fluctuations are at a minimum.

Several Statham unbonded strain gages have been received for test. The smallest gage had a range of 0.003 in. and a high electrical output of full scale deflection (about 20 mv). Unfortunately these are not recommended for use above 200°F. The strain sensitive elements are 0.001 constantan wires stretched between sapphire pins. If calibration tests are satisfactory the unit will be irradiated and retested. Pre-irradiation tests await return of a Templin extensometer calibrator from the Bureau of Standards where its accuracy is being verified. A high-temperature short-duty cycle microformer (possibly cobalt core) small enough to fit in the hot zone is being considered. By overloading it by several thousand percent for very short periods when readings are being taken, it may be possible to make an instrument sufficiently sensitive and yet with a minimum of mass to be heated by the gamma flux. The

(12) "Micrometre Pneumatique Differential," *Mécanique* 306 (Oct. 1942).

feasibility of a capacitative extensometer comprising, with a small inductance, a tuned circuit whose resonant frequency is measured by loosely coupling it to a variable frequency voltage source outside the pile is being investigated. If no satisfactory extensometer is developed the test will probably be run without extensometers, and the total strain will be measured after irradiation.

Since tensile stressing of the specimens in the LITR will require a member to transmit the force from the experiment to the pile face, the design of an experimental hole facility to permit loading is complicated. The heat from the experiment and the gamma-ray heating will require cooling of the experimental thimble, so an experimental water-cooled plug has been designed for submission to the Experimental Review Committee. For its shielding the plug will depend on a liner which completely fills the hole; the inside of the liner will be filled with water which has passed and cooled the experimental apparatus. Present calculations by J. B. Trice indicate that this will give adequate neutron shielding and, with the addition of a lead plug 6 in. thick near the outer end of the hole, sufficient gamma-ray shielding. The outer end of the liner will be removable to permit insertion and withdrawal of experiments after the water has been pumped out. The experimental can will be provided with lugs which can be rotated into engagement with recesses in the interior of the liner. This will assure accurate orientation (required in the cantilever apparatus) as well as provide an anchor against which a tensile force may be exerted on a specimen in the can. Lead wires will be sealed in a tube extending from the apparatus back to the pile face where they will emerge through a gland in the outer end of the plug. Insertion and withdrawal procedures are being designed to minimize exposure of personnel to the gamma beam emerging from the open hole (about 40 r/hr). A withdrawal shield is also being designed for apparatus and leads. The activity of sodium-containing experiments may require as much as 8 in. of lead for safety in withdrawal.

Two experiments are being prepared for irradiation in the LITR, one to study length changes in a stressed wire to verify the possible radiation expansion noted in NAA-SR-121,[8] the other to study the creep of aluminum as measured by type SR-4 strain gages; they are still awaiting sustained operation of that reactor.

A series of type 347 stainless steel specimens have been maintained (unstressed) at temperatures of 1400, 1500, and 1600°F for periods up to 500 hr to permit comparison studies of their structure with that existing in the creep specimens at the end of tests. The specimens are now being polished for metallographic examination.

The flux-dependent change in output voltage of a microformer reported in our last quarterly progress report[7] is now being investigated.

4. ENGINEERING PROPERTIES

LIQUID-METALS LOOP

C. D. Baumann O. Sisman
R. M. Carroll W. W. Parkinson
C. Ellis

Lithium at 1000°F was circulated through hole 58 of the graphite reactor for one week, and detailed description of the experiment was presented in the last quarterly progress report.[1] The principal components of the apparatus include a 1/4-in.-i.d. type 316 stainless steel loop which extends to the center of the pile and is connected to a 3/16-in.-i.d. loop external to the pile, an electromagnetic pump and electromagnetic flow meter, and three ionization chambers to measure the activity at various points on the external circuit of the lithium loop.

The primary purpose of this experiment is to study the Bremsstrahlung activity from the decay of Li^8 created by the reaction $Li^7(n,\gamma)Li^8$, which decays with an 0.88-sec half-life, giving a 12.7-Mev beta. The beta is absorbed in the lithium stream and the container walls (1/16-in. stainless steel) producing the Bremsstrahlung activity. The data have not yet been corrected for the efficiency of the counter for this particular energy radiation, and the neutron flux is still in the process of being determined. Figure 4.1 shows the Bremsstrahlung activity, uncorrected for the above two variables, at the three ionization chambers (or three different distances from the active lattice) for various velocities of the lithium stream. By extrapolating back to infinite velocity, the Bremsstrahlung activity for zero decay is found to be 2×10^9 Mev/sec per cubic centimeter of natural lithium (at a flux of about 2×10^{11} n/cm^2-sec). Figure 4.1 shows absorption curves for the Bremsstrahlung activity using iron and copper absorbers. The average energy of the photons was determined to be 0.06 Mev. The radiation is identified as that from Li^8, since it shows the 0.88-sec half-life by its decay while moving from one chamber to the next.

The loop was operated continuously at an in-pile temperature of 1000°F or slightly higher for the week of July 16, 1951 through July 23, 1951. It was planned to operate one week at 1000°F and a second week at the highest temperature attainable up to 1500°F. However, while increasing the temperature during the regular Monday pile shutdown period, the in-pile heating circuit failed. After

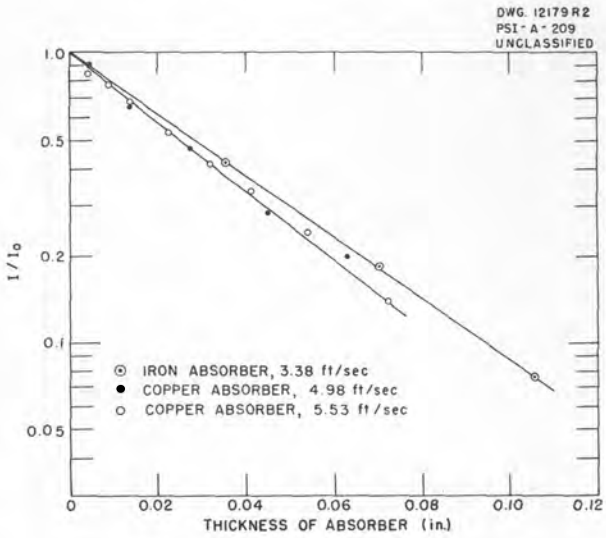

Fig. 4.1. Absorption of Bremsstrahlung Activity from Li^8 Beta.

[1] C. D. Baumann, R. M. Carroll, and O. Sisman, "Liquid-Metal Loops," *Physics of Solids Institute Quarterly Progress Report for Period Ending April 30, 1951*, ORNL-1095, p. 69 (Nov. 12, 1951).

examination of a portion of the in-pile loop it appears that cracks gradually developed in the copper tube connections between the lead wires and the heaters and that as the power was increased the cracks completely opened up. Why the cracks developed has not as yet been fully determined.

During the week of operation of the loop the velocity of the lithium stream was maintained most of the time at approximately 3 ft/sec in the external loop (approximately 1¾ ft/sec in the in-pile loop because of the larger diameter tubing). The velocity was changed only during the periods when runs of activity vs. velocity were made (Fig. 4.2) and when the absorption curves (Fig. 4.1) were determined. The velocity was increased for the absorption measurements in order to increase the starting activity. The curves of activity vs. reciprocal velocity (Fig. 4.2) were taken periodically during the entire week of operation, but since no significant change occurred, only one set of curves is presented. Since the intercepts and slopes of these curves showed no significant variation with time it may be concluded that there was no appreciable corrosion of the tube by the circulating lithium. If there had been a significant amount of corrosion, both the zero intercept and the slope for each counter would have increased with time. That there was no significant amount of corrosion is further shown by the results of counting the lithium from a 9-in. section of the tubes adjacent to the active pile lattice. The total count as obtained in a 100% geometry counter was only twice background.

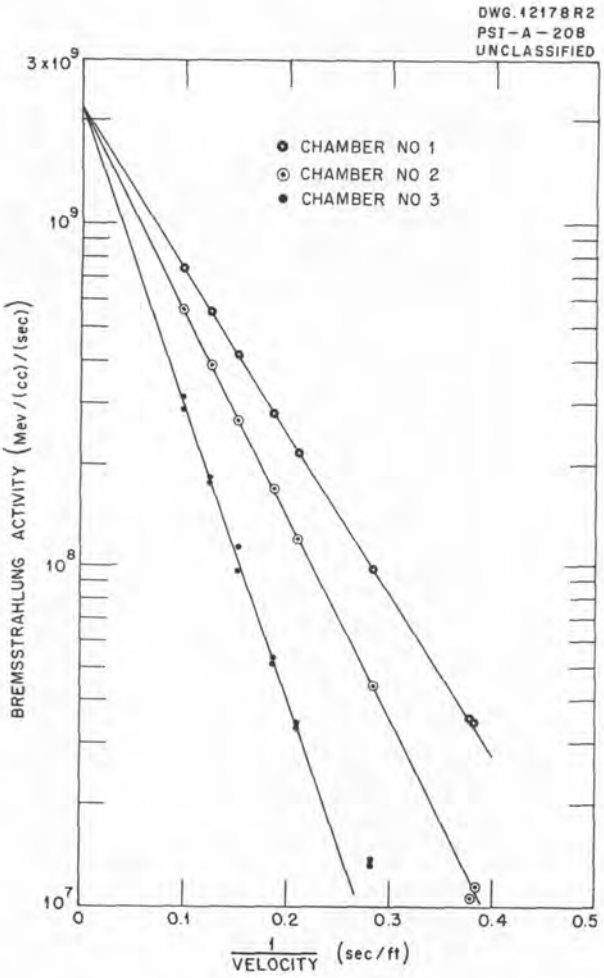

Fig. 4.2. Bremsstrahlung Activity from In-Pile Lithium Loop.

From Fig. 4.1, where the variation in activity with thickness of copper or iron (interspersed between the tube containing the circulating lithium and No. 2 counter) is shown, the half thickness of copper was found to be 0.025 in. and that of the iron 0.030 in. Using these figures, in conjunction with "The Mass Absorption Coefficient for X-Rays,"[2] and ignoring the scattering cross-section, the average energy of the Bremsstrahlung was found to be 0.063 and .058 Mev, respectively. Thus, the average energy of the Bremsstrahlung arising from the circulation of lithium in type 316 stainless steel tubes is of the order of 0.06 Mev.

---

[2] W. S. Snyder and J. L. Powell, Supplement 3, *Absorption of γ-Rays*, ORNL-421 (Mar. 14, 1950).

The ion chambers used in this experiment were air-filled at atmospheric pressure and cylindrical in shape (4 in. in diameter and 4 in. in height) with one of the bases being a thin-walled aluminum "window." The walls of the chamber were maintained approximately 150 volts above ground. In order to prevent any possible short to ground, the entire surface of the chamber was covered with 1/16 in. Teflon.

The chambers and their amplifying and recording equipment were bench tested with three glass tubes filled with standard solutions of Co^{60} of various strengths so as to simulate the line sources of the circulating lithium in the external pile loop. A lead brick with a 2-in.-diameter hole was placed between the source and the counter to act as a collimator, thus reducing stray radiation falling upon the counter.

The in-pile loop with all the controlling, measuring, and recording equipment was shipped from Y-12 to the X pile where it was assembled at the north end of hole 58. Here the chambers were calibrated in position with the three Co^{60} sources. In this way the natural and pile backgrounds were automatically taken into account. The calibration curves were approximately linear and of the form $S = AR - b$ where S is the source strength per unit length of pipe, R is the recorder reading (the amplified chamber response), A is a constant inversely proportional to the distance of the source from the counter, and b is the background correction which varies directly as pile power level, inversely as the distance of the counter from the pile, and also includes the natural background.

A cursory visual examination of the tube from which the lithium had been removed showed no signs of damage. Further investigation will be made when the tubes become somewhat less radioactive.

Rather than pursue the corrosion due to lithium any further at this time, it has been decided to use sodium in inconel for the next loop and study the corrosion by lithium at higher temperatures at a later date. It is planned to run the sodium loop at temperatures up to 1500°F.

LIQUID-METALS IN-PILE STRESS-CORROSION LOOP

A. S. Olson and W. E. Brundage

Work has begun on the design of a liquid-sodium circulating loop to be placed in the LITR. A pneumatic-type micrometer for measuring extensions of 0.010 to 0.020 in. with an accuracy of 1% is also in the design stage. This micrometer will be used for creep measurements of a portion of the sodium loop.

It is planned to circulate liquid sodium at 1500°F through the loop with a velocity of approximately 10 ft/sec. The loop is to be fabricated from inconel; it will have a 5-in. test section, to be stressed at 1500 psi for creep measurements at this temperature. The entire apparatus, including the pneumatic micrometer and a gas-operated circulating pump, will occupy about 2 ft of space in one of the 6-in.-diameter channels of the LITR.

NUCLEAR HEATING

J. B. Trice

An investigation was started to determine the rates of heat production induced in various materials by nuclear bombardment. The objective of this is to provide a general basis

for predicting the cooling required for experimental rigs in the LITR and the MTR.

Several estimates of nuclear heating rates for materials placed in the X pile, the LITR, and the MTR have been made by previous investigators. Of the two experimental sets of determinations, one of these, used to map the nuclear heating rates in the LITR, employed a graphite ionization chamber to measure absorption of gammas. The other experimental determination was a direct calorimetric measurement in the X pile.

Using Richardson's[3] experimental value for the rate of heating due to gammas in a gram of water irradiated in hole 12 of the X pile, gamma heating rates were estimated for several other materials. Heating by neutrons was also calculated using an $(nv)_{th}$ of 7×10^{11} n/cm^2-sec, and the neutron energy spectrum was measured by Bopp and Sisman in hole 19. The results of these estimates are summarized in Table 4.1. The two values listed for the LITR are normalized to an $(nv)_{th}$ of 7×10^{11} n/cm^2-sec in order to permit comparison between nuclear heating rates for materials placed in two entirely different types of reactors operating at approximately the same maximum neutron density. The much greater nuclear heating rate for materials in the LITR indicated that heating by gammas predominates.

In order to verify by direct measurement the nuclear heating rates determined in the LITR with the graphite ionization chamber, two calorimeters were constructed. The first one was built to test the feasibility of design. It consists of a closed horizontal aluminum can 5 in. in diameter and 5 in. long with water inlet and outlet pipes built into each end. Three thin-wall aluminum wells ½ in. in diameter and 3 in. deep extend into the can from the top and are held at a constant temperature by circulating water. The test specimen is a cylinder machined with small ridges at the top and bottom so as to fit loosely into one of the aluminum wells. The ridges on the specimen insure a minimum area of thermal contact with the well wall. A small copper-constantan thermocouple measures temperature at the center of the specimen, and a thin aluminum cap fits into the top of the well to prevent external heat loss from the specimen.

In a calibration test the specimen is heated to about 300°C and then dropped into one of the wells in the constant temperature water bath. The aluminum cap is secured and specimen temperature as a function of time is recorded on a Brown Electronik Recorder. The heat given off from the specimen between any two temperatures taken from the record is given by

$$\text{(calories)}\ \Delta H = C_p M \Delta T ,$$

or, in terms of rate of temperature fall, the rate of heat loss per gram is given by

$$\frac{1}{m}\frac{dH}{dt} \quad C_p \left[\frac{dT}{dt}\right]_T ,$$

where C_p is known and dT/dt is computed directly from the cooling curve as a function of temperature.

The rate of heat loss is thus found as a function of specimen temperature. The calorimeter, containing the specimen, can be placed near the active lattice of the LITR. The specimen

[3] D. M. Richardson, *Calorimetric Measurement of Radiation Energy Dissipated by Various Materials Placed in the Oak Ridge Pile*, ORNL-129 (Oct. 1, 1948).

TABLE 4.1

Nuclear Heating Rate for Several Materials[a]

MATERIAL	HEAT DUE TO PILE NEUTRONS (μcal[b]/g-sec)				HEAT DUE TO PILE GAMMAS (EXTERNAL GAMMAS) (μcal/g-sec)	TOTAL HEAT (μcal/g-sec)		
	ELASTIC	CAPTURE	SATURATION β DECAY	SATURATION γ EMISSION		CALC.	EXP.	EXPERIMENTAL TOTAL FOR LITR[c]
H[d]	6700				740	7440		
D[d]	1930				370	2300		
O[d]	60				370	430		
H_2O[d]	800				410	1210	1200	10,000
D_2O[d]	430				370	800	770	
C[d]	80				370	450	470	
Al[d]	23	40	110	5	370	548	600	
C	90		0		370	460		
Cu	6		270		370	626		
Fe	7	300	0		370	677		
Ni	8		1.5		370	380		
Be	250		0		370	620		9000
Zn	1		4.5		370	375		
Cr	1		15		370	385		
Mn	1		2600		370	2970		

[a]All values except last column are for X-10 graphite pile.

[b]Microcalories.

[c]$(nv)_{th} = 7 \times 10^{11}$ n/cm^2-sec.

[d]Values due to Richardson (hole 12).

temperature at equilibrium is then measured and the rate of nuclear heating per gram is recorded from the calibration curve.

Tests indicate that the temperature difference between the specimen and the water bath will be large enough during irradiation to permit accurate measurements. Figure 4.3 shows the rate of heat loss as a function of temperature for a calorimeter water temperature of 22.4°C and a copper specimen weighing 44.5 g. The maximum rate of heat production for a material placed in the LITR is estimated to be about 0.1 cal/g-sec. From Fig. 4.3 it is observed that this corresponds to a temperature difference of 140°C between specimen and water.

The second type of calorimeter is similar to the first, except that it

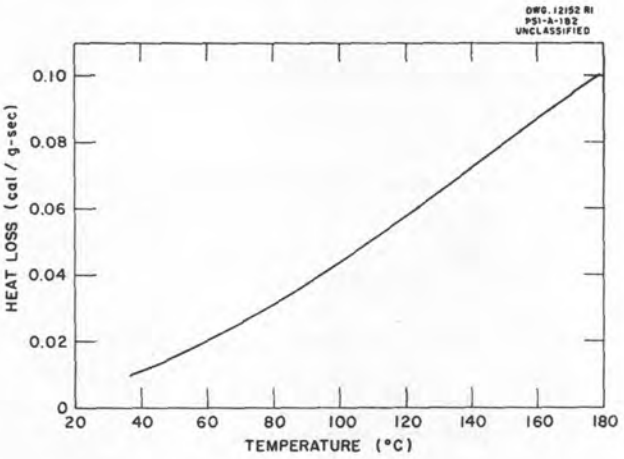

Fig. 4.3. Run No. 1, Rate of Heat Loss as Function of Temperature for Copper Specimen in Large Calorimeter.

has room for only one specimen. It is completely contained inside the end of a long ¾-in.-o.d. aluminum tube, and it is designed to function in either an air or a water medium. It is planned to use the second calorimeter in the active lattice and the experimental holes in the LITR.

PILE-INDUCED RADIATION

C. D. Bopp R. L. Towns
O. Sisman W. K. Kirkland

Pile-induced gamma activity from four of the hastelloy alloys is shown in Figs. 4.4 through 4.6. The decay curves were taken after irradiating for six months in the X reactor. Activity measurements were made on thin shavings with a 100% geometry ionization chamber as described in earlier reports.[4] Absorption curves for lead were determined after 600 hr

(4) "Experimental," *Materials Testing Reactor Project Progress Report for Period Ending February 28, 1950*, ORNL-628, p. 27, esp. pp. 28-30 (April 10, 1950); "Pile-Induced Radiation," *General Reactor Engineering Research Quarterly Progress Report for Period Ending November 20, 1950*, ORNL-973, p. 21 (April 5, 1951).

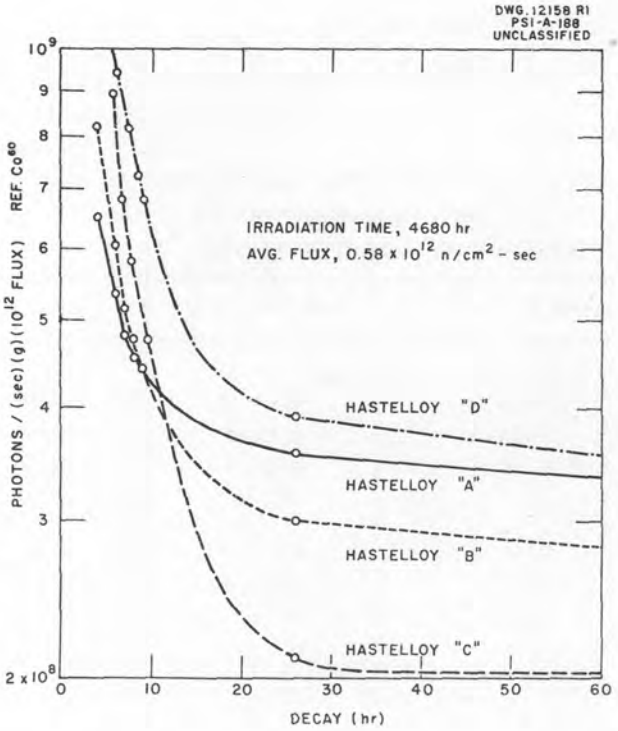

Fig. 4.4. Short Time Gamma Decay of Hastelloy.

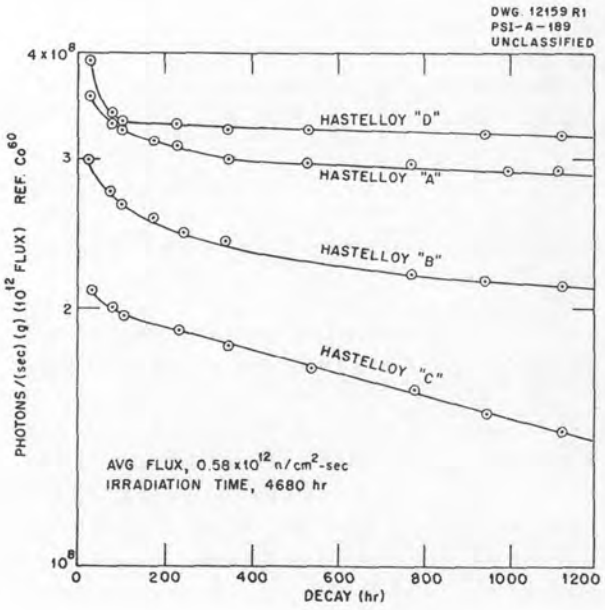

Fig. 4.5. Long Time Gamma Decay of Hastelloy.

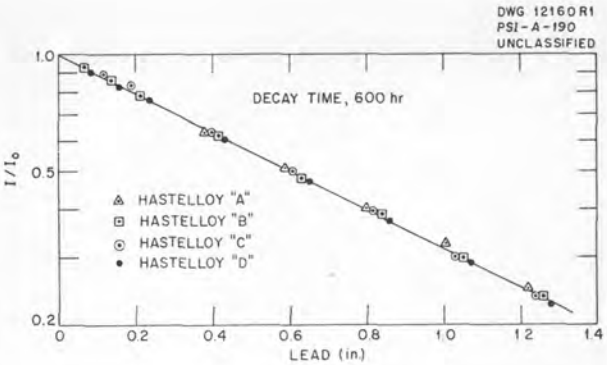

Fig. 4.6. Absorption of Gamma Radiation from Hastelloy.

decay and are shown in Fig. 4.6. Nominal composition of the hastelloy is listed below.

Hastelloy A: 17 - 21% Mo; 17 - 21% Fe; balance Ni.
Hastelloy B: 24 - 32% Mo; 3 - 7% Fe; 0.02 - 0.12% C; balance Ni.
Hastelloy C: 14 - 19% Mo; 4 - 8% Fe; 0.04 - 0.15% C; 12 - 16% Cr; 3 - 5.5% W; balance Ni.
Hastelloy D: 8 - 11% Si; 2 - 5% Cu; 1% Al; balance Ni.

Decay curves for several samples of thorium after irradiation for one month in the ORNL reactor are presented in Fig. 4.7. These materials were supplied by R. E. Adams of the

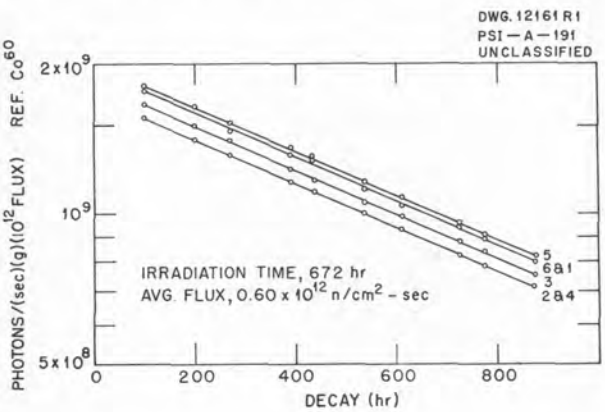

Fig. 4.7. Gamma Decay of Thorium.

Metallurgy Division and were identified as follows:

1. Ames thorium
2. Iodide thorium
3. Ames thorium, +~4% Be
4. Ames thorium, +~2% Cb
5. Ames thorium, +~2% Zr
6. Ames thorium, +~2 or 4% Ti

The curves show the predominant activity to be that of 27.4-day Pa^{233}. The energy of the radiation also checks that given for Pa^{233} (~0.3 Mev); no significance is to be attached to the separation of the curves since very small samples were used and the error in weighing the sample is about ±5%.

PHYSICAL PROPERTIES OF IRRADIATED ELASTOMERS

O. Sisman W. K. Kirkland
C. D. Bopp R. L. Towns

Eight commercial elastomers are being studied for resistance to pile radiation. The compositions of these materials are given in the last quarterly progress report.[5] Results of the tests to date are shown in Figs. 4.8 through 4.15. The following properties are reported: tensile strength, elongation, set at break, compression set, strain at 400 psi compression, change in weight, specific gravity, Shore Durometer hardness and Shore elasticity.

The elastomers are irradiated in hole 19 of the X reactor. Hole 19 is water-cooled to between 25 and 40°C. The average thermal flux as measured with cobalt foils[6] was

[5] O. Sisman, C. D. Bopp, R. L. Towns, and W. K. Kirkland, "Physical Properties of Plastics," ORNL-1095, *op. cit.*, p. 75.

[6] O. Sisman and C. D. Bopp, *Physical Properties of Irradiated Plastics*, ORNL-928 (June 29, 1951).

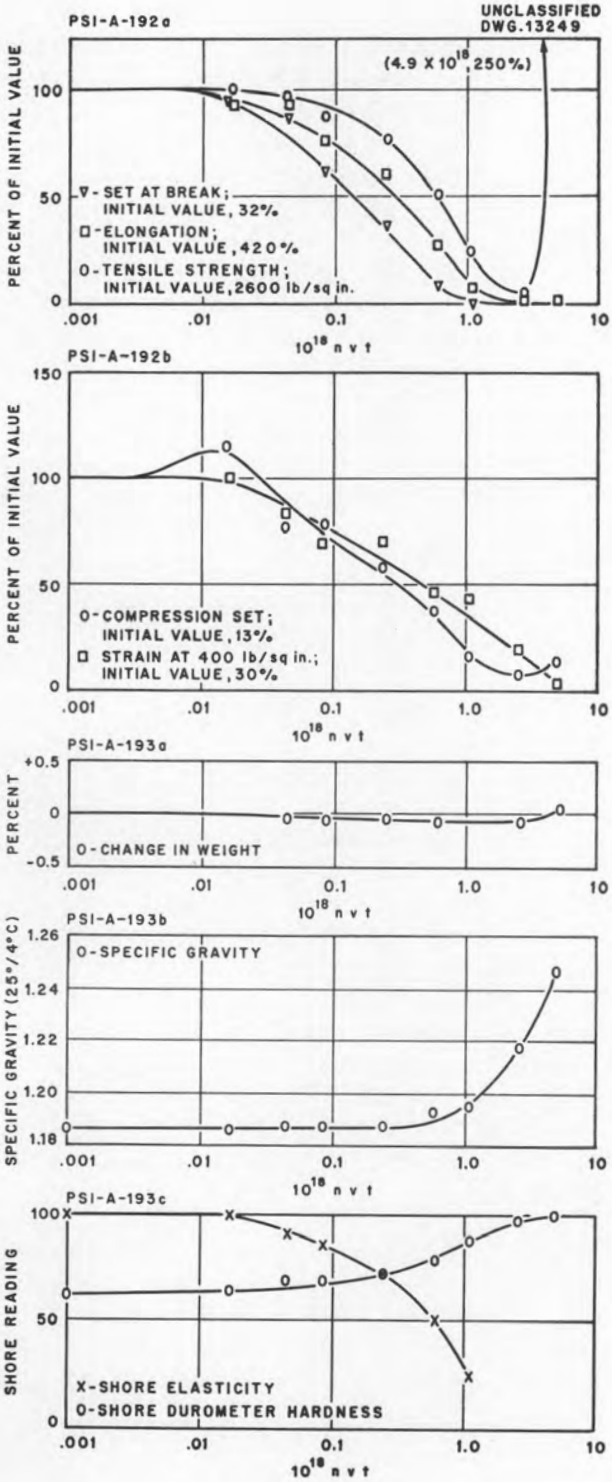

Fig. 4.8. Physical Properties of Irradiated Natural Rubber.

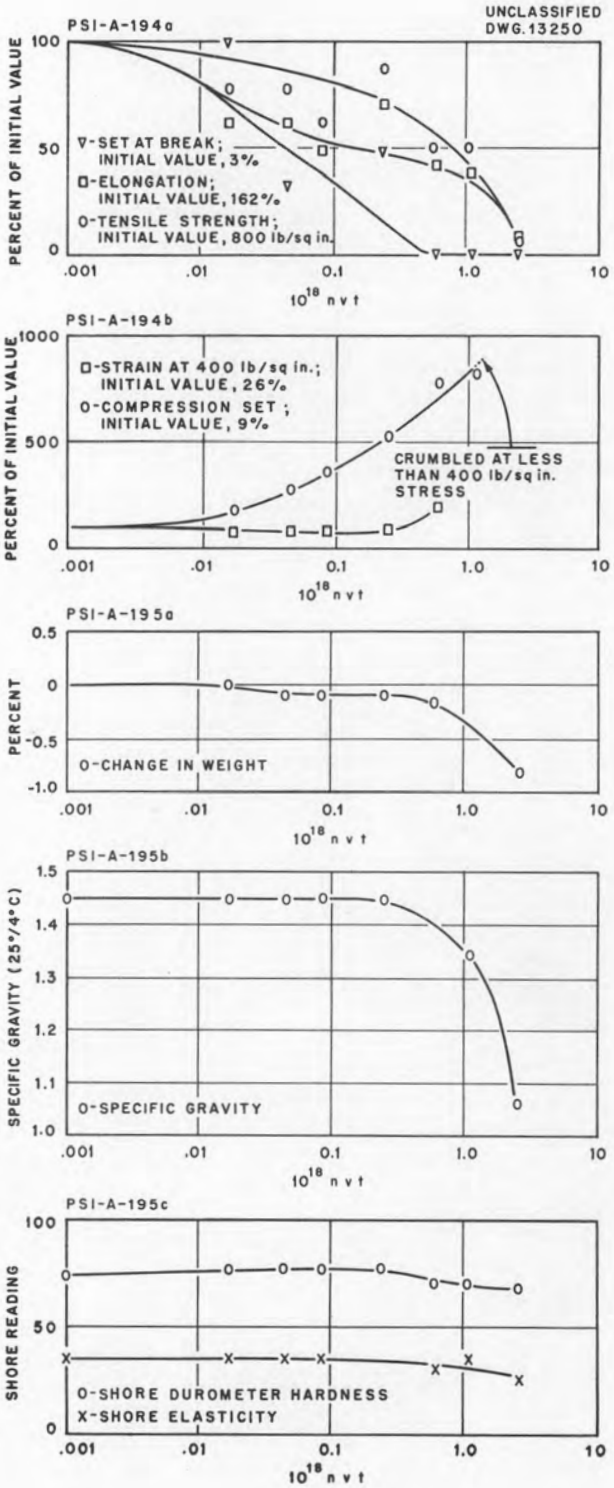

Fig. 4.9. Physical Properties of Irradiated Thiokol ST.

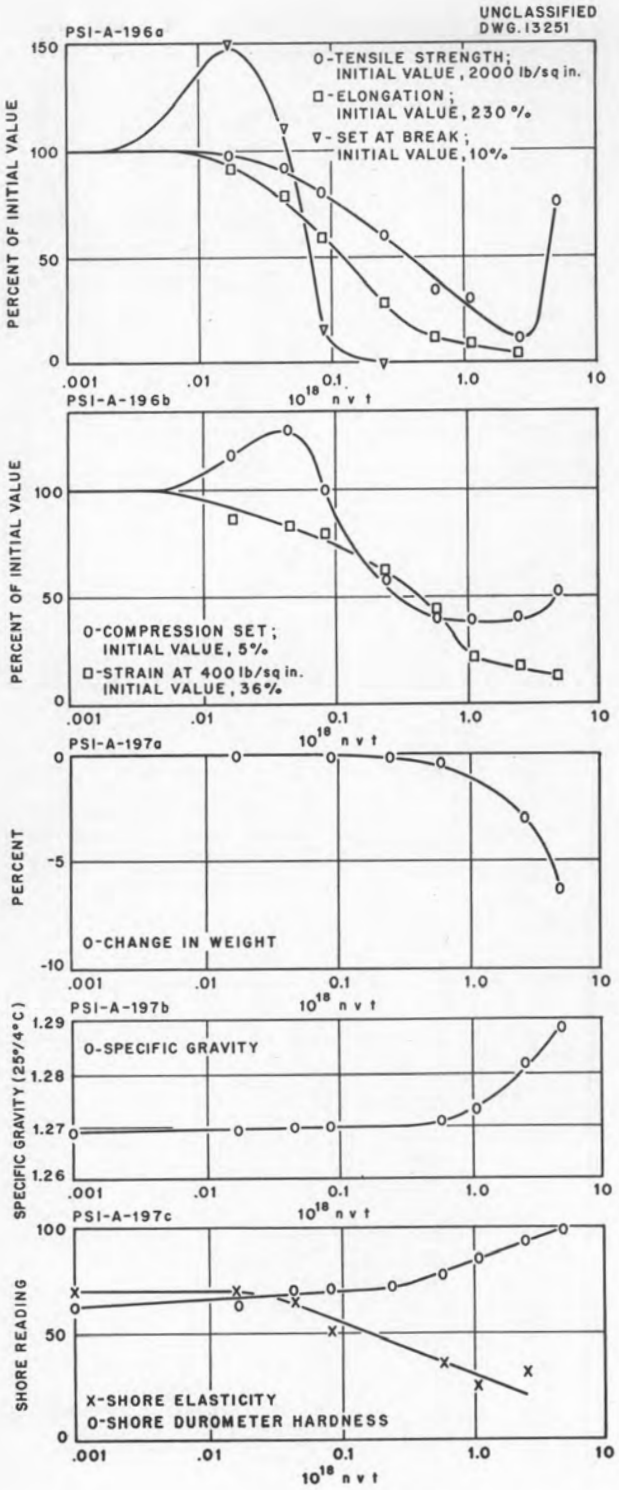

Fig. 4.10. Physical Properties of Irradiated Hycar PA-21.

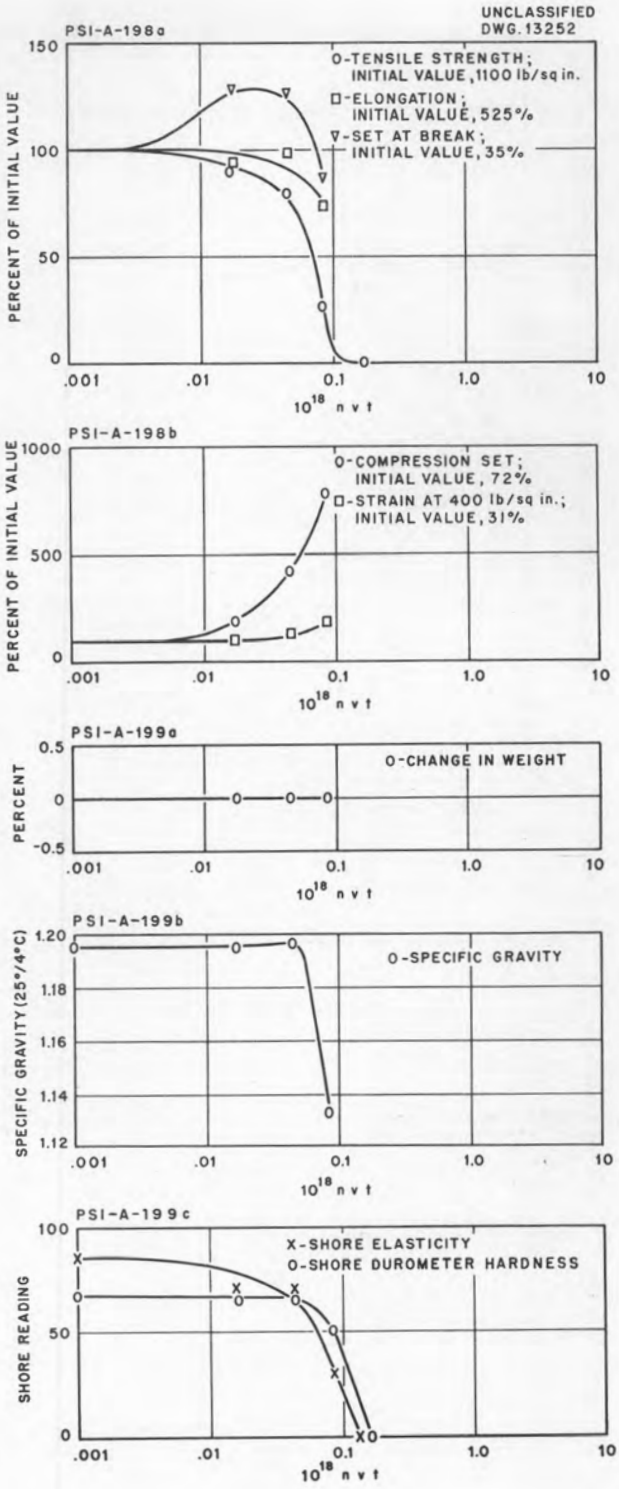

Fig. 4.11. Physical Properties of Irradiated GR-I50.

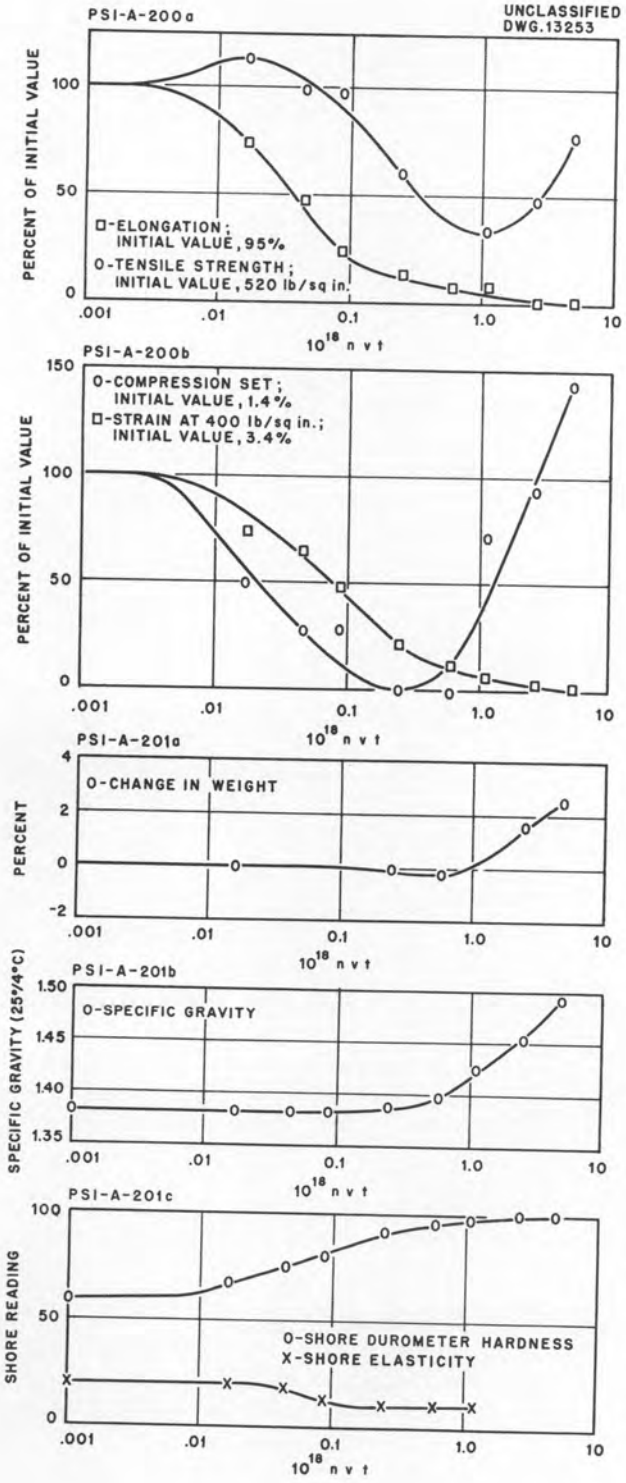

Fig. 4.12. Physical Properties of Irradiated Silastic 7-170.

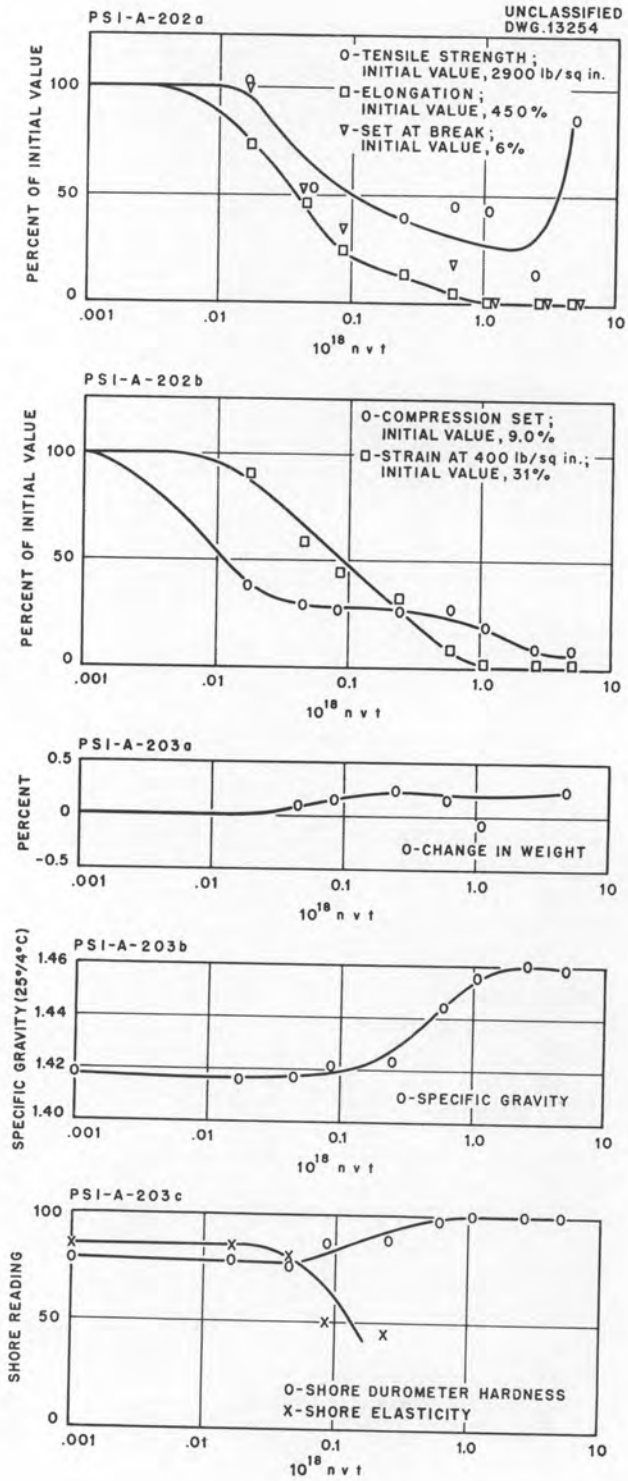

Fig. 4.13. Physical Properties of Irradiated Neoprene W.

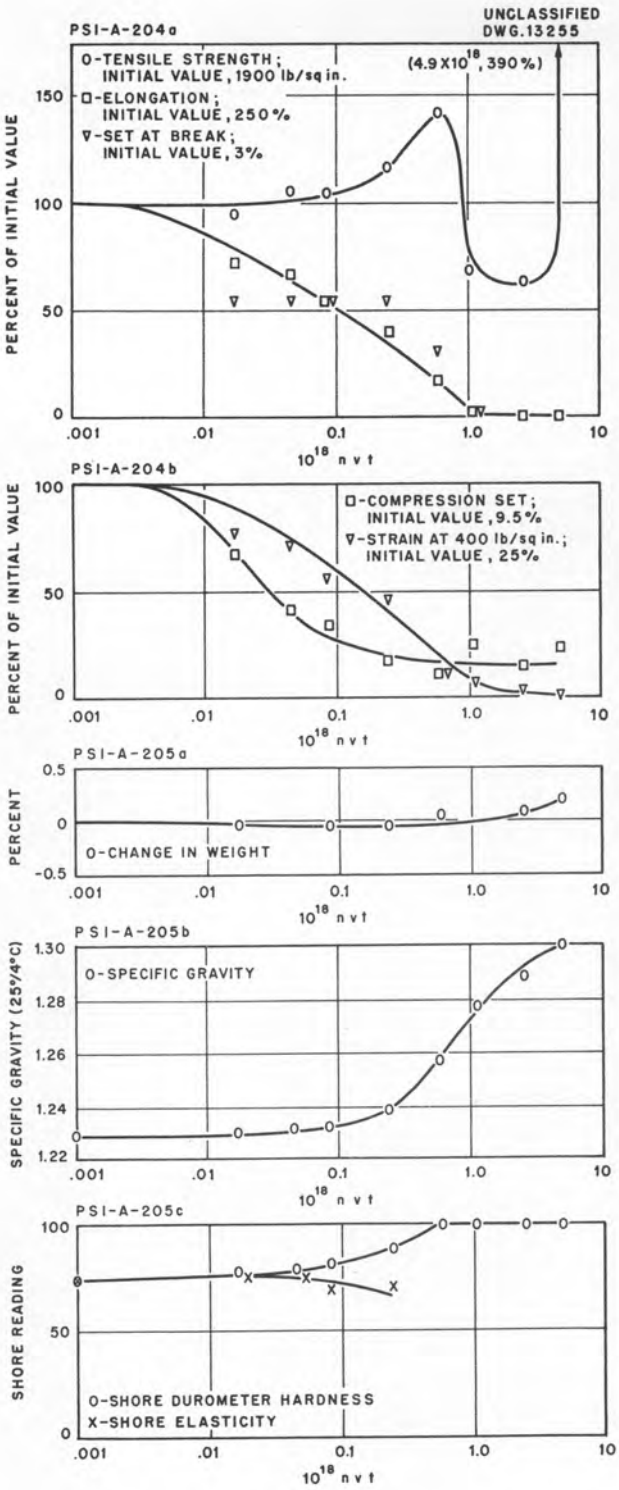

Fig. 4.14. Physical Properties of Irradiated Hycar OR-15.

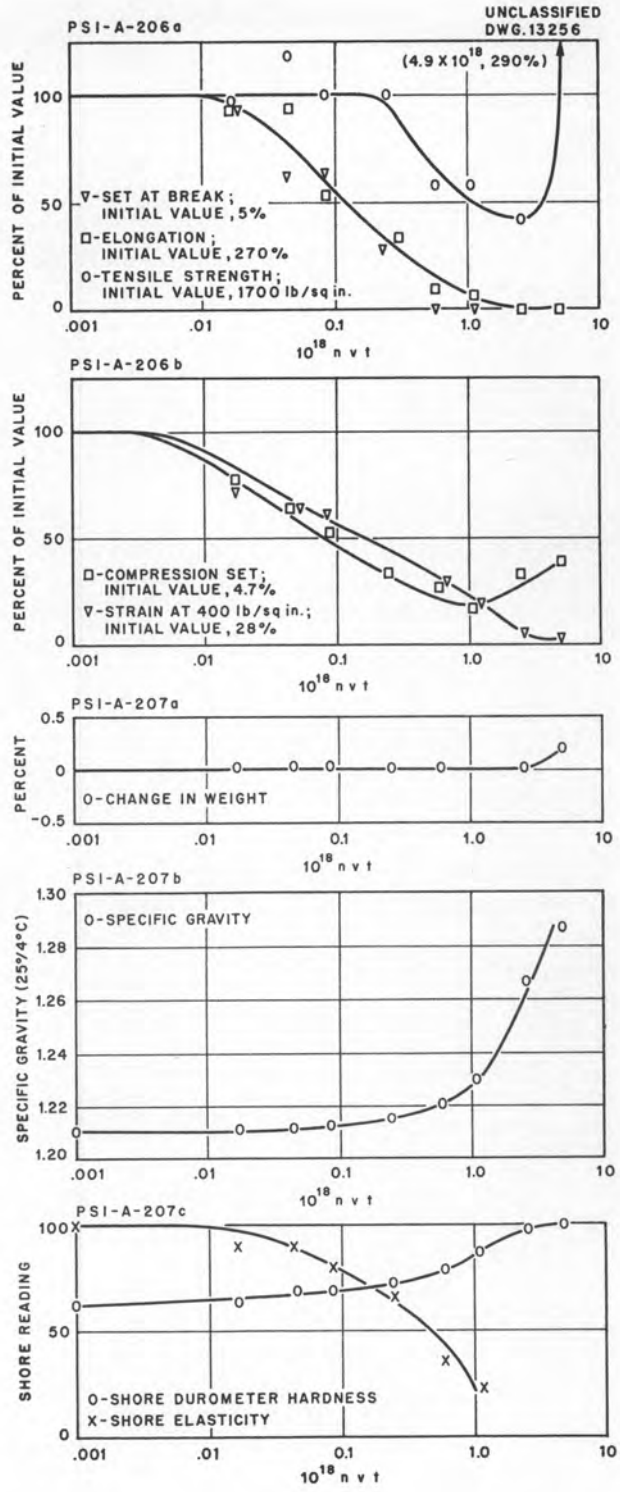

Fig. 4.15. Physical Properties of Irradiated GR-S50.

1.0×10^{12} n/cm^2-sec. Neutrons entering the specimen cans in this hole are attenuated by 3/16 in. of water and 1/8 in. of aluminum in addition to the graphite surrounding the hole. The fast flux spectrum is given in ORNL-525.[7]

After specimens are conditioned for at least 24 hr at 25°C and 50% relative humidity, dimensional measurements are taken. The specimens are then irradiated. Following irradiation the specimens are again conditioned for 24 hr at 25°C and 50% relative humidity before testing.

Exposure of radiation hardens Silastic, Neoprene, GR-S, Hycar OR, natural rubber, and Hycar PA, but it softens butyl (GR-I) and Thiokol. Both butyl and Thiokol finally become sticky and tarry; however, Thiokol withstands 20 times the radiation dose that butyl withstands.

The tensile strength and, very markedly, the elongation of all elastomers are eventually decreased by irradiation, although Silastic and Hycar OR initially increase in tensile strength. After the elongation has decreased to less than 1% of the initial value, the tensile strength, of the group of elastomers that harden with irradiation, increases; however, these materials are then very brittle. Tests are in progress to determine how long these brittle materials will withstand irradiation before crumbling apart.

Set at break decreases with irradiation following the elongation closely except that for Hycar PA and butyl there is an initial increase in the set at break while there is no corresponding change in elongation. Silastic showed zero set at break for all times of irradiation.

Compression set decreased, following closely the strain at 400 psi compressive load. After the strain at 400 psi decreases to less than 20% of the initial value, the compression set of Silastic increases markedly and the compression set of butyl, natural rubber, and Hycar PA increases to a lesser extent.

The specific gravity increases for the elastomers that harden; the specific gravity of the elastomers that soften decreases. A marked loss in weight occurs only for Thiokol and Hycar PA.

Neoprene decreases in dielectric strength and volume resistivity. The dielectric strength drops from 280 to 120 volts/mil; the volume resistivity drops from 10^{11} to 10^5 ohm-cm. The dielectric strength and the volume resistivity do not change markedly for the other elastomers tested.

The testing procedure employed for the tensile testing is a modification of ASTM test D412-49T.[8] A Baldwin-Southwark universal testing machine is used with the Baldwin extensometer and Scott grips for testing nonrigid plastic materials. For elastomers with at least 3% elongation the speed of testing is the rate of travel of the platen-adjusting motor, about 4 in./min; however, for materials embrittled by irradiation so that elongation is less than 3%, the rate of loading is reduced in order to prevent failure by impact at the start of stressing. For brittle

[7] C. D. Bopp and O. Sisman, *The Neutron Flux Spectrum and Fast and Epithermal Flux in Hole 19 of the ORNL Reactor*, ORNL-525 (July 28, 1950).

[8] 1949 Book of A.S.T.M. Standards, *Electrical Insulation, Plastics, Rubbers*, p. 887, American Society for Testing Materials, Philadelphia, 1950.

materials with less than 3% elongation the speed of testing is 400 lb/min. The percent elongation is defined as the extension at breaking divided by the original distance between gage marks. Set at break is obtained by piecing together the broken specimen and measuring the distance between gage marks.

Compressive set tests are intended to measure the ability of rubber compounds to retain elastic properties during prolonged action of compressive stress. Compression set is taken as the percent decrease in thickness of the test specimen measured 30 min after removal from a loading device in which the specimen has been subjected for 22 hr to 400 lb/sq in. compressive load at 70°C. The strain is recorded at the moment of application of the 400 lb/sq in. compressive stress.

The test for specific gravity is given in ASTM D-792-48T.[9]

The test for durometer hardness is given in ASTM-D-676-49T.[10] The durometer consists of a pressure foot from which protrudes a spring-loaded indentor. The distance the indentor penetrates when the presser foot is brought into contact with an elastomer is read on the scale of the instrument. Zero penetration gives a reading of 100.

The Shore elastometer consists of a similar pressure foot with an opening from which a needle is pushed into the elastomer. The distance the needle returns into the presser foot when the force pushing it into the elastomer is released is read on the scale of the instrument. If the needle returns all of the way back, the reading is 100; if it returns none of the way, the reading is zero.

[9] *Op. cit.*, p. 728.

[10] *Ibid*, p. 1039.

IRRADIATION OF GRAPHITE-URANIUM RODS

R. H. Kernohan

As a preliminary step in the study of fission-fragment damage to graphite as a function of uranium particle size, 12 bars of uranium-free graphite were irradiated in the X-10 pile. Investigation of the uranium-free material was necessary in order to distinguish between neutron damage and fission-fragment damage as much as possible.

The 12 bars were fabricated by Battelle Memorial Institute and are described in Table 4.2.

Measurements taken on the bars prior to irradiation were taken in order as follows: dimensions, weight, natural vibration frequency to determine elastic modulus, relative thermal conductivity, electrical resistivity. The samples were irradiated in the center of doughnut hole 1768 for two weeks which corresponds to an integrated flux of $1 \times 10^{18}/cm^2$.

Although the activity of the specimens was quite low, measurements were taken on the latest remote control apparatus for the hot cells in order to check their operation.

After irradiation, measurements were taken in order as follows: dimensions, weight, electrical resistivity, vibration frequency, and relative thermal conductivity. No significant changes were observed in dimensions or weight. Five of the specimens increased in weight slightly, possibly because of absorbed moisture. Significant percentage changes in order properties are shown

TABLE 4.2

Graphite Bars Fabricated by BMI

SPECIMEN	DESCRIPTION
M1-9 and 23	Extruded, resin-bonded graphite, baked at 2500°F to carbonize binder
M1-19 and 20	Extruded, resin-bonded graphite, bonded at 4500°F to graphitize binder carbon
L34-4 and 8	Molded, resin-bonded graphite, baked at 2500°F to carbonize binder
L34-5 and 6	Molded, resin-bonded graphite, baked at 4500°F to graphitize binder carbon
AGOT-1 and 2	Extruded, pitch-bonded cake, fully graphitized; project grade, cut parallel to extrusion axis
AGOT-5 and 6	Same as above, but cut perpendicular to extrusion axis

TABLE 4.3

Radiation Induced Changes in Graphite Bars

$nvt = 1 \times 10^{18}\ n/cm^2$

SPECIMEN	TREATMENT	ELASTIC MODULUS, E (% increase)	THERMAL CONDUCTIVITY, K (% decrease)	ELECTRICAL RESISTIVITY	
				INITIAL, ρ_1 (% increase)	FINAL,[a] ρ_2 (% increase)
M1-9	Extruded	32	10	40.7	22.5
M1-23		29.5	13	34.9	21.3
M1-19	Extruded and graphitized	55	25	49.0	22.0
M1-20			34	47.0	19.3
L34-4	Molded	46	9	34.3	22.0
L34-8		27	15	35.0	21.4
L34-5	Molded and graphitized	67	16	36.6	19.1
L34-6		62	19	37.7	20.2
AGOT-1	Cut parallel to extrusion		46	77.9	47.2
AGOT-2			41	77.3	51.5
AGOT-5	Cut perpendicular to extrusion	44	15	29.9	20.9
AGOT-6		80	31	73.5	55.3

[a] After thermal measurements.

in Table 4.3. Electrical resistivity measurements were the most accurate, being correct to within .3%. Measurements of elastic modulus were not entirely satisfactory and a different measurement technique is being considered. Some error is also apparent in the thermal conductivity changes.

Since the thermal measurements necessitated heating the specimens for about 2 hr to temperatures in the range of 100 to 200°C, there existed the possibility of annealing out some of the damage. A second measurement of electrical resistivity showed that about half the damage had been annealed out during the thermal conductivity measurements. These changes are shown in Table 4.3.

A container for holding the uranium-graphite bars in the X-10 pile was designed and submitted to the Research Shops for fabrication. Battelle is in the process of obtaining the enriched uranium and fabricating the final test bars.

5. LIQUID FUELS

RADIATION DAMAGE TO LIQUID FUELS

G. W. Keilholtz C. C. Webster
J. G. Morgan H. E. Robertson

Liquid fuels (NaF, KF, and UF_4 mixtures) have been bombarded in the X reactor for 200-hr periods, and corresponding bench tests without radiation have been made. The resulting samples are now being examined by the Metallurgy and Analytical Chemistry Divisions for corrosion effects and chemical stability of the fuel. This includes photomicrographs and the analysis for uranium, fluorine, iron, chromium, and nickel. The temperature was maintained at 1500°F and continuous pressure measurements were recorded during the 200-hr test. The container was filled to 58 psi with helium at the 1500°F temperature, and the pressure did not deviate appreciably during the test period.

Figures 5.1 and 5.2 show the equipment, including the Baldwin strain gage (0 to 250 lb capacity). Helium gas served as the pressure transferring medium through stainless steel tubing. Figure 5.1 shows the construction of the inconel sample container with thermocouple well and pressure fittings.

Radiation damage studies on the fuel material ($NaF-KF-UF_4$) are going ahead on the Y-12 cyclotron and the details are discussed under the heading "Y-12 Cyclotron Studies," p. 51.

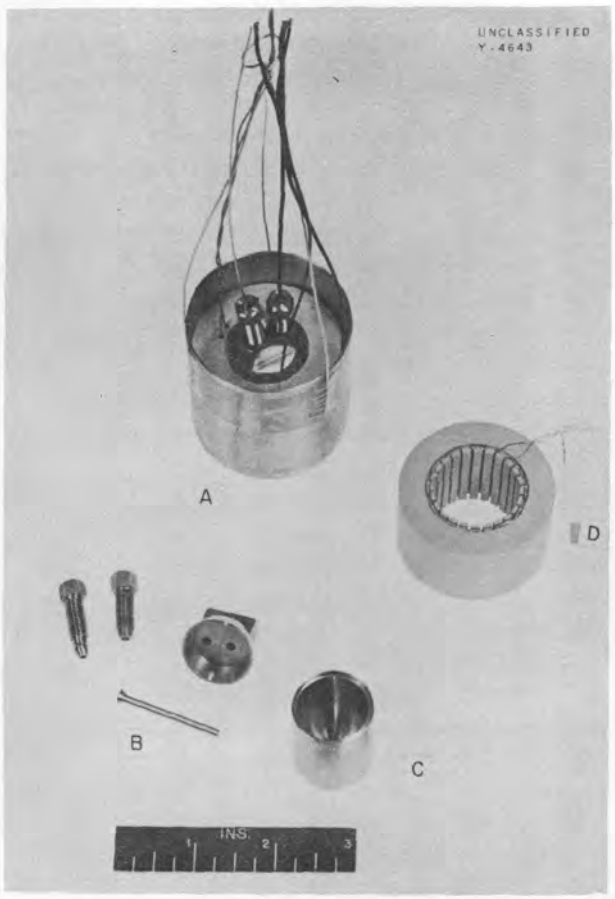

Fig. 5.1. Liquid-Fuel Sample Container with Thermocouple Well and Pressure Fittings. A, assembly; B, thermocouple well, pressure fittings, and capsule lid; C, capsule; D, heater.

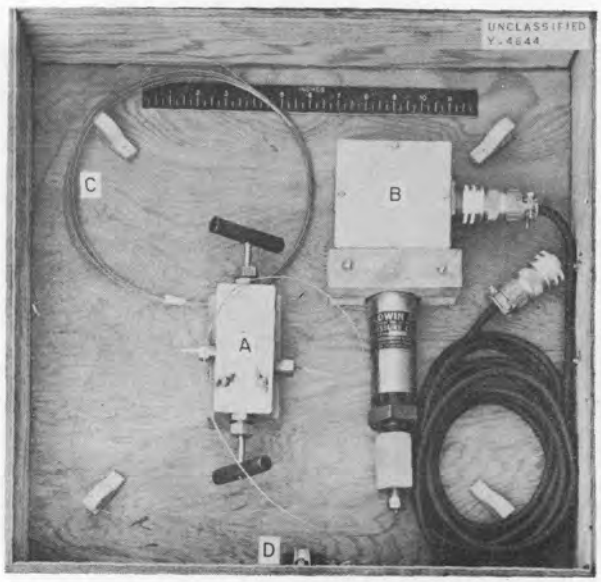

Fig. 5.2. Capsule and Pressure Measuring Device. A, high-pressure valve; B, Baldwin strain gage; C, pressure line; D, capsule.

6. CRYSTAL PHYSICS

Y-12 CYCLOTRON STUDIES

W. J. Sturm M. J. Feldman
X-10
R. J. Jones J. S. Luce
C. L. Viar
Y-12

The efforts of this group have recently been devoted exclusively to radiation damage studies for the ARE. Specifically, the experiments have been directed toward the determination of the effects of proton bombardment upon inconel-encased eutectic fluoride mixture ARE fuel elements. Three types of fuel pin cyclotron target cooling are to be used during bombardment: (1) radiation, (2) water, and (3) liquid sodium. It is a general policy that, whenever practical, new type cyclotron targets are given a preliminary bombardment in the high flux of low-energy protons in the calutron, thus simulating the beam-induced thermal effects of the cyclotron and generally reducing the probability of target failure in the cyclotron. A series of nine fuel elements, consisting of four cyclotron-bombarded samples and associated control specimens, have thus been prepared for analysis. Only preliminary analytic results are available at this time and will be discussed below.

Radiation-Cooled Targets. The eutectic-containing fuel pin for the cyclotron measurements is an evacuated 6-in. length of 1/4-in.-o.d. inconel tubing with a 0.010-in. wall, having a 4-in. flattened portion (Fig. 6.1) of thickness slightly greater than the range of the bombarding protons. The cylindrical portion serves as a void into which the eutectic can expand upon heating. In order to estimate the amount of energy which can be dissipated by heat radiation alone, thermocouples were welded to the bombarded face and upper leading edge, and this target was mounted in the calutron. Bombardment was made

DWG. 13259
PSI-A-186
UNCLASSIFIED

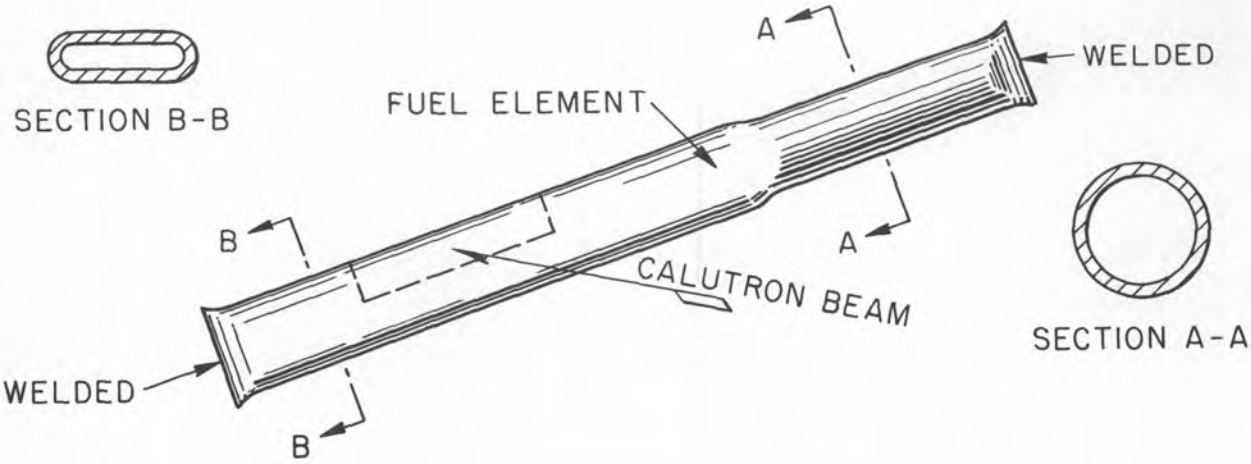

Fig. 6.1. Eutectic-Containing Fuel Pin.

with 12.5-Kev protons, and by varying the beam current the power was made to range from zero to about 40 watts. This power was expended upon a 1/2- by 3/16-in. area on the face of the fuel pin. The equilibrium temperature of the pin as measured just outside the bombarded area is plotted in Fig. 6.2 as a function of proton beam power. Accordingly, it was estimated that to maintain the front face of the pin at the proposed reactor temperature of 1500°F, by proton bombardment and radiation cooling, approximately 22 watts of beam would be required. Since the irradiated area of the fuel tube for the calutron bombardment was made to approximate that for the cyclotron, it was estimated that 1 μa of 20-Mev protons in the cyclotron should provide the required heat input. Actually, because of differences in beam baffling and in the shape and temperature of the tank area, differences in heat input of a factor of 3 to 4 can be expected.

The bombarded members of the series of nine fuel pins mentioned above were radiation cooled and were maintained at temperature by beam heating. A cyclotron target dolly,

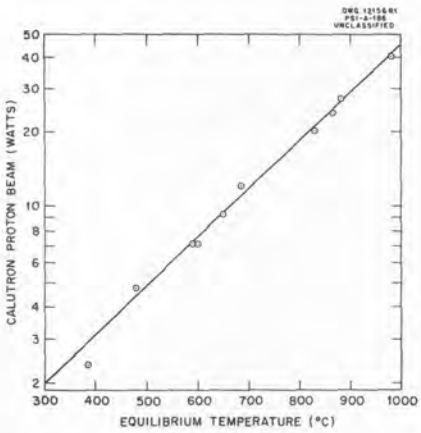

Fig. 6.2. Equilibrium Temperature of Eutectic-Containing Fuel Pin as a Function of Proton Beam Power.

redesigned for these experiments, was equipped with two sets of thermocouple leads, and provision was made for mounting and baffling the fuel elements. During the irradiation the beam current was varied to maintain the front face of the pin at a constant temperature in the region of 700 to 725°C. Temperature was indicated by a chromel-alumel couple welded to the tube near the center of the bombarded area, and cyclotron beam current variations were made to maintain this temperature at a constant value. Four fuel pins were bombarded in this manner with beam currents of 2 to 3 μa of 20-Mev protons. The first of these, allowed to rise to 875°C, was melted in the region of an intense beam; subsequent samples, however, held in the lower temperature range, survived and were considered worthy of analysis.

Two targets were bombarded for 1 hr, and two for 4 hr, each under approximately the same conditions of beam current and temperature. For the sake of comparative analytic results, several unirradiated pins of the same inconel stock, similarly produced, evacuated, and filled with fluoride mixture (UF_4-NaF-KF), were heated to the same temperature and for the same period of time as were cyclotron targets.

The analytic procedure, as it now stands, consists of four parts. The first, analysis of the eutectic for trace quantities of inconel components iron, nickel, and chromium, is done spectroscopically; quantities found are in the range of hundreds of parts per million, and accuracy is estimated to be ±20%. The second analysis is an assay of the fuel for the elements uranium and fluorine. Changes in the ratio of these elements might be expected to yield data about fluoride decomposition and recombination with the inconel wall. The accuracy

claimed for this analysis is ±1%. The third type of analysis is mass spectrographic, quantitatively evaluating the relative abundances of the various fluorides of uranium before and after irradiation as an indication of fluoride decomposition and recombination. At the present time, little about the accuracy of this analysis can be said; it is expected, however, that a change of less than 1% in the abundance of the UF_4 component can be measured. The fourth analysis is metallurgical, including examination for corrosion, intergranular penetration, and grain type alteration.

To date only one of the 1-hr cyclotron-bombarded fuel pins has been partially analyzed. Energy dissipation during the irradiation was about 40 watts/cc for this sample. No change outside experimental error was noted in the trace elements or in relative uranium to fluorine abundance. Mass spectrographic analysis has not been completed. Metallographic studies show no detectable corrosion; however, on the few pins thus far studied, an increase of about three diameters in grain size over that of the "as received" sample of inconel tubing appears in both the bombarded and control samples. Since the change in grain size appears outside the irradiated area in the cyclotron sample and appears as well in the unirradiated control sample, it seems that the effect is, at least primarily, due to the cold work introduced in fabricating the flattened tube section used for both cyclotron target and control specimens. Subsequent thermal history very likely accounts for the recrystallization observed. Further study will be directed toward determining the reality of the effect; efforts will be made to increase the precision of the temperatures of the control specimens, and bombardment of thick samples of inconel will be undertaken for metallurgical analysis.

Water-Cooled Targets. To increase the maximum energy which can be dissipated at the target without exceeding 1500°F at the front face, several types of water-cooled targets have been designed. The first consists of a 3/8 × 1/2 × 2.5 in. cooling bar of stainless steel brazed to a flattened 1/2-in. copper tube through which water is circulated. Fuel elements and other targets are mounted on this block.

Preliminary irradiations in the calutron indicated that without exceeding 1500°F on the target, as much a 3 kw of proton beam could be dissipated on this stainless steel cooling surface. However, with a fuel pin mounted on this surface, it was not possible to introduce more than about 400 watts to the target without exceeding the 1500°F boundary condition on the fuel pin. This discrepancy, unresolved for some time, was removed with the recent evaluation of the very low thermal conductivity of the eutectic mixture. Calculations based upon this conductivity value indicate that about 320 watts can be dissipated in this geometry, in the absence of significant convection effects. One fuel element has been bombarded on the water-cooled mount using a thermocouple mounted on the irradiated face to control the beam current. A beam current of about 20 amp (about 400 watts) maintained the target at the required temperature, in essential quantitative agreement with the indicated calculation.

The fuel pin thus bombarded showed at 5 ft several roentgens of radioactivity at the end of a 1 hr irradiation and thus far has not been analyzed. The pin itself, except for

the manner of cooling, was identical with the series of radiation-cooled pins discussed above, and analytic results can be compared directly with the control samples of the earlier series.

Two further types of water-cooled targets are at various stages of completion; each has water channels and thin window fuel chambers and is machined from a single inconel block. One of each type has been prepared and is ready to be filled with the fluoride eutectic.

X-RAY WORK

G. E. Klein and F. A. Sherrill

A Hilger HRX X-ray-diffraction unit has been installed and placed in operating condition. Slight modifications were made in the vacuum system to insure satisfactory operation. The Hilger tube has four windows and its anode contains sectors of copper, cobalt, chromium, and silver. It is possible to simultaneously obtain several different radiations from the various windows and to quickly shift the radiation being given off at any particular window. This is a distinct advantage when working with materials not suited to the use of the conventional copper radiation and also where it is advantageous to use more than one radiation in the examination of a single sample.

A North American Philips Geiger-counter spectrometer has been placed in operation using the X-ray radiation from the Hilger unit since this is the only X-ray source available at the present time. It is proposed to install a Philips copper-target tube and tube head on a separate table which will be used to provide the X-ray source for the spectrometer during normal operations and to reserve the radiation from the Hilger unit only for times when radiations other than copper are required. The Philips tube will be serviced from the power supply of the Hilger unit. The basic reason for using the Philips tube with the spectrometer is that a sealed-off tube such as the Philips tube provides a much more constant X-ray energy output than that which is provided by a continuously evacuated tube such as the Hilger tube. A constant X-ray output is required for the efficient operation of a Geiger-counter spectrometer. Three additional openings in the Philips tube head will be utilized for powder and back-reflection work.

A dark room has been constructed in Laboratory 9, and an X-ray development tank has been installed and connected. Electrical installations have been provided and most of the necessary fixtures have been installed.

Two 114.59-mm diameter X-ray powder cameras, a Norelco film measuring scale and film viewer, and a film viewer for the dark room have been received. A back-reflection camera and sample holder have been built along with necessary attachments for use with the Hilger unit.

The X-ray equipment has been utilized to take back-reflection patterns for determining orientation of zinc and copper single crystals. Powder patterns were made for positive identification and comparison of numerous materials in which minor impurities or structural changes were suspected. Tin at temperatures below 16 °C was examined with the spectrometer to determine whether the methods used had been successful in producing gray tin. Examination showed no evidence of gray tin.

High-tension cable which is yet to be received will provide a connection between the Hilger power supply and the spectrometer to be placed in the hot cell and between the Hilger power supply and the Philips X-ray tube. When the complete installation is made it will be possible to operate any one of the three units at any particular time by simple change of connections.

When completely equipped, the X-ray laboratory will be in a position to handle X-ray problems concerned with both normal and irradiated specimens. The versatility of the equipment will make it possible to employ the most advantageous method to the material under investigation.

IN-PILE THERMAL CONDUCTIVITY OF STRUCTURAL MATERIALS AT HIGH TEMPERATURES

A. Foner Cohen

One sample of inconel has been subjected to in-pile tests. The thermal conductivity appears to decrease by a factor of two in less than one week of exposure in the X pile and then reaches an approximately constant value. The sample temperature was approximately 820°C for the above experiment. The effect of an in-pile temperature anneal by increasing the temperature of the specimen approximately 70°C for 40 min and then returning the specimen to a temperature of 820°C caused annealing out of approximately 20% of the damage, after which, with further irradiation, the thermal conductivity decreased by this amount before reaching an equilibrium value. The results discussed above are to be considered preliminary until more samples are measured. Other experiments are in progress on types 316 and 310 stainless steel and pure nickel. The experiments in progress are planned to give information on the flux dependence of the thermal conductivity in the alloys. More detailed information concerning the annealing out of the damage is also anticipated.

ELECTRICAL AND THERMAL CONDUCTIVITY OF METALS

A. Foner Cohen and L. C. Templeton

Circuitry for the in-pile measurement of electrical conductivity of pure metals and for relative changes in the thermal conductivity has been completed. Most of these measurements will be made at temperatures not exceeding 400°C. The first material in this class of materials is pure nickel. A preliminary apparatus for measuring the magnetoresistance of metals or alloys before and after pile irradiation at temperatures up to approximately 800°C has been designed and some of the parts have been made.

METAL CRYSTALS

T. H. Blewitt R. R. Coltman, Jr.
R. E. Jamison

During the past quarter the work described in previous reports[1,2] has been continued, additional experiments have been started, and new experimental facilities have been added. The status of each of these will be discussed in some detail.

---

[1] T. H. Blewitt, R. R. Coltman, and F. A. Sherrill, "Study of the Effect of Radiation on Metal Crystals," *Physics of Solids Institute Quarterly Progress Report for Period Ending January 31, 1951*, ORNL-1025, p. 22 (July 17, 1951).

[2] T. H. Blewitt and R. R. Coltman, "Metal Crystals," *Physics of Solids Institute Quarterly Progress Report for Period Ending April 30, 1951*, ORNL-1095, p. 17 (Nov. 12, 1951).

TABLE 6.1

Electrical Resistivity of Copper Crystals

T = temperature (°C); ρ_T = resistivity at temperature T; $\Delta\rho_T$ = change in resistivity at temperature T.

SAMPLE	TREATMENT	T (°C)	ρ_T (μohm-cm)	ρ_{20} (μohm-cm)	T' (°C)	$\rho_{T'}$ (μohm-cm)	$\rho_{-196.0}$ (μohm-cm)	$\Delta\rho_{20}$ (μohm-cm)	$\Delta\rho_{-196.0}$ (μohm-cm)
19A	Annealed	18.27	1.6732	1.6846	-196.03	.19692	.19412		
		17.58	1.6686	1.6846	-196.01	.19678	.19685	.0000	-.0003
		15.81	1.6569	1.6847				+.0001	
	Exposed to	17.48	1.6680	1.6846	-195.91	.19726	.19666	.0000	-.0005
	3.28×10^8r	18.19	1.6729	1.6849	-196.01	.19642	.19649	+.0003	-.0006
	γ rays	12.43	1.6347	1.6848				+.0002	
21A	Annealed	18.59	1.6731	1.6824	-195.99	.19922	.19915		
		20.86	1.6877	1.6819	-196.02	.19885	.19898	-.0005	-.0002
		17.03	1.6628	1.6825	-196.03	.19926	.19945	+.0001	+.0003
	Exposed to	13.85	1.6418	1.6825	-196.00	.19941	.19941	+.0001	+.0003
	3.2×10^8r	8.28	1.6046	1.6822	-196.11	.19828	.19902	-.0002	-.0001
	γ rays								
14B	Annealed	19.19	1.6777	1.6830	-195.99	.20129	.20107		
		18.53	1.6733	1.6830	-196.02	.30118	.20131	.0000	+.0002
	After	19.64	1.6855	1.6879	-195.97	.20608	.20588	+.0049	+.0048
	2×10^{18}nvt	19.77	1.6890	1.6904	-196.04	.20599	.20586	+.0074	+.0048
		18.94	1.6812	1.6882	-196.07	.20537	.20584	+.0052	+.0048
		19.96	1.6885	1.6887	-196.02	.20543	.20555	+.0057	+.0045
		18.72	1.6799	1.6884	-196.03	.20565	.20585	+.0054	+.0048
		18.31	1.6766	1.6878				+.0048	
		15.82	1.6631	1.6908				+.0078	
17A	Annealed	18.43	1.6774	1.6878	-195.98	.20248	.20235		
		18.01	1.6748	1.6880	-196.02	.20222	.20235	+.0002	+.0000
	After	19.77	1.6914	1.6929	-196.05	.20643	.20677	+.0051	+.0044
	2×10^{18}nvt	20.25	1.6946	1.6929	-196.04	.20640	.20666	+.0051	+.0043
		19.25	1.6892	1.6942	-196.01	.20677	.20677	+.0064	+.0044
		18.26	1.6822	1.6937	-196.01	.20680	.20687	+.0059	+.0045
		21.57	1.7043	1.6939				+.0061	
16A	Annealed	17.80	1.6724	1.6870	-195.99	.20305	.20298		
		17.81	1.6726	1.6871	-196.04	.20269	.20296	+.0001	.0000
	After	20.70	1.6974	1.6928	-196.03	.20755	.20775	+.0058	+.0048
	2×10^{18}nvt	17.12	1.6745	1.6936	-196.06	.20720	.20760	+.0066	+.0046
		20.37	1.6955	1.6931	-195.94	.20755	.20715	+.0061	+.0042

TABLE 6.1 SUMMARY

Sample 19A:
- ρ at 20°C is 1.6846 ± .0001 μohm-cm and 1.6848 ± .0001 μohm-cm after γ exposure;
- ρ at -196°C is .19698 ± .00014 μohm-cm and .19658 ± .00008 μohm-cm after γ exposure.

Sample 21A:
- ρ at 20°C is 1.6823 ± .0002 μohm-cm and 1.6824 ± .0002 μohm-cm after γ exposure;
- ρ at -196°C is .19921 ± .00018 μohm-cm and .19922 ± .00020 μohm-cm after γ exposure.

Sample 14B:
- ρ at 20°C is 1.6830 ± .0000 μohm-cm and 1.6889 ± .0010 μohm-cm after 2×10^{18} nvt;
- ρ at -196°C is .20119 ± .00012 μohm-cm and .20580 ± .00010 μohm-cm after 2×10^{18} nvt.

Sample 17A:
- ρ at 20°C is 1.6879 ± .0001 μohm-cm and 1.6935 ± .0005 μohm-cm after 2×10^{18} nvt;
- ρ at -196°C is .20235 ± .00000 μohm-cm and .20677 ± .00005 μohm-cm after 2×10^{18} nvt.

Sample 16A:
- ρ at 20°C is 1.6871 ± .0001 μohm-cm and 1.6933 ± .0003 μohm-cm after 2×10^{18} nvt;
- ρ at -196°C is .20297 ± .00001 μohm-cm and .20750 ± .00023 μohm-cm after 2×10^{18} nvt.

Change in Resistivity of Copper Crystals from Pile Irradiation. Table 6.1 shows the results of measurements made at liquid nitrogen and room temperatures on copper crystals before and after a pile irradiation of 2×10^{18} nvt. The experimental procedure used is described in some detail in a previous report.[1] The potential drop across a known gage length was measured by a Rubicon type C thermofree microvolt potentiometer. The potential leads were sintered on the sample, and the temperature was measured by a copper constantan thermocouple.

The results obtained appear to be anomolous in that the radiation-induced resistance seems to be temperature dependent. The change in resistivity is some 25% greater at 290°A than at 90°A. The magnitude of the radiation-induced change is so small that further verification of this phenomena is required although the observed effects are in excess of the probable error. It is interesting to note that the magnitude of change measured at 90°A agrees very well with those previously found.[1] The older results were obtained by assuming that radiation added only to the temperature independent component of resistance, the residual resistance. To a first approximation, however, the method used to reduce the data gave the magnitude of the change in resistivity at 90°A.

Further verification of this temperature dependence is being made at present. As outlined in a previous report,[2] the accuracy of the measurement can be improved by the use of a control sample to eliminate a temperature measurement.* Measurements have been made at 90 and 290°A will results repeatable to a few hundredths of a percent accuracy. The results are shown in Table 6.2. Since measurements will also be made at either liquid helium or at liquid hydrogen so as to determine the residual resistivity directly, the diameter has been reduced to 1/8 in. The irradiation of these samples will be made in the LITR reactor in a

*In previous work, recovery of radiation hardness without recrystallization at 400°C was observed while no recovery was observed at 250°C.

TABLE 6.2

Measurements of the Electrical Resistance of Copper Single Crystals by Comparison with the Resistance of a Standard Control Specimen

	RESISTANCE (μohm) AT ROOM TEMPERATURE		RESISTANCE (μohm) AT LIQUID NITROGEN TEMPERATURE	
	I = 1.5 amp	I = 1.0 amp	I = 5.0 amp	I = 4.0 amp
Trial I				
Control 42-A	57.9150	57.9043	6.8920	6.8859
Specimen 39-A	57.9204	57.9060	6.9219	6.9134
Difference	0.0054	0.0017	0.0299	0.0275
Trial II				
Control 42-A	57.8014	57.8073	6.8857	6.8802
Specimen 39-A	57.8121	57.8128	6.9160	6.9073
Difference	0.0107	0.0055	0.0303	0.0271
Avg. Difference (Trials I and II)	0.0058 ± 0.0024		0.0287 ± 0.0014	
Trial I				
Subcontrol 39-B	58.5987	58.5828	6.91737	6.91308
Specimen 39-A	57.8328	57.8138	6.90643	6.89979
Difference	-0.7659	-0.7690	-0.01094	-0.01329
Trial II				
Subcontrol 39-B	58.5160	58.5153	6.9289	6.9228
Specimen 39-A	57.7502	57.7492	6.9179	6.9093
Difference	-0.7658	-0.7661	-0.0110	-0.0135
Avg. Difference (Trials I and II)	-0.7667 ± 0.0011		-0.0122 ± 0.0012	

facility described later in this report. It is estimated that the fast flux will be up by a factor of 5 or 10 over that of the irradiations previously made in the X pile.

Further experiments have been started on the samples for which the data shown in Table 6.1 was determined. It seems desirable that experimental evidence be obtained to show a correlation between radiation hardness and the increase in resistivity resulting from radiation; consequently, these samples will be annealed at temperatures ranging from 250 to 400°C,[1] and the resistivity and stress-strain subsequently will be determined. Since it is desirable to perform the annealing in a vacuum a Wilson seal has been constructed so that the samples can be given a specified heat treatment in a vacuum. It is interesting to note that increase in resistivity induced by work hardening is reduced at temperatures below that

required to cause recovery of the work hardening, indicating that at least a portion of the observed increase in resistivity is not directly associated with work hardening.

The temperature dependence of the increase in resistivity observed from radiation effects in Table 6.1 may be the results of a radiation-induced change in the elastic constants of copper. G. Dienes[3] has calculated the effect of interstitial and vacancy atoms on the elastic constants. These calculations indicate that interstitial atoms in copper increase the elastic constants by several orders in excess of that expected from a bulk effect, whereas vacancy atoms decrease the elastic constants only to the extent of that expected from a bulk effect. Apparently the effect of interstitial atoms only need to be considered. Dienes' calculations show that 1% interstitial atoms will increase the elastic constants in accordance with the figures shown in Table 6.3. The dependence of the Debye characteristic temperature on the elastic constants can be expressed as

$$\theta_D = \frac{K^{1/2}C}{\left\{ 2\left[\frac{2(1+\sigma)}{3(1-2\sigma)}\right]^{3/2} + \left[\frac{1+\sigma}{3(1+\sigma)}\right]^{3/2} \right\}^{1/3}},$$

where

K = bulk modulus,

$$C = \frac{3.6 \times 10^{-3}}{A^{1/3}\rho^{1/3}}$$

(A = atomic weight; ρ = density),

σ = Poisson's ratio.

For an order of magnitude calculation it can be assumed that the copper crystals are isotopic, and we then have the following relationships between the elastic constants.

$$\sigma = -\frac{S_{12}}{S_{11}},$$

where S_{ij} are elastic moduli. It can be shown for *fcc* crystals that the relationship between the elastic moduli, S_{ij}, and the elastic constant, C_{ij}, is

$$-\frac{S_{12}}{S_{11}} = \frac{C_{12}}{C_{12} + C_{11}}.$$

Then in accordance with the assumptions made we can write

$$\theta_D = \frac{K^{1/2}C}{\left\{ 2\left[\frac{2(C_{11} + 2C_{12})}{3(C_{11} - C_{12})}\right]^{3/2} + \left[\frac{C_{11} + 2C_{12}}{3C_{11}}\right]^{3/2} \right\}^{1/3}}.$$

To a first-order approximation changes in the elastic constants will affect

[3] G. J. Dienes, *A Theoretical Estimate of the Effect of Radiation on the Elastic Coefficients of Simple Metals*, NAA-SR-80 (June 20, 1951).

TABLE 6.3

Effect of Interstitials on the Elastic Coefficients of Copper
(Data taken from G. J. Dienes)[3]

	ELASTIC CONSTANTS (dynes cm^{-2})		
	PERCENT INTERSTITIALS		
	x = 0%	x = 1%	x = 5%
$c_{11} - c_{12}$ (unirradiated)	5.1×10^{11}		
$c_{11} - c_{12}$ (irradiated)		5.3×10^{11}	6.1×10^{11}
$\Delta[c_{11} - c_{12}]$		0.2×10^{11}	1.0×10^{11}
$\Delta[c_{11} - c_{12}]/[c_{11} - c_{12}]$(%)		3.9	19.6
c_{44} (unirradiated)	8.6×10^{11}		
c_{44} (irradiated)		9.4×10^{11}	12.6×10^{11}
Δc_{44}		0.8×10^{11}	4.0×10^{11}
$\Delta c_{44}/c_{44}$ (%)		9.3	46.5
K (unirradiated)	1.33×10^{12}		
K (irradiated)		1.45×10^{12}	1.93×10^{12}
ΔK		0.12×10^{12}	0.6×10^{12}
$\Delta K/K$ (%)		9.0	45.0
E_1 (unirradiated)	2.125×10^{12}		
E_1 (irradiated)		2.32×10^{12}	3.11×10^{12}
ΔE_1		0.195×10^{12}	0.985×10^{12}
$\Delta E_1/E_1$ (%)		9.2	46.3
E_2(unirradiated)	1.355×10^{12}		
E_2 (irradiated)		1.417×10^{12}	1.655×10^{12}
ΔE_2		0.062×10^{12}	0.3×10^{12}
$\Delta E_2/E_2$ (%)		4.56	22.1

only the numerator. Thus, for an order of magnitude calculation

$$\theta_D \cong K^{1/2}C^1 .$$

Substituting Dienes' calculated effects on the elastic constants we obtain

$$\frac{\theta_{DB}}{\theta_{DA}} = \left[\frac{1.33 \times 10^{12}}{1.45 \times 10^{12}}\right]^{1/2} ,$$

where θ_{DB} is the Debye characteristic temperature before irradiation and θ_{DA} is the Debye characteristic temperature after irradiation. If one takes for θ_{DB} a value of 333°A,[4] then θ_{DA} = 319°A. It should be emphasized that the magnitude of the change in Debye temperature is probably much too great as the number of retained interstitial atoms is probably considerably less than 1% assumed.[1]

The effect of this change in characteristic temperature on the electrical resistivity can be estimated by the use of Gruniesen's equation, which gives

$$\rho = CTG\left[\frac{\theta_D}{T}\right] (1 + \gamma T + \beta T^2),$$

where ρ is the electrical resistivity, C, β, E and γ are constants, T is the absolute temperature, and G is the Gruniesen function having a fifth power dependence on (θ_D/T). The term $(1 + \gamma T + \beta T^2)$ will in general be small and will be neglected here. Then

$$\frac{\rho_A}{\rho_B} \cong \frac{G(\theta_{DA}/T)}{G(\theta_{DB}/T)} .$$

For copper at 300°A we have

$$\rho_A \cong 1.006\ \rho_B$$

and

$$\Delta\rho = \rho_A - \rho_B \cong .006\ \rho_B \cong .0100\ \mu\text{ohm-cm},$$

and for copper at 90°A we have

$$\rho_A \cong 1.053\ \rho_B$$

and

$$\Delta\rho = \rho_A - \rho_B \cong .053\ \rho_B \cong .0103\ \mu\text{ohm-cm}.$$

These calculations then show that if 1% interstitial atoms are present and if they affect the elastic constants in accordance with Dienes' calculation, the Debye temperature should decrease; in the case of copper this decrease should be from 333 to 319°. The electrical resistivity of copper will then be raised by 6/10 percent at room temperature and by about 5 percent at liquid nitrogen temperatures. The magnitude of the change resistance, however, at these two temperatures will be approximately equal, the low-temperature increment being somewhat greater. It should be noted that only the change in the thermal component of resistance has been considered here and that the interstitials will also cause an increase in the resistivity. If one takes seriously the suggestion[1] that the interstitial atoms should behave like zinc impurities, the

---

[4] N. F. Mott and H. Jones, *The Theory of the Properties of Metals and Alloys*, Clarendon Press, Oxford, 1936.

magnitude of this change should be .3 μohm-cm, which is considerably in excess of the decrease arising from the change in the elastic constant. It can be seen that the magnitude of the changes induced by changes in elastic constants will be an order of magnitude lower than those induced from the residual resistivity. Therefore, to a good approximation it can be assumed in the case of copper that the Debye characteristic temperature remains constant during bombardment, hence, the anomolous results reported there cannot be explained from changes in the Debye temperature.

Effect of Radiation on the X-Ray Reflection Coefficients. A single crystal of copper was irradiated in a low-energy beam of protons at Y-12. The energy was 2 Mev and the exposure was 15 μamp-hr. Half of the crystal was shielded from the beam. X-ray studies were then made by rocking the crystal very slowly through the Bragg angle (1° per hour) and detecting the reflected radiation with a Geiger tube. Filtered copper Kγ radiation was used for the source of X rays. The results are indicated in Fig. 6.3. If the slight change observed near the tail of the curve is real it is

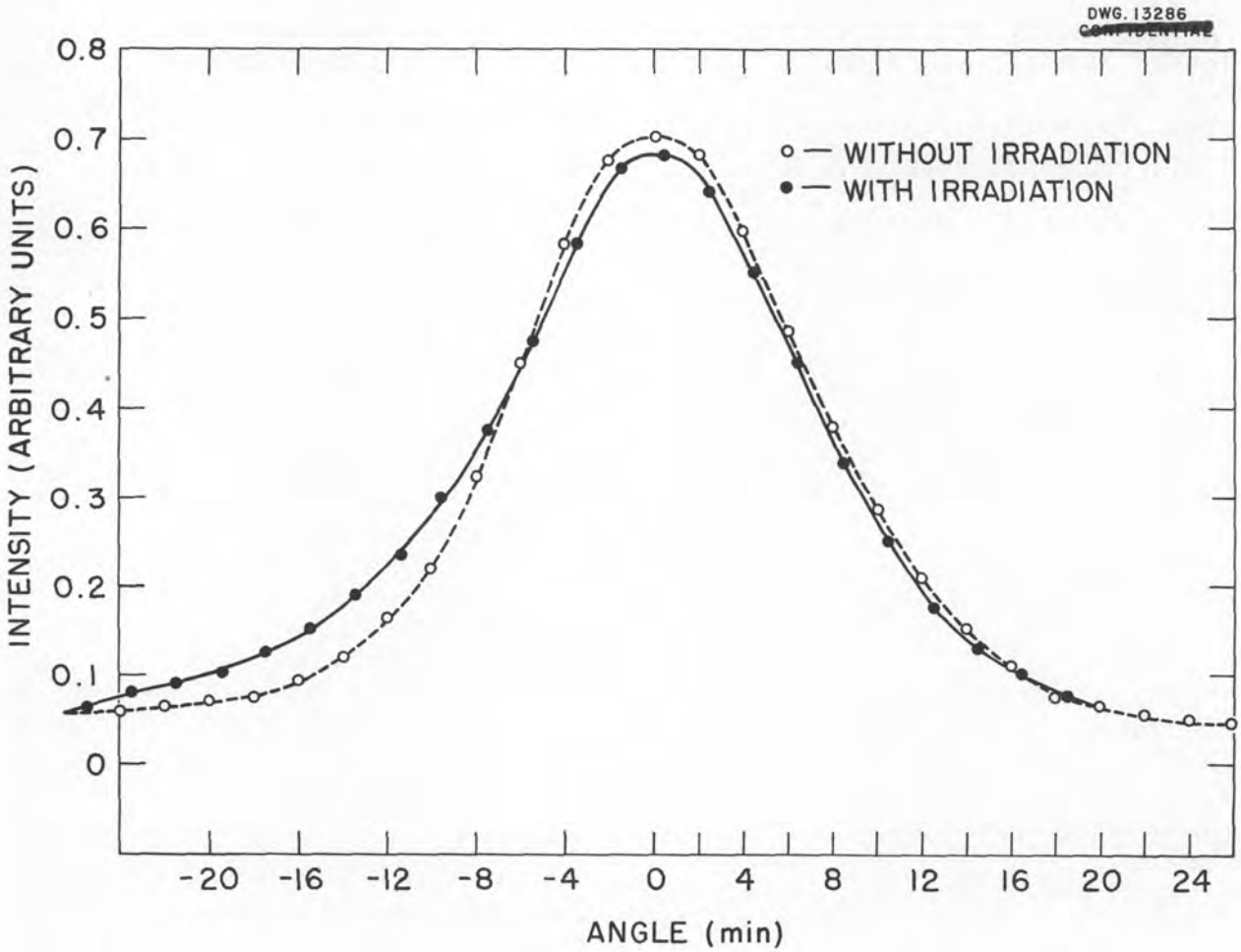

Fig. 6.3. The 220 Reflection from an Unirradiated and an Irradiated Copper Crystal.

indicative of a decrease in the reflection coefficients. Apparently the extinction increases slightly, indicating an increase in the perfection of the crystal.

Effect of Radiation on the Stress-Strain Curves of Polycrystalline Copper. Four standard .505-in. tensile specimens were machined from the same piece of OFHC copper. These were then given an identical heat treatment of 1 hr at 950°C in a vacuum of 10^{-5} mm of mercury. Two of the samples were then placed in the pile and irradiated in a neutron flux of 2×10^{18} nvt. The stress-strain curve was subsequently measured on all four samples. A Baldwin Southwark 120,000-lb machine was used. The strain was measured by a microformer. The results are shown in Fig. 6.4. It is clear that the elastic limit is raised substantially as one would expect from the data[1] obtained on single crystals. It appears that ultimate strength is decreased slightly.

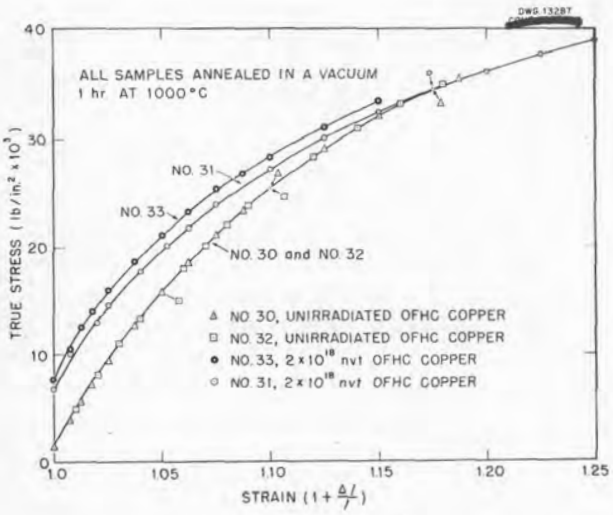

Fig. 6.4. Effect of Radiation on the Stress-Strain Curves of Polycrystalline Copper.

Study of the Radiation Effects on Disordered Cu_3Au. An experiment is now under way which promises to give some insight into the mechanism of radiation damage. Considerable work has been done[5,6] in the past on the effects of radiation on ordered and disordered Cu_3Au. The results of these experiments clearly showed that disorder resulted from the neutron bombardment in the case of the ordered system. It was observed, however, by the observers at Harwell that the ordered sample at first seemed to reach a slightly higher degree of order which then decreased rapidly with further bombardment. The observers at Chalk River found a similar effect and further found that in some cases a disordered alloy apparently was ordered. There was a slight indication in the Siegel and Billington data that some ordering occurred in a disordered sample as the electrical resistivity decreased slightly after correction for the mercury formed by transmutation. It is interesting to note that cold work of ordered Cu_3Au crystals shows a behavior similar to that reported for the irradiation of ordered Cu_3Au by the Harwell observers, namely, the order apparently increases for small damage and then apparently decreases rapidly.

Siegel and Billington have suggested that the disorder is produced by the highly localized temperature of the thermal spikes which is then rapidly quenched, leaving the alloy in the vicinity of the thermal spike in high-temperature phase. It seems that radiation ordering can be understood by a consideration of the effect of the imperfections induced by the

---

[5] S. Siegel, "Effect of Neutron Bombardment on Order in the Alloy Cu_3Au," *Phys. Rev.* 75, 1823 (1949).

[6] L. G. Cook and R. L. Cushing, *Effects of Neutron Irradiation on the Structure of the Order-Disorder Alloy Cu_3Au*, NP-3235 (May 25, 1951).

neutron knock-ons on the diffusion process. Huntington and Sietz[7] have shown theoretically that diffusion should occur by a vacancy mechanism, and recent experiments support their theory; consequently, if an appreciable number of vacancies are generated by a pile irradiation then the diffusion rate should increase substantially and the relaxation time of the ordering process should be lowered.

Let us now consider the effect of a 2-Mev neutron on sample Cu_3Au. The neutron will knock on an atom, causing it to be displaced from its lattice site with a kinetic energy of several hundred Kev. This energy will then be lost, largely by inelastic collision, until a threshold energy is reached, and then the remaining energy will be lost, primarily by elastic billiard ball type collisions. In this latter process further atoms will be displaced from the equilibrium conditions by this primary knocked-on atom, some with sufficient energy to be displaced from their lattice sites and others with only sufficient energy to oscillate about their lattice position in a manner equivalent to thermal oscillation. In the case of a disordered sample this equivalent thermal oscillation will have little effect since the sample is already in the high-temperature equilibrium condition. The rapid dissipation of the lattice oscillations will be equivalent to a rapid quench. A phase stable at high temperatures will thus be retained in the region in the vicinity of the knocked-on atom. In the case of ordered alloys the disordered phase is stable at high temperatures. However, in the vicinity of the knocked-on atom there will also be a large number of interstitial and vacancy atoms. Order of magnitude calculations can be made to find the number of vacancies and interstitials created by bombardment. The number of primary knock-ons will be given by

$$N_p = \sigma_s (nv) tN ,$$

where

σ_s = scattering cross-section,

nv = neutron flux,

t = time,

N = number of atoms per cubic centimeter.

For copper σ_s is about 7 barns for thermal neutrons and for fast neutrons an assumption of about 3 barns will be made. Then for a 1-month bombardment in the center of the X pile,

$$N_p = 3 \times 10^{-24} \times 2 \times 10^{18} \times 10^{23} = 6 \times 10^{17} .$$

Each primary displacement will in turn cause secondary and ternary knock-ons. The total number of knock-ons will then be given by

$$N_d = N_d \cdot N_i .$$

Seitz[8] has calculated the number of displaced atoms per primary knock-on for several light elements and, if it is assumed that his calculations for aluminum can also be used for copper and gold, then

$$N_d = 6 \times 10^{17} \times 10^2 = 6 \times 10^{19} .$$

[7] H. B. Huntington and F. Seitz, "Mechanism for Self-Diffusion in Metallic Copper," *Phys. Rev.* 61, 315 (1942).

[8] F. Seitz, "On the Disordering of Solids by Action of Fast Massive Particles," *Disc. Faraday Soc.*, No. 5, 271 (1949).

It should be noted that the value of N_i used is probably too low. This value of 6×10^{19} displaced atoms is of the same order as that obtained from the measured values of the change in electrical resistance of copper single crystals from a 1-month bombardment in the X pile. Thus the total number of displaced atoms would be about .06% if they were homogeneously distributed. However, these displaced atoms will be highly localized in the vicinity of the primary displacement. If we assume that the range of the displaced atoms is such that the order of 10^4 atoms then there will be 6% interstitial atoms in this localized region. This should appreciably increase the diffusion rate and lower the relaxation time for the formation of order in the thermal spike. If, then, a sample of disordered Cu_3Au is irradiated or annealed at a temperature which is low enough to prohibit order without the presence of the additional vacancy atoms but sufficiently high so that appreciable ordering will occur in the presence of the high number of vacancy atoms, then the result will be a number of ordered regions essentially the size of the thermal spikes. The size and number of ordered regions can be readily determined from X-ray and electrical resistivity measurements. It may be possible that the number of vacancies can also be estimated from the relaxation time after bombardment.

The following experiment is now being performed. A sample of Cu_3Au has been synthesized in the laboratory following the procedure given in reference.[9] The sample was homogenized by an anneal at 900°C for 5 hr and then drawn to a 10-mil wire. Some of the wire was subsequently annealed at 825°C for 4 hr and then wound on a 1/4-in. lavite spool to form a helix with a pitch of 10 turns per inch. Potential probes were welded near the ends of the helix, and the assembly was then sealed in an evacuated glass tube (1×10^{-5} mm pressure) and held at 450°C for 4 hr in a vertically mounted tape furnace. The glass tube was then suspended in the furnace with a piece of nickel wire which was cut at the end of the anneal, dropping the glass tube with the assembly into a water bath. The glass broke on contact with the water, giving a rapid quench and retaining the disordered phase. This sample was mounted in a hollow lavite cylinder with a nichrome winding so that a predetermined temperature could be reached. The whole assembly was then mounted in a stainless steel capsule with the potential, current, thermocouple and heater leads brought through kovar seals, and the capsule was evacuated to better than 10^{-3} mm pressure. This sample will shortly be irradiated at 250°C, and the electrical resistivity will be measured as a function of irradiation. The temperature of 250°C was determined for the following reasons. In previous calculations we have shown that for a 1-month bombardment in the X pile 3×10^{17} primary knock-ons should result. If it is assumed that there are 10^4 atoms in the thermal spike and that the equilibrium degree of order will result at 250°C as a result of the additional vacancies, then approximately 1% of the total volume will be ordered. This will be equivalent to a change in electrical resistivity of about 3%. At 200°C the relaxation time for material quenched about the critical temperature is in excess of 10,000 hr. However, the relaxation time for order within a domain in the absence of antiphase boundaries is of the order of 55 hr, consequently at 250°C

[9] C. Sykes and H. Evans, "The Transformation in the Copper-Gold Alloy Cu_3Au," *J. Inst. Metals* 58, p. 255 (1936).

the thermal spikes can nucleate the order which can then continue at an accelerated rate. The flux is so low in the X pile that it is felt that some magnification such as is received at this temperature is necessary to obtain measurable results.

Other samples have been prepared for bombardment in the LITR facility described in the following section of this report. These samples have been annealed at 625°C rather than at 900°C following the wire drawing in order to secure a grain size suitable for X-ray powder patterns. They will then be irradiated at room temperature in the LITR, after which they will be annealed at various temperatures and times, and the X-ray powder patterns and electrical resistivities will then be studied. An anneal at 200°C will, for example, inhibit growth except in the vicinity of the added vacancies which will result in the volume of the ordered domain being the size of the thermal spike. This size can be determined by the breadth of the superlattice lines if they exceed 20°A. If the sample is further annealed at 250°C this ordered domain will grow until they become adjacent to each other. The size of the domains and the number of nuclei can then be determined. From the electrical resistivity and the intensity of the superlattice line, the degree of order within each domain can be computed and hence the relaxation can be computed. From this date it should be possible to estimate the number of vacancy atoms present from each knocked-on atom.

It should be noted that the presence of these localized vacancies should not appreciably alter the macroscopic diffusion rates since the average mean free path of the vacancy should be relatively small. In the case of the Cu_3Au alloy, however, each movement of an atom will be registered due to its ordering phenomena. The diffusion of the elements of an unordered alloy cannot normally be detected unless motion of an appreciable distance is considered.

LITR Facility. In order to obtain the maximum fast flux in the LITR a hollow fuel element has been built which will be placed in the active lattice. Nine of the fuel plates have been removed from the element and a rectangular slot 1-1/8 by 2-7/16 in. has been built into the element. A 2S aluminum torpedo will be used to hold the samples. Removal tools have been built so that the torpedoes and the fuel element can readily be moved. In addition to the obvious advantage of high flux the samples are cooled by the water in the reactor. In addition, samples can easily be removed without damage and in the case of samples with short lives they can be stored in the reactor water, alleviating the necessity of carriers. It is estimated that the fast flux in this facility will be between 5×10^{13} and 1×10^{13} nv.

SECRET

SECURITY INFORMATION

RESTRICTED DATA

This document contains Restricted Data as defined in the Atomic Energy Act of 1946. Its transmittal or the disclosure of its contents in any manner to any unauthorized person is prohibited.

SECRET

SECURITY INFORMATION